ΠΑΝΕΠΙΣΤΗΜΙΟ ΙΩΑΝΝΙΝΩΝ
ΣΧΟΛΗ ΕΠΙΣΤΗΜΩΝ & ΤΕΧΝΟΛΟΓΙΩΝ
ΤΜΗΜΑ ΜΗΧΑΝΙΚΩΝ ΕΠΙΣΤΗΜΗΣ ΥΛΙΚΩΝ

Ρόλος του Διαχωρισμού και Κατακρημνισμάτων στους Μηχανισμούς Διεπιφανειακής Ενίσχυσης Κράματος Αλουμινίου Ενισχυμένου με SiC όταν υπόκειται σε Θερμομηχανική Κατεργασία

Δημήτριος Μυριούνης

ΔΙΔΑΚΤΟΡΙΚΗ ΔΙΑΤΡΙΒΗ

ΙΩΑΝΝΙΝΑ 2009

'To the memory of my beloved sister'

'Στη μνήμη της πολυαγαπημένης μου αδελφής'

TABLE OF CONTENTS

Chapter IV - Tensile and Fatigue Behaviour of SiC particulate reinforced aluminium alloy composites

PREFACE

This report describes a split PhD work carried out in two Universities under the Cooperation Agreement signed by both institutes. This Agreement is entered between the Sheffield Hallam University, located in England, United Kingdom and the University of Ioannina, located in Ioannina, Greece from December 2004 to May 2009. The submission of the report is in accordance with the requirements for the award of the degree of Doctorate of Philosophy in Materials Engineering under the auspices of both Universities.

ACKNOWLEDGEMENTS

At this point, I would like to thank my family for their valuable support at every level. I have a real debt of gratitude to my mother, my father for their unremitting zeal and helpfulness. Also special thanks to all my friends and colleagues for helping and encouraging me to achieve my goals, to broaden my horizons and realise my ambitions. I hope to give them more joy and happiness in the future. Finally, I would like to thank my supervisors Professor Theodore Matikas and Dr. Syed Hasan who truly believed in me all these years, for giving me the chance to start fulfilling my dreams.

ABSTRACT

Metal Matrix ceramic-reinforced composites are rapidly becoming strong candidates as structural materials for many high temperatures and aerospace applications. Metal matrix composites combine the ductile properties of the matrix with a brittle phase of the reinforcement, leading to high stiffness and strength with a reduction in structural weight. The main objective of using a metal matrix composite system is to increase service temperature or specific mechanical properties of structural components by replacing existing superalloys.

The satisfactory performance of metal matrix composites depends critically on their integrity, the heart of which is the quality of the matrix-reinforcement interface. The nature of the interface depends on the processing of the metal matrix composite component. At the micro-level the development of local stress concentration gradients around the ceramic reinforcement, as the metal matrix attempts to deform during processing, can be very different to the nominal conditions and play a crucial role in important microstructural events such as segregation and precipitation at the matrix-reinforcement interface. These events dominate the cohesive strength and subsequent mechanical properties of the interface.

At present the relationship between the strength properties of metal matrix composites and the details of the thermo mechanical forming processes is not well understood.

The purpose of the study will is to investigate several strengthening mechanisms and the effect of thermo-mechanical processing of SiC particulate reinforced A359 aluminium alloy composites on the particle-matrix interface and the overall mechanical properties of the material. From experiments performed on composite materials subjected to various thermo-mechanical conditions and by observation using SEM microanalysis and mechanical testing, data were obtained, summarised and mathematically/statistically analysed upon their significance.

An analytical model to predict the interfacial fracture strength in the presence of material segregation was also developed during this research effort. Its validity was determined based on the data gathered from the experiments.

Chapter I - Aims & Objectives

The main objective of the current work is the design of SiC particulate-reinforced aluminium alloy composite systems with enhanced mechanical properties (Figure I.1). This is achieved by microstructural modification of the raw MMC material using appropriate heat treatment processing. During thermo-mechanical processing, several strengthening mechanisms such as segregation and precipitation phenomena occur influencing the particle-matrix interface properties. Different heat treatment conditions result in tailored interfacial mechanical behaviour (see Chapter III).

In order to design a SiC particulate-reinforced aluminium alloy composite system, a thermodynamics-based damage mechanics model has been developed enabling determination of the interfacial mechanical property using input from various experimental measurements (Chapter V). This analytical model correlates the microstructural with the macroscopic behaviour of the composite and predicts the interfacial fracture strength in the presence of material segregation.

The experimental approach (Chapter IV) of this work involves:

(a) Metallographic, SEM imaging and microhardness measurements to obtain data on the size of the SiC particulates, the phases present, as well as microhardness values in the matrix and the interface.

(b) Tensile testing to obtain mechanical parameters of the composite such as the tensile strength and the Young's modulus.

(c) Fracture mechanics testing to determine the fracture toughness of the material.

(d) Fatigue testing to determine the fatigue crack growth rate.

In order to use the model and determine the interfacial fracture strength, properties measured experimentally are used as input parameters. The results demonstrate that the model succeeds in predicting the trends in relation to the segregation and the interfacial fracture strength behaviour in Al/SiCp materials processed in different heat treatment conditions.

It was finally shown that Al/SiCp composites processed in specific thermo-mechanical conditions in order to attain higher values of interfacial fracture strength due to precipitation hardening and segregation mechanisms, also exhibited enhanced bulk mechanical and fracture properties.

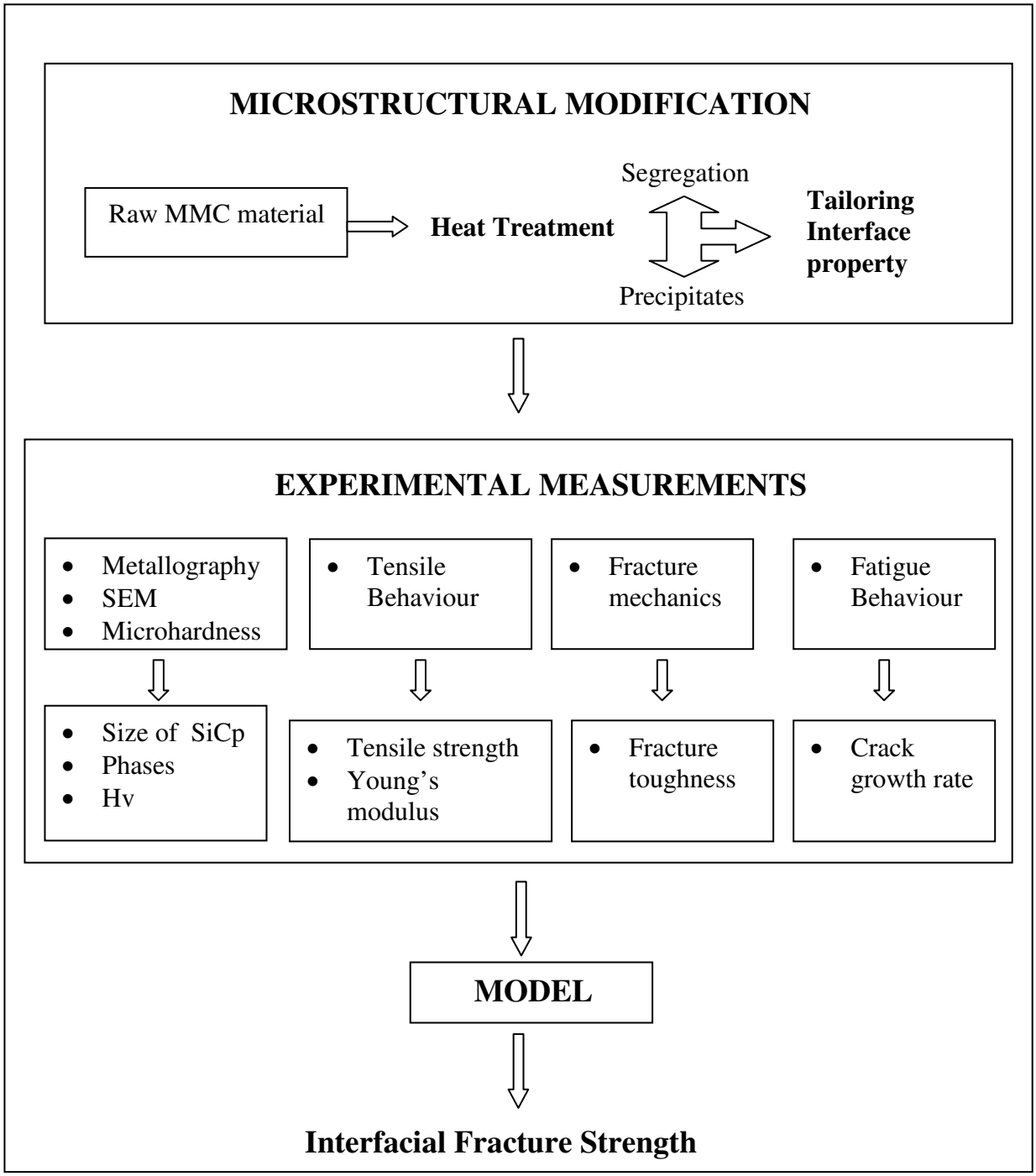

Figure I.1. The design of SiC particulate reinforced aluminium alloy composite system with tailored mechanical properties.

Chapter II - Introduction

II.1 History of Composite Materials

The concept of composite materials is ancient: to combine different materials to produce a new material with performance unattainable by the individual constituents.

Practically everything in this world is a composite material. In a broad sense the word ‘composite’ means ‘made of two or more different parts’. For example, a common piece of metal is a composite (polycrystal) of many grains (or single crystals). Strictly speaking, the idea of composite materials is not new or recent. For instance, wood is a composite material as it is a fibrous composite consisted of cellulose fibres in a lignin matrix. The cellulose fibres have high tensile strength but are very flexible (low stiffness), while the lignin matrix joins the fibres and furnishes the stiffness. Some more recent examples, but before engineered materials became prominent, are carbon black in rubber, steel rods in concrete, cement/asphalt mixed with sand, fibreglass in resin etc [1].

For man-made composites, there are three big categories of composite materials: metal matrix composites (MMCs), polymer matrix composites (PMCs), and ceramic matrix composites (CMCs). These are made by adding various reinforcements such as particulates, fibres or whiskers, into metal, polymer or ceramic matrix respectively. In the case of metal matrix composites (MMCs) the metal used more often as a matrix can be aluminium or titanium and the reinforcement can be particulates or fibres of silicon carbide (SiC) or Titanium Carbide (TiC). Polymer matrix composites (PMCs), also known as FRP - fibre reinforced polymers, use a polymer-based resin as the matrix, and a variety of fibres such as glass and carbon as the reinforcement. For example ‘fibreglass’, the first successful modern composite, is one of the polymer matrix

composites. Finally, ceramic matrix composites (CMCs) are used in very high temperature environments and these materials use a ceramic as the matrix and short fibres or particulates as reinforcement, such as those made from silicon carbide and boron nitride [2].

The idea of man made making composite materials came from the need for stronger and stiffer yet lighter composites in fields as diverse as aerospace, energy, automotive, and civil construction. Since the early 1960s, there has been an increasing research and development effort in these materials. Today, given the most efficient design, new materials and manufacturing processes we can make a composite material that meets or even exceeds the performance requirements. Most of the savings from the introduction of these materials are in weight and cost. These are measured in terms of ratios such as stiffness/weight, strength/weight and cost/weight ratios [3].

Throughout these decades scientists and engineers have implemented new advanced technologies that made composite materials become better than monolithic materials. Design and analysis of composite materials became more flexible, in a way that the designer can create a different material for each application aiming in weight and cost savings. Yet another development is the manufacturing and design integration at all levels, from conception to fabrication of a material, as well as failure analysis. Thus, composite material has a more 'controlled' life cycle compared with monolithic materials, in a sense that these man made materials are carefully designed for a specific purpose, therefore are more likely to overcome any problems concerning the application that are made for.

Although nature has invented the way of composting materials, man made composite materials are the ones that have advanced properties and are designed in order to meet specific engineering roles, by exploiting the desirable properties of the components whilst minimising the harmful effects of their less desirable properties.

Most commonly, composite materials have a bulk phase, which is continuous, called the matrix, and one dispersed, non-continuous phase, called the reinforcement, which is usually harder and stronger. The essence of the concept of composites is the following: the bulk phase accepts the load over a large surface area, and transfers it to the reinforcement, which being stiffer, increases the strength of the composite. The significance here lies in that there are numerous matrix materials and as many reinforcement types, which can be combined in countless ways to produce just the desired properties [4].

II.2 Metal Matrix Composites (MMCs)

According to the bibliography, metal matrix composites play a crucial role in the engineering field both for industrial as well as research environments and can play a pretty important role in the revolution of the technological material future applications [4].

Metal matrix composites are rapidly becoming strong candidates as structural materials for many high temperature and aerospace applications. These materials combine metallic properties and ceramic properties, leading to high stiffness and strength with a reduction in structural weight. The main objective of using a metal matrix composite system is to increase service temperature or specific mechanical properties of structural components by replacing existing superalloys.

In many cases, the performance of metal matrix composites is superior in terms of improved physical, mechanical and thermal properties (specific strength and modulus, elevated temperature stability, thermal conductivity, and controlled coefficient of thermal expansion), although substantial technical and infrastructure challenges remain.

Metal Matrix Composite is a composite material in which one constituent is a metal or alloy forming at least one percolating network. The other constituent is embedded in this metal matrix and usually serves as reinforcement. A significant volume fraction of a stiff non-metallic phase in a ductile metal matrix results in phenomena that are specific to reinforced metals.

The performance of metal matrix composites depends on the matrix-reinforcement interfacial bond. This interfacial cohesion can be improved by the appropriate heat treatment processing. At the micro level the development of local concentration gradients around the reinforcement, as the metal matrix attempts to deform during processing can be very different to the nominal conditions and play a crucial role in important microstructural events such as segregation of the interface [5].

Furthermore, in the past few years, there has been a significant advance in the understanding of these materials and of phenomena specific to their fabrication and behaviour. Also, scientific investigations have addressed the governing principles of their processing and general laws have been identified for the influence exerted by the reinforcement on the microstructural evolution of the matrix. Finally, advances in computational mechanics have brought to light practically important micromechanical phenomena that were often ignored in analytic treatments [4].

The composite materials design has shifted emphasis to pursue light weight, environment friendliness, low cost, quality, and performance. Parallel to this trend, Metal Matrix Composites have been attracting growing interest. MMCs' attributes include alterations in mechanical behaviour (e.g., tensile and compressive properties, creep, notch resistance, and tribology) and physical properties (e.g., intermediate density, thermal expansion, and thermal diffusivity) by the filler phase; the materials' limitations are thermal fatigue, thermochemical compatibility, and low-transverse creep resistance.

II.3 Reinforcement in Matrix

The reinforcement material is embedded into the matrix. The reinforcement does not always serve a purely structural task (reinforcing the compound), but is also used to change physical properties such as wear resistance, friction coefficient, or thermal conductivity. The reinforcement can be either continuous, or discontinuous.

Discontinuous MMCs can be isotropic, and can be worked with standard metalworking techniques, such as extrusion, forging or rolling. Continuous reinforcement on the other hand uses monofilament wires or fibres such as carbon fibre or silicon carbide. Because the fibres are embedded into the matrix in a certain direction, the result is an anisotropic structure in which the alignment of the material affects its strength. One of the first MMCs used boron filament as reinforcement. Discontinuous reinforcement uses "whiskers", short fibres, or particles. The most common reinforcing materials in this category are alumina and silicon carbide [2].

Reinforcement materials can be introduced into the matrix in different ways, including blending of the reinforcement throughout the matrix material prior to consolidation, or adding shaped forms - called preforms - before consolidation. In the blending approach, reinforcement particles are uniformly dispersed in the matrix by stirring in molten aluminum for the manufacture of Aluminium MMCs. The particles are slurried with alumina and spray dried for the manufacture of Al_2O_3 CMCs [6]. In the preform approach used for Aluminium MMCs, reinforcements, typically in the form of fibres, chopped fibres, particulates or whiskers, are blended with low and high temperature binders and formed into the desired selective reinforcement shape or preform using vacuum forming, pressing or injection molding forming techniques. Vacuum forming is the most common method for manufacturing simple shaped preforms, such as the plates/disks, rings or cylinders used in the manufacture of

Aluminium MMCs for pistons and cylinder liners. Pressing of plastic or granulated reinforcements is currently being developed to make more complex preform shapes required for new applications. Injection molding has also been used to some extent to make very complex preform shapes, but preform density is limited based on the need to maintain a flowable plastic body, which is then heated or cooled to provide adequate green strength for removal from the die without distortion [7].

II.3.1 Reinforcement Selection

The MMC types (Figure II.1) are commonly subdivided according to whether the reinforcement is in the form of [8-9]:

- Particle reinforced MMCs
- Short fibre or whisker reinforced MMCs
- Continuous fibre or sheet reinforced MMCs

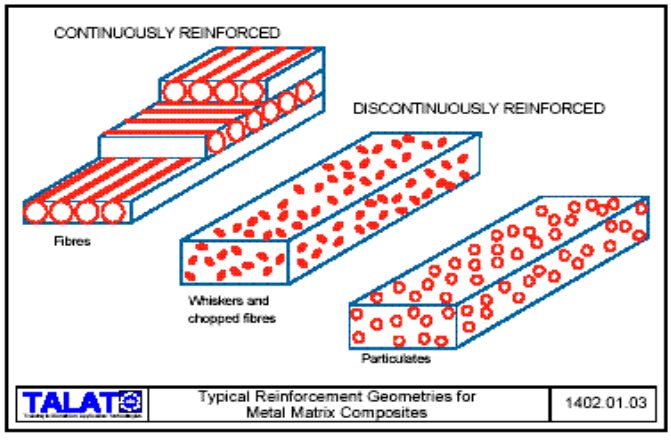

Figure II.1. Typical reinforcement geometries for MMCs.

Proper ceramic reinforcement selection is critical to achieve the required composite properties. Several reinforcement materials can be found in particle, fibre, chopped or milled fibre, and whisker forms. Typical particle reinforcements include

SiO_2, Al_2O_3, TiC and SiC particles that are used to reinforce the entire matrix material. These materials are relatively low in cost and are available in several particle sizes [8].

The next group of materials is often referred to as 'white fibres' and includes alumino-silicate fibres and alumina fibres. These materials are available in both fibre and chopped or milled fibre form, depending on whether anisotropic (exhibiting different values when measured in different directions) or isotropic (exhibiting the same values when measured in different directions) properties are desired in the composite. These medium-performance materials cost more than particles but offer engineers the ability to selectively reinforce the matrix by forming the fibre into a porous preform shape.

Another type of reinforcement is SiC whiskers which are single crystal acicular shaped particles that possess the highest strength and modulus of all reinforcements. This is currently the highest-cost reinforcement, but it offers the optimum strength, modulus, fatigue and wear resistance properties depending on the reinforcement percentage addition. The use of preforms and selective reinforcement can provide a cost effective solution when using SiC whiskers.

The table below shows examples of some important reinforcements used in metal matrix composites and their aspect ratios and diameters. In particular, particulate or discontinuously reinforced MMCs have become very important because they are inexpensive and they have relatively isotropic properties compared to fibre reinforced composites. The important aspect in this matter is whether they remain stable during processing and service.

Type	Aspect Ratio	Diameter, μm	Examples
Particles	~1-4	1-25	SiC, Al_2O_3, BN
Short Fibre or whisker	~10-1000	0.1-25	SiC, Al_2O_3, C
Continuous fibre	>1000	3-150	SiC, Al_2O_3, C, B, W

Table II.1. Typical reinforcement used in metal matrix composites

Furthermore, a number of metal wires including tungsten, beryllium, titanium, and molybdenum have been used to reinforce metal matrices. Currently, the most important wire reinforcements are tungsten wire in superalloys and superconducting materials incorporating niobium-titanium and niobium-tin in a copper matrix. The reinforcements cited above are the most important at this time. Many others have been tried over the last few decades, and still others undoubtedly will be developed in the future [10].

II.3.2 Particulate MMCs

Particulate MMCs is being used or developed for a range of industrial applications. While these are often focussed on Aluminium alloy matrices, Ti-, Fe- and Mg-based systems are also of interest. The particulate is most commonly SiC or Al_2O_3, but others (TiB_2, B_4C, SiO_2, TiC, WC, BN, ZrO_2, W etc) have been investigated. Chemical reaction during processing can occur in some cases [11].

Particulate MMCs are most commonly manufactured either by melt incorporation and casting technique or by powder blending and consolidation. Other routes include reactive processing or spray co-deposition. Quality control objectives include the elimination of excessive interfacial reaction during processing, particularly for melt routes, and also the avoidance of microstructural defects such as poor interfacial bonding, internal voids and clustering of the reinforcement [12].

II.4 Advantages and Disadvantages of MMCs

As aforementioned the performance advantage of metal matrix composites is their tailored mechanical, physical, and thermal properties that include low density, high specific strength, high specific modulus, high thermal conductivity, good fatigue

response, control of thermal expansion, and high abrasion and wear resistance. In general, the reduced weight and improved strength and stiffness of the MMCs are achieved with various monolithic matrix materials [13]. Compared to monolithic metals, MMCs have:

- Higher strength-to-density ratios
- Higher stiffness-to-density ratios
- Better fatigue resistance
- Better elevated temperature properties
    - Higher strength
    - Lower creep rate
- Lower coefficients of thermal expansion
- Better wear resistance

The advantages of MMCs over polymer matrix composites are:

- Higher temperature capability
- Fire resistance
- Higher transverse stiffness and strength
- No moisture absorption
- Higher electrical and thermal conductivities
- Better radiation resistance
- No outgassing
- Fabricability of whisker and particulate-reinforced MMCs with conventional metalworking equipment.

The major drawback of these materials, however, is their less than ideal ductility, fracture toughness and fatigue crack growth rate properties. A major disadvantage of MMCs is that they offer increased performance but at increased cost. However, there may be a misconception here; that is, if an aluminium based MMC is

offered against a conventional aluminium component, then a major increase in performance is vital if the significant increase in costs is to be justified. However, it is often the case that an aluminium based MMC is offered in replacement of a titanium or polymeric composite part, competing on both performance and cost [14]. Some of the disadvantages of MMCs compared to monolithic metals and polymer matrix composites are:

- Higher cost of some material systems
- Relatively immature technology
- Complex fabrication methods for fibre-reinforced systems (except for casting)
- Limited service experience

Finally, for aluminium matrix composites materials their main advantage is the low cost over most other MMCs. In addition, they offer excellent thermal conductivity, high shear strength, excellent abrasion resistance, high-temperature operation, nonflammability, minimal attack by fuels and solvents, and the ability to be formed and treated on conventional equipment.

II.5 Background on interface strengthening in SiC particulate-reinforced aluminium alloy composites

Aluminium-based metal matrix composites (MMCs) are very promising for high temperature and strength as well as wear resistant applications. Aluminium alloys are important materials in many industrial applications, including aerospace. Silicon carbide (SiC) particulate-reinforced aluminium alloy composites (Al/SiCp) are especially attractive due to their superior strength, stiffness, low cycle fatigue properties, corrosion fatigue behaviour, creep and wear resistance compared with corresponding wrought

aluminium alloys which are used extensively for various critical structural applications [15-18].

An important feature of the microstructure in the SiC particulate reinforced aluminium alloy composites is the higher density of dislocations and larger residual internal stresses in comparison to the unreinforced alloys, which are introduced by the large difference in coefficients of thermal expansion between the reinforcement and the matrix. The introduction of the reinforcement plays a key role in both the mechanical and the thermal ageing behaviour of the matrix alloy, as well as the composite material. Micro-compositional changes which occur during the thermo-mechanical forming processes of these materials may cause substantial changes in mechanical properties such as ductility, fracture toughness and stress corrosion resistance [19-22].

The apprehension of the work hardening behaviour of particulate reinforced metal matrix composites is crucial in optimising the parameters for deformation processing of these materials. The particulate composite material is not homogeneous; hence material properties are not only sensitive to the constituent properties, but also to the interfacial ones. The strength of the particulate composites depends on the size of the particles, the inter-particle spacing, and the volume fraction of the reinforcement [15].

The strengthening of a pure metal is carried out by alloying and supersaturating, to the extent, the excess alloying additions precipitate (ageing) using suitable heat treatment. To study the deformation behaviour of precipitate hardened alloy or particulate reinforced metal matrix composites the interaction of dislocation with the reinforcing particles is much more dependent on the particle size, the spacing and the density than on the composition [16]. Furthermore, when a particle is introduced in a matrix, an additional barrier to the movement of dislocation is created and the dislocation must react by either cutting through the particles or by taking a path around the obstacles [23].

At present, the relationship between the strength properties of metal matrix composites and the details of the thermo-mechanical forming processes is not well understood. The kinetics of precipitation in the solid state has been the subject of much attention. Early work of Zener on growth kinetics has been developed by Aaron and Aaronsson [24] for the grain boundary case and by Aaron et al [25] for intragranular precipitation. These approaches have been integrated to produce a unified description of the inter- and intra-granular nucleation and growth mechanisms by Shercliff and Ashby [26] and Carolan and Faulkner [27]. More recently, successful attempts have been made to combine models of precipitate growth at interfaces with concurrently occurring segregation in aluminium alloys [28]. Studies of the relationship between interfacial cohesive strength and structure have only recently become possible. This is due to the remarkable advances in physical examination techniques allowing direct viewing of interface structure and improved theoretical treatments of grain boundary structures.

The ability of the strengthening precipitates to support the matrix relies on the properties of the major alloying additions involved in the formation of these precipitates. The development of precipitates in Al-based alloys can be well characterised through heat treatment processing. Heat treatment affects the matrix properties and consequently the strain hardening of the composite. Furthermore, the distribution and concentration of these precipitates greatly affects the properties of the material where homogenous distribution of small precipitates provides the optimum results.

The role of the reinforcement is crucial in the micro deformation behaviour. The addition of SiC to Aluminium alloy increases the strength and results in high internal stresses, in addition to the ones caused by the strengthening precipitates. A great deal of attention has recently been devoted to understanding the strengthening mechanisms in metal matrix composites, which are distinguished by a large particulate volume fraction

and relatively large diameter. Another important matter in understanding and modelling the strength of particulate MMCs is to consider the effect of particle shape, size and clustering [29-31]. Lewandowski et al. [32] illustrated the important effects of clustering of reinforcement on the macroscopic behaviour as well as the effects of segregation to SiC/Al interfaces. Rozak et al. [33] presented the effects of casting condition and subsequent swaging on the microstructure, clustering, and properties of Al/SiC composites.

II.6 MMCs Fabrication –Processing Routes

II.6.1 Essential Requirements for any production route

Before analysing the processing routes there are some important concerns affecting the production of the composite. These are,

- The reinforcement must be distributed in a controlled manner in the metal matrix, i.e. either uniformly distributed throughout or placed in designated locations of the component.
- Minimal porosity and full density would result in the final component.
- Typically, volume fractions of 10% – 40% of reinforcement need to be incorporated in the matrix.
- Reactions at the reinforcement/matrix interface should be controlled to promote optimum bond strength and avoid reinforcement degradation.
- The reinforcement should be incorporated into the matrix without breakage. This is particularly important factor when processing continuous fibre and whisker reinforced MMCs.

- During composite joining and forming, minimal reinforcement degradation of either chemical or physical means should result. Reinforcement alignment and distribution should be maintained.
- The route should be as flexible as possible in terms of matrices and reinforcements to which it can be applied.
- The route should be capable of producing components with high degree of reproducibility at minimum product variability, minimum cost and maximum productivity.
- Highly desirable flexibility in a variety of shapes can be produced.
- Finally, any proposed process route should be amenable to scale-up.

Processing of Metal Matrix Composites can be broadly divided into three categories of fabrication techniques: Solid State-Liquid State-Vapor State Processing [34].

There is a multitude of fabrication techniques of metal matrix composites depending on whether they are aiming at continuously or discontinuously reinforced MMC production. The techniques can further be subdivided, according to whether they are primarily based on treating the metal matrix in a liquid or a solid form. The production factors have an important influence on the type of component to be produced, on the micro-structures, on the cost and the application of the MMC.

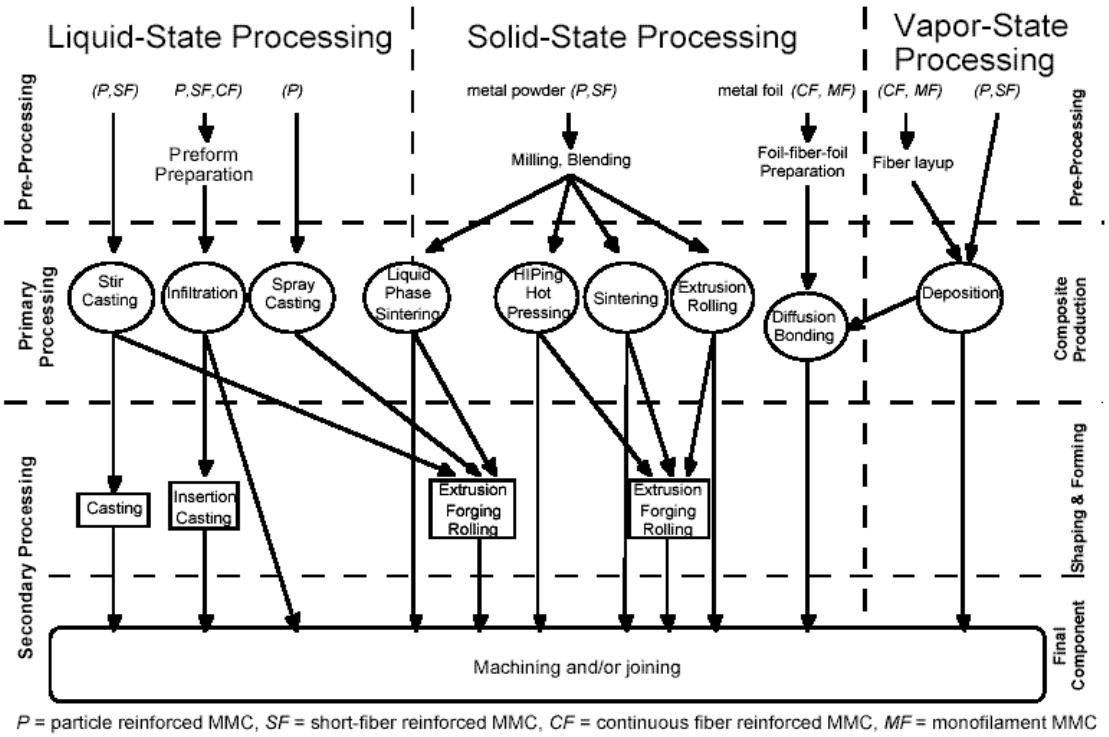

Figure II.2. Overview flow chart of MMC processing routes.

As depicted in Figure II.2, [35] processes can be classified according to whether the matrix is in the liquid, solid or vapour phase while it is being combined with the reinforcement. The individual composite production operations are briefly outlined below under these groupings.

II.7 Liquid State Processing

Liquid State processing technologies can be divided into:

- Infiltration
- Dispersion
- Spraying

II.7.1 Infiltration Process

Infiltration process (Figure II.3a, b) involves holding a porous body of reinforcing phase within a mould and infiltrating it with molten metal that flows through interstices to fill the pores and produce a composite.

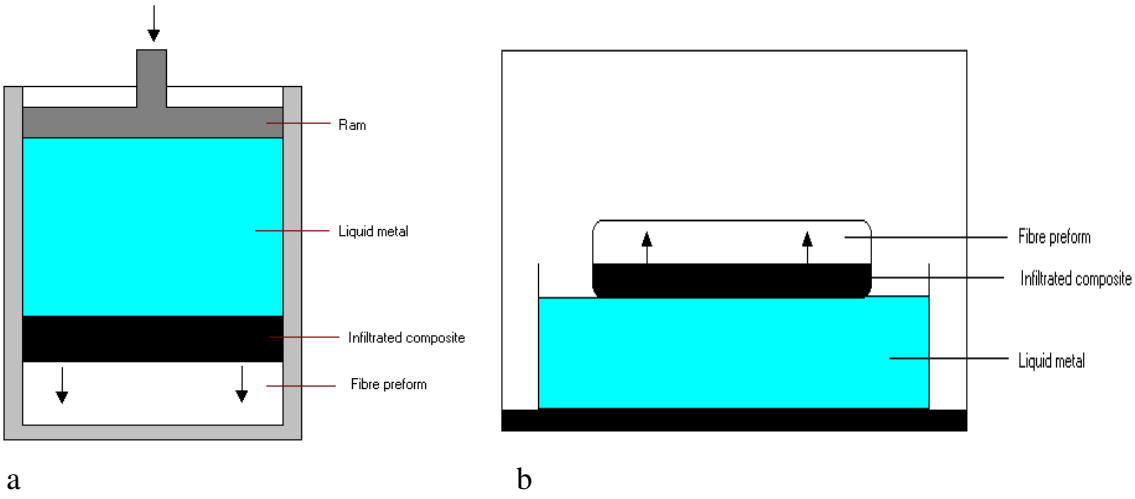

Figure II.3a, b. Infiltration process.

In infiltration, the molten metal penetrates a pretreated, formed, and prepared particulate bed or preform with pressure or without pressure (pressureless infiltration). In the latter case, however, the molten alloy infiltrates the reinforcement by percolation. This method is normally carried out in air, inert gas, or evacuated atmosphere. The preform is normally formed by pressing, slip casting, joining, or injection molding. In air or under a preferred gas, the molten alloy slips through the preform and oxidises or chemically reacts with the preform material. The final composite phases consist of the oxidation (or reaction) products and the remaining matrix material. By this method, a dense composite shape is usually achieved [36-37].

II.7.2 Stir Casting

This involves stirring the melt with solid ceramic particles and then allowing the mixture to solidify. This can usually be done using fairly conventional processing equipment and can be carried out on a continuous or semi-continuous basis. A concern is to ensure that good particle wetting occurs. Difficulties can arise from the increase in viscosity on adding particles or, especially, fibres to a melt. However, this increase is typically only by a factor of 2 or so with up to about 20 vol. % particulate, provided that the particles remain well-dispersed. This viscosity is sufficiently low to allow casting operations to be carried out. Microstructural inhomogeneities can arise, notably particle agglomeration and sedimentation in the melt. Redistribution as a result of particle pushing by an advancing solidification front can also be a problem.

This is reduced when solidification is rapid, both as a result of a refinement in the scale of the structure and because there is a critical growth velocity, above which solid particles should be enveloped rather than pushed.

Stir casting usually involves prolonged liquid-ceramic contact, which can cause substantial interfacial reaction. This has been studied in detail for Al-SiCp composites where the formation of Al_4C_3 and Si can be extensive. Therefore, the degradation of the final properties of the composite raises the slurry's viscosity leading to difficult casting. The rate of reaction is reduced, and can become zero, if the melt is Si-rich, either by prior alloying or as a result of the reaction [38-39].

II.7.2.1 MC-21 Rapid Mixing Process

The materials used in this research have been supplied by a company named MC-21. In the MC-21's stir-casting approach, the desired aluminum alloy is melted,

and carefully sized ceramic (silicon carbide or aluminum oxide) particles are stirred in by means of an efficient vacuum-assisted mixing process (Figure II.4). The process allows good wetting and a very strong bond between the ceramic particles and aluminum matrix and uses inexpensive raw materials. The equipment is flexible, relatively inexpensive, and allows the production of a broad range of MMCs containing a variety of types and volume fractions of ceramic particulate and of aluminum alloy matrices.

They have created improved mixing technology that reduces the time required for uniform incorporation of a wide range of ceramic particle reinforcement volume fractions to well under 60 minutes. Batch mixing times of this order allow the mixing to be done in “real time” in the foundry environment, enabling the concept of having a modular production unit on the foundry floor feeding molten composite to one or more casting machines to be realised. This eliminates the need for careful remelting of the melt stock currently required for MMC ingot produced by other processes, saving time, minimizing the chance for overheating and ruining of the melt, and reducing energy consumption.

Other benefits of the rapid mixing process include its demonstrated ability to produce a much wider range of reinforcement size and volume fraction combinations.

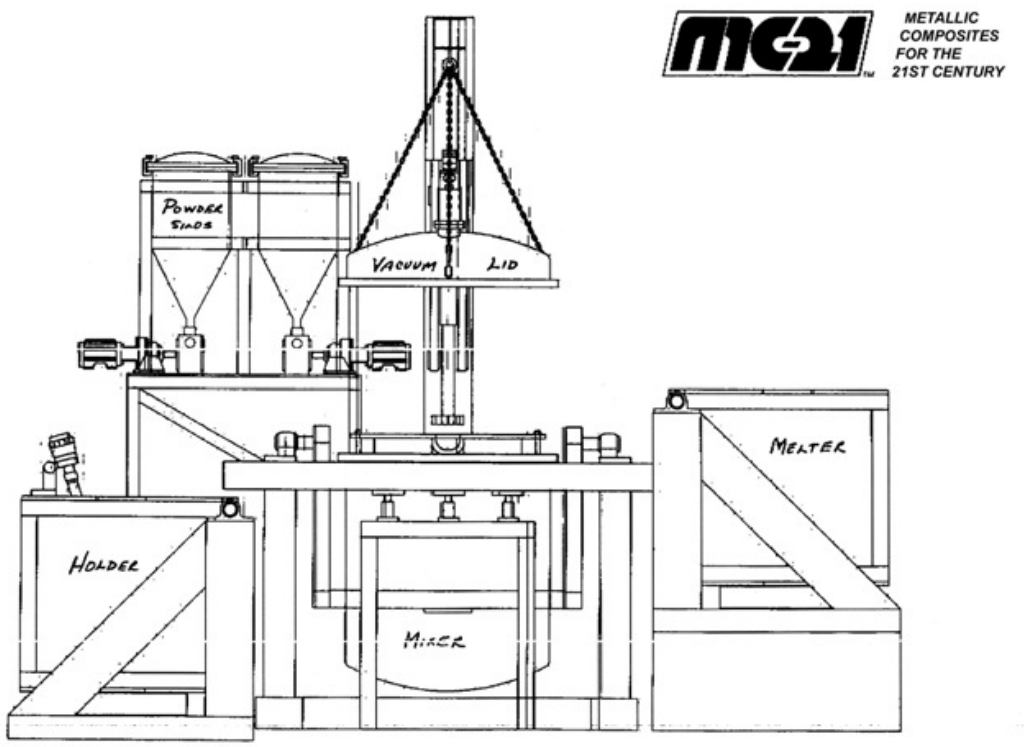

Figure II.4. A schematic drawing of the 600 kg unit is shown in the accompanying figure, illustrating the melting, mixing, and holding units that comprise a stand-alone modular unit. Also included are powder silos for containing and feeding the ceramic particle reinforcement into the mixing unit as well as a vacuum lid to seal the mixing unit.

In summary, the short process cycle time, relatively simple equipment, and ability to use low cost reinforcement materials result in an aluminum metal composite material that can be produced for on the order of $1/pound as it is ready to enter the mould [40].

II.7.3 Squeeze Infiltration

Liquid metal is injected into the interstices of an assembly of short fibres, usually called a preform. Usually, the preform is designed with a specific shape to form an integral part of a finished product in the as-cast form (Figure II.5). Preforms are

regularly fabricated by sedimentation of short fibres from liquid suspension. The process can also be adapted for production of particulate MMCs. In order for the preform to retain its integrity and shape, it is often necessary for a binder to be used. Various silica- and alumina-based mixtures have been popular as high temperature binders. The binding agent is normally introduced via the suspension liquid, so that it deposits or precipitates out on the fibres, often forming preferentially at fibre contact points, where it serves to lock the fibre array into a strong network.

The pressure required for infiltration can readily be calculated on the basis of the necessary meniscus curvature and corrections can be made for melt/fibre wetting. In practice, substantial pressures in the MPa range are likely to be needed. In most cases, fibres do not act as preferential crystal nucleation sites during melt solidification. One consequence of this is that the final liquid to freeze, which is normally solute-enriched, tends to be located around the fibres. Such prolonged fibre/melt contact, often under high hydrostatic pressure and with solute enrichment, has a tendency to favour formation of a strong interfacial bond. Other forms of defect are, however, common in squeeze infiltrated composites. These include porosity and local variations in fibre content and in average alloy composition [41].

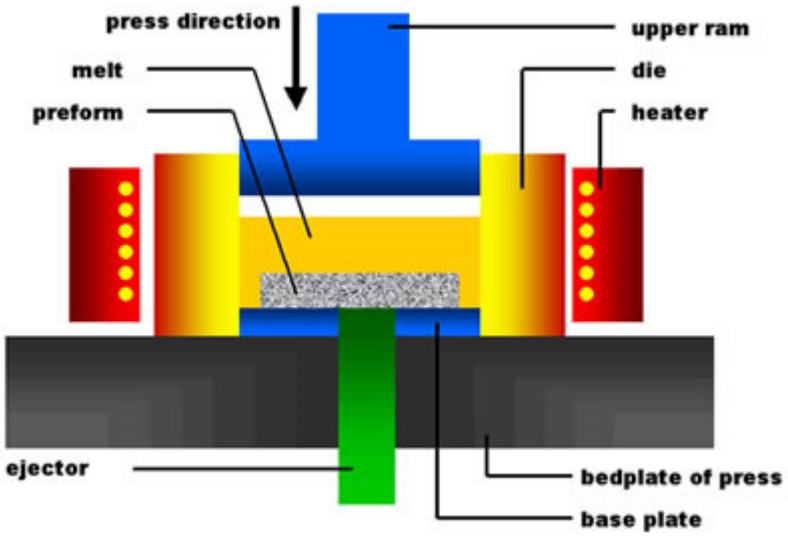

Figure II.5. Squeeze Casting.

II.7.4 Dispersion processes

In dispersion processes the reinforcement is incorporated in loose form into the metal matrix. Due to poor wetting characteristic of metal-reinforcement systems, mechanical force is required to combine these phases.

The simplest dispersion process is the Vortex method, which consists of vigorous stirring of the liquid metal and the addition of particles in the vortex. In the vortex method, the pretreated and prepared filler phase is introduced in a continuously stirred molten matrix and then cast. The use of an inert atmosphere or vacuum than air is essential to avoid the entrapment of gases. Mixing can be affected ultrasonically or by reciprocating rods, centrifuging, or zero-gravity processing that utilises an ultrahigh vacuum and high temperatures for long periods of time. A method of inertial injection has been developed for this process [42]. Difficulties, such as the segregation/settling of secondary phases in the matrix, agglomeration of ceramic particulate, particulate fracture during agitation, and extensive interfacial reactions, are often encountered [43].

However, the problems of matrix-particulate reactivity and particle-segregation effects are somewhat encountered. The vortex method seems attractive because of its ease of operation and relatively low cost. For the fabrication of MMCs by stir casting, a requirement for a good stirring unit is to provide intimate contact while minimizing gas absorption.

This installation provides a sharp dose of separated powder particles to the required point of the melt preceded by the displacement caused by the impeller (Figure II.6) [44].

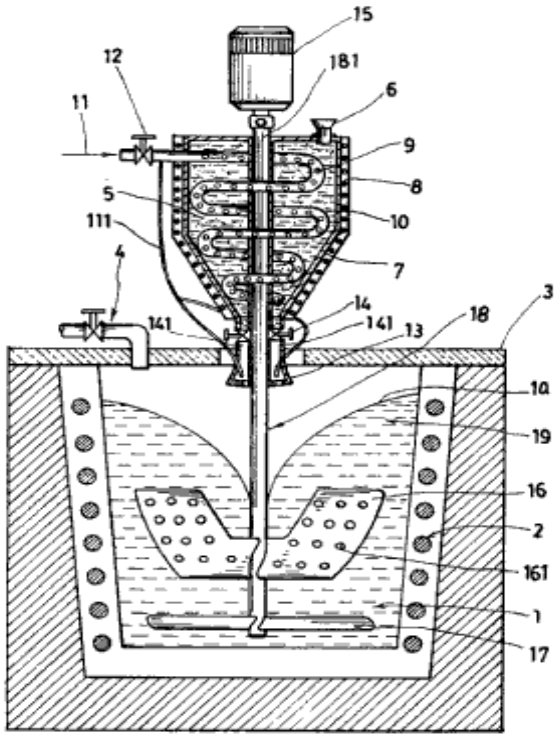

Figure II.6. Vortex method.

This is achieved through a mechanism where the powder-supply tube rotates with the impeller, and, as a result, the powder carried by the flow of inert gas always penetrates the zone of the melt with the highest turbulence. Increased particle content raises melt viscosity such that it can become non-Newtonian, but increased shear rate at rising temperatures appears to minimise the viscosity. Also, particles recovery and microstructural homogeneity in cast composites prepared with the use of a mechanical impeller have been found to depend on the stirring rate and length of time at temperature, matrix-alloy composition, physicochemical nature of the reinforcement, feed time and feed rate, and crucible-to-impeller diameter ratio.

Mixing of particles and metal can also be achieved while the alloyed metal is kept between solidus and liquidus temperature. This process is known as Compocasting or Rheocasting. The advantage of using semi-solid metal is the increase in the apparent viscosity of the slurry. This process permits the introduction of the pretreated particulate or short fibres into the solidifying, highly viscous, and thixotropic dendritic slurry of the

molten matrix by agitation. This mechanically entraps the ceramic reinforcements and prevents any form of segregation. Continued stirring then reduces the viscous mass to low-viscous, fine, nondendritic slurry. This results in a mutual interaction between the matrix melt and the filler phase, which enhances wetting and bonding between the two phases. Pressure is usually used to affect a sound casting, especially when the volume fraction (Vf) of the particulate material is greater than 0.3 or 0.15, in the case of short fibres. This is because the composite viscosities increase as Vf increases, which is limiting at lower volume fractions. Fibre damage/degradation due to vigorous agitation is another difficulty. Owing to these effects, rheocasting lends itself only to particulate composites with a very low Vf of low to medium density particulates. A fundamental characteristic of this technique is that the matrix alloy is isothermally held within the freezing range of the alloy and, together with the reinforcement, is mechanically stirred. Stirring and agitation help to break the solid phases into smaller forms, releasing any particulate clusters that also break down in the process. New particle-matrix bonding can then take place, through which particulate agglomeration and gravity-induced settling is eliminated.

Another method to mix semi-solid metal and particulates is the Thixomoulding process, whereby metal pellets and particles are extruded through an injection moulding apparatus. Critical to the success of dispersion processes is the control over generally undesirable features such as porosity resulting from gas entrapment during mixing, oxide inclusions, reaction between reinforcement and metal matrix, particle migration and clustering during and after mixing [43-44].

II.8 Spray Atomisation/Codeposition

Spray Disposition (SD) is gaining recognition in the synthesis of discontinuously reinforced MMCs. [45]. The process involves the incorporation of fine ceramic particulates in inert-gas-atomized droplets of the molten matrix such that the matrix contains both liquid and solid phases. The matrix material is usually finely dispersed in droplets by the high-velocity spray of the inert-gas jets.

The materials and structural-design advantage of this process is that desired multiphase matrix materials or discontinuous reinforcement, while entrained in a gas jet, could be incorporated at a localized portion. Unwanted reactions are avoided because the contact time and the thermal exposure between the particulate and the partially solidified matrix phases are reduced.

II.8.1 Spray Processes

In these processes droplets of molten metal are sprayed together with the reinforcing phase and collected on a substrate where metal solidification is completed. Alternatively the reinforcement may be placed on the substrate and molten metal may be sprayed onto it. The critical parameters in spray processing are the initial temperature, size distribution and velocity of the metal drops, the velocity, temperature and feeding rate of the reinforcement. Most spray deposition processes use gases to atomise the molten metal into fine droplets. The particles can be injected within the droplet stream or between the liquid stream and the atomising gas. The advantage of spray deposition techniques resides in the resulting matrix microstructure that features fine grain size and low segregation. One of the drawbacks of the process is the amount of residual porosity and the resulting need to further process the materials.

Spray deposition techniques fall into two distinct classes, depending whether the droplet stream is produced from a molten bath, or by continuous feeding of cold metal into a zone of rapid heat injection. The process was developed for building up bulk metallic material by directing an atomised stream of droplets onto a substrate. Adaptation to particulate MMC production by injection of ceramic powder into the spray has been extensively explored, although with limited commercial success. Droplet velocities typically average about 20-40 m s-1. A thin layer of liquid, or semi-solid, is often present on the top of the ingot as it forms. MMC material produced in this way often exhibits inhomogeneous distributions of ceramic particles. Ceramic-rich layers approximately normal to the overall growth direction are often seen. This may be the result of hydrodynamic instabilities in the powder injection and flight patterns or possibly to the repeated pushing of particles by the advancing solidification front in the liquid or semi-solid layer, until the ceramic content is too high for this to continue. Porosity in the as-sprayed state is typically about 5-10% [46].

Thermal spraying differs in several respects from melt atomization processes. Deposition rates (usually ~ 1 g s-1) are slower, but particle velocities (~50-400 m s-1) are higher. Quenching rates for each individual splat can be very high (~106 K s-1). Porosity levels are typically at least a few %. Thermal spraying onto arrays of fibres to form MMCs has received some attention. An attraction here is the possibility of producing composite material in an operation involving only very brief exposure to high temperatures. Provided the void content and distribution are such that full consolidation could be effected with little further heat treatment, this would allow problems of excessive fibre/matrix chemical reaction during processing to be avoided - a particularly important objective for Ti-based MMCs. Unfortunately, it has proved very difficult to spray onto fibre arrays so as to produce MMCs with acceptably low void contents and there are also problems in maintaining a uniform fibre distribution.

II.9 Solid State Processing

Solid State processes are generally used to obtain the highest mechanical properties in MMCs, particularly in discontinuous MMCs. Because segregation effects and brittle reaction product formation are at a minimum for these processes, especially when compared with liquid-state processes powder metallurgy is the most common method for fabricating metal – metal composites. With the advent of rapid solidification technology, the matrix alloy is produced in a prealloyed powder form rather than starting from elemental blends. After blending the powder with particulate reinforcements, cold isostatic pressing is utilised to obtain a green compact that is then thoroughly degassed and forged or extruded [47].

In some cases hot isostatic pressing of the powder blend is required, prior to which complete degrassing is essential. Consolidation of matrix powder with ceramic fibres has also been achieved but the difficulties encountered when attempting to maintain uniform fibre spacing. Although, powder based routes for MMC production tend to be more expensive than liquid based routes and therefore generally occupy the more specialist high cost markets for MMCs [48].

II.9.1 Powder Metallurgy

P/M is used in the synthesis of both AMCs and ceramic-matrix composites through the relatively low-cost methods of single compaction, double compaction, and mechanical deformation following hot pressing as well as through high-cost hydrostatic and isostatic compaction, hot dynamic compaction, or explosive compaction methods. P/M involves the blending of well-characterized matrix powders and discontinuous reinforcement, compaction at ambient or hot conditions, degassing, and consolidation.

In these solid-state techniques, subfusion temperature regimes are normally attained in consolidation for optimum results. Depending on the morphology of the reinforcement or the desirable properties, further processing by mechanical-deformation mechanisms is applied [49].

II.10 Characteristics – Mechanical Properties

II.10.1 MMC Properties

Properties for MMCs depend on the matrix metal and the volume percent of composite reinforcement, which are optimised for specific applications. The superior mechanical properties of MMCs drive their use. An important characteristic of MMCs, however, and one they share with other composites, is that by appropriate selection of matrix materials, reinforcements, and layer orientations, it is possible to tailor the properties of a component to meet the needs of a specific design. For example, within broad limits, it is possible to specify strength and stiffness in one direction, coefficient of expansion in another, and so forth. This is rarely possible with monolithic materials. Monolithic metals tend to be isotropic, that is, to have the same properties in all directions. Some processes such as rolling, however, can impart anisotropy, so that properties vary with direction. The stress-strain behavior of monolithic metals is typically elastic-plastic. Most structural metals have considerable ductility and fracture toughness. The wide variety of MMCs has properties that differ dramatically. Factors influencing their characteristics include [50]:

- Reinforcement properties, form, and geometric arrangement
- Reinforcement volume fraction

- Matrix properties, including effects of porosity
- Reinforcement-matrix interface properties
- Residual stresses arising from the thermal and mechanical history of the composite
- Possible degradation of the reinforcement resulting from chemical reactions at high temperatures, and mechanical damage from processing, impact, etc.

Particulate-reinforced MMCs, like monolithic metals, tend to be isotropic. The presence of brittle reinforcements and perhaps of metal oxides, however, tends to reduce their ductility and fracture toughness. Continuing development may reduce some of these deficiencies [51].

Another factor that has a significant effect on the behavior of particulate-reinforced metals is the frequently large difference in coefficient of expansion between the two constituents. This can cause large residual stresses in composites when they are subjected to significant temperature changes. In fact, during cool down from processing temperatures, matrix thermal stresses are often severe enough to cause yielding. Large residual stresses can also be produced by mechanical loading.

II.10.2 Fracture Mechanics of Composites

Fracture mechanics provides a methodology evaluating the structural integrity of components containing such defects, and demonstrating whether they are capable of continued, safe operation. The basic criterion in any fracture mechanics analysis is to prevent failure. To do so, the crack driving force must be less than the material resistance to cracking [52].

The complexity of fracture behaviour of metal matrix composites can greatly complicate the application of the fracture mechanics methods. Nevertheless, some useful generalisations can be made. The order of sections is the following: description

of macro mechanism, definition of damage parameters, driving force and analysis of engineering approaches.

For fibre composites the damage parameters are fractions of fibre breaking, delamination and volume eliminated from the carrying system. The mechanism of fracture is step-by-step enlargement of the damaged zone. The governing parameter of the stress-strain-damage state of the composite is one of energy characteristics and/or nominal strain. The engineering approach can yield the critical strain value and, consequently, the critical stress value.

Damages of components in particulate reinforced composites are sufficiently different. Brittleness and plasticity of the components affect the fracture mechanisms and strength parameters of the composites. In large-scale composite structures microdamages may reduce rigidity over certain zone, enlarge further the area and lead to a macrocrack growth. Energy parameters for the damaged zone define the moment of full-scale fracture initiation. The engineering approaches use S-N curves.

II.10.3 Fracture Toughness

Fracture toughness is a material property and indicates the amount of stress required to propagate a preexisting flaw. It is a very important material property since the occurrence of flaws is not completely avoidable in the processing, fabrication, or service of a material/component. Flaws may appear as cracks, voids, metallurgical inclusions, weld defects, design discontinuities, or some combination thereof. Since engineers can never be totally sure that a material is flaw free, it is common practice to assume that a flaw of some chosen size will be present in some number of components and use the linear elastic fracture mechanics (LEFM) approach to design critical components. This approach uses the flaw size and features, component geometry,

loading conditions and the material property called fracture toughness to evaluate the ability of a component containing a flaw to resist fracture.

A parameter called the stress-intensity factor (K) is used to determine the fracture toughness of most materials. A Roman numeral subscript indicates the mode of fracture and the three modes of fracture are illustrated in Figure II.7. Mode I fracture is the condition in which the crack plane is normal to the direction of largest tensile loading. This is the most commonly encountered mode and, therefore, for the remainder of the material we will consider K_I [53].

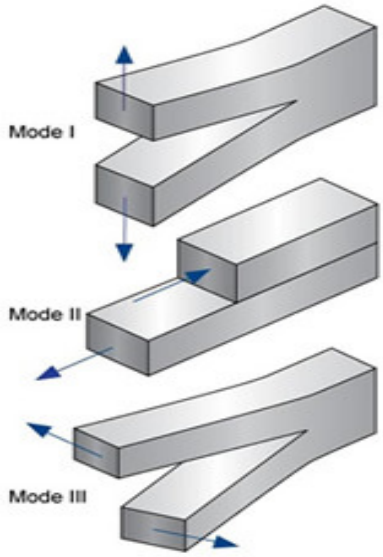

Figure II.7. The three modes of fracture.

The stress intensity factor is a function of loading, crack size, and structural geometry. The stress intensity factor may be represented by the following equation II.1:

$$K_I = \sigma\sqrt{\pi a \beta} \qquad \text{II.1}$$

II.11 MMCs Applications

To date, much of the research has focused on the high-performance lightweight needs of the aerospace industry, where the unique requirements of the defense and advanced research organisations render cost a minor factor and reductions in structural weight are affected by reducing the alloy density and increasing its modulus.

Metal-matrix composites are either in use or prototyping for the Space Shuttle, commercial airliners, electronic substrates, bicycles, automobiles, golf clubs, engine blocks, pistons, brake-system components, seals, solid lubricants, wear- and abrasion-resistant structures, electromechanic contacts, chassis components and a variety of other application. While the vast majorities are aluminum matrix composites, a growing number of applications require the matrix properties of superalloys, titanium, copper, magnesium, or iron [22].

Aluminum MMCs are produced by casting, powder metallurgy, in situ development of reinforcements, and foil-and-fibre pressing techniques. Consistently high-quality products are now available in large quantities, with major producers scaling up production and reducing prices. They are applied in brake rotors, pistons, and other automotive components, as well as, machinery components, extruded angles and channels, and a wide variety of other structural and electronic applications. Some of the major MMCs applications used are described as follows:

- Military tank track shoes – Under sponsorship of the U.S. Army Tank-automotive and Armaments Command (TACOM), Al MMC track shoes are being developed for military land and amphibious tracked vehicles. Using selective reinforcement SiC whisker technology weight savings of up to 25% are being realized over the existing forged steel track shoes, which weigh nearly three tons per set.

- Aerospace structures – Lightweight, near-net shape Al MMCs are being developed for critical missile support structures to replace higher-cost, heavily machined titanium. Al MMC SiCw's low CTE and high modulus make it an acceptable alternative to titanium for use in the demanding aerodynamic environment [54] (Figure II.8).

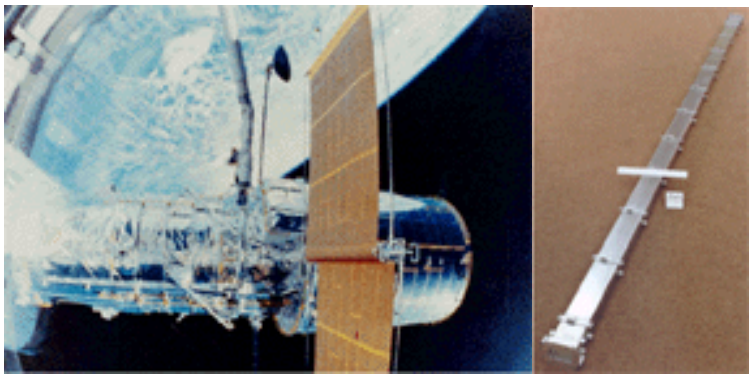

Figure II.8. The P100/6061 Al high-gain antenna wave guides/ boom for the Hubble Space Telescope (HST) shown (a-left) before integration in the HST, and (b-right) on the HST as it is deployed in low-earth orbit from the space shuttle orbiter.

- Electronic substrates – SiC particulate aluminum MMCs are being used in electronic substrate applications, where the MMC serves as the heat sink for a silicon device. The MMC has a coefficient of thermal expansion (CTE) closer to that of silicon, reducing the stresses that lead to device cracking or debonding, and offers high thermal conductivity for enhanced heat dissipation [55] (Figure II.9).

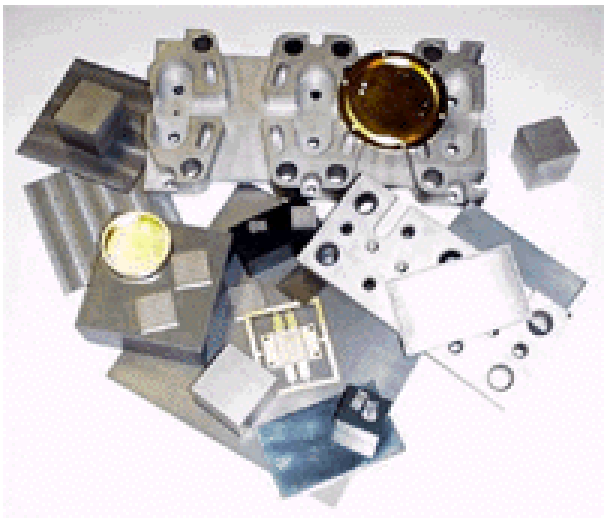

Figure II.9. Discontinuously reinforced aluminum MMCs for electronic packaging applications: (a-top) SiCp/Al electronic package for a remote power controller (photo courtesy of Lockheed Martin Corporation), and (b-bottom) cast Grp/Al components (photo courtesy of MMCC, Inc.).

- Pistons – Use of Al MMC in the dome region enables operation at higher cylinder firing pressures, particularly important in advanced high performance gas and diesel engines. The ability to selectively reinforce areas such as the ring belt can reduce wear rate and noxious emissions with no penalty in reciprocating mass [56].
- Cylinder liners – Selective reinforcement of the cylinder bore for cast aluminum engines would provide superior thermal conductivity and durability performance compared to traditional cast iron liners. Blending of SiCw with a secondary reinforcement of nickel powder or graphite could also improve sliding characteristics.
- Disk brake rotors – SiC particulate has been used for homogeneous reinforcement of the rotor. Activities are ongoing to further improve wear characteristics using fibre and whisker preform technology.

- Driveshafts and torque tubes – Use of MMCs for driveshafts and other components responsible for transfer of torque enable them to be lighter and stiffer. MMC driveshafts also reduce noise resulting from vibration.
- Recreational and sports – Bicycles, golf clubs and racing horseshoes are among the "recreational and sports" applications for MMCs. Applications for these categories are driven by their light weight and wear resistance features.

II.12 MMCs Market Barriers

During the past decades, there have been many changes in the industry and shifts in priorities. In the early 1990s, it was forecast that defense/aerospace applications would account for approximately 80% of the metal matrix composite market in 2000. While the military aerospace market remains an important target for metal matrix composites, opportunities have emerged in other industries. The push for better fuel economy and lighter vehicles has opened the door to expanded usage of metal matrix composites in automobiles. Ever higher performance, heat-generating computer chips have elicited increasing interest in thermal management applications for metal matrix composites.

As a small yet strategic global market, MMCs are a critical and essential element in many advanced technologies. The present state of the MMC business, however, is changing. A global recession and September 11 particularly affected commercial aerospace and other end-use markets for MMCs, and led to diminished demand. At the same time, new entrants and expansions by existing producers resulted in additional capacity. In turn, this led to lower operating rates for many producers, and a more competitive market, and pricing pressures. These "drivers" will continue.

Use of MMCs has recovered and in the long term will continue expand, as a result of technological advancements, both in the area of new methods for producing MMCs, as well as in evaluating MMCs various applications. With the rapid changes in the industry structure and in the accelerated rise of new, expanding applications, a technology/marketing report update with a unified view of materials and applications is needed.

In addition, realistic market data (including time series) for MMCs have proven elusive, especially on a global basis. Because product innovation is important, the industry is relatively secretive, with no central reporting organization as is found in the plastic resins and textile fibres. A paucity of company information also exists as many companies either are small privately held organizations, or if part of a larger company, represent a relatively small part of the operations and are usually integrated into the final product organization [57].

II.13 Limitations to Wide MMC Acceptance

It is worth considering the limitations that may hamper the full commercialisation of metal composites. The gap between the materials experts' knowledge of the performance of new material and real engineering application must be bridged. This would involve in helping the engineering community to design MMCs by providing property data, covering key aspects of performance and apply appropriate processing techniques (e.g. forming, machining, joining etc).

Chapter III – Microstructure and matrix/particle interface of SiC particulate reinforced A359 aluminium alloy Composites

The microstructure of the Silicon carbide particulate reinforced aluminium alloy composites is discussed in this Chapter. The modification of the microstructure is achieved by the appropriate heat treatment processing, whereas segregation and precipitation phenomena are affecting the microstructure and the interfacial strength. Observations of these strengthening mechanisms are demonstrated and analysed through advanced microscopy and other techniques discussed in detail. The tailoring of the interfacial properties of the composites is examined and as a result the enhancement of the composites mechanical properties could be achieved.

III.1 Introduction to Al/SiCp Composites

Silicon carbide particulate reinforced aluminium alloy composites are engineering materials with great prospects for a variety of structural applications, due to their superior strength, stiffness, low cycle fatigue and corrosion fatigue behaviour, creep and wear resistance, compared to the aluminium monolithic alloys.

An important feature of the microstructure in the Al/SiC composite system is the increased amount of thermal residual stresses, compared to unreinforced alloys, which are developed due to mismatch in thermal expansion coefficients of matrix and reinforcement phases. The introduction of the reinforcement plays a key role in both the mechanical and thermal ageing behaviour of the composite material. Micro-

compositional changes which occur during the thermo-mechanical forming process of these materials can cause substantial changes in mechanical properties, such as ductility, fracture toughness and stress corrosion resistance.

Particulate-reinforced composites are not homogeneous materials; hence bulk material properties not only are sensitive to the constituent properties, but also strongly depended on the properties of the interface. The strength of particulate-reinforced composites depends on the size of the particles, interparticle spacing, and the volume fraction of the reinforcement [58].

In the case of particulate-reinforced aluminium composites, the microstructure and mechanical properties can be altered by thermo-mechanical treatment as well as by varying the reinforcement volume fraction. The strengthening of monolithic metallic material is carried out by alloying and supersaturating, to an extent, that on suitable heat treatment the excess alloying additions precipitates out (ageing).

III.2 Precipitation Hardening

Properties in particulate-reinforced aluminium matrix composites are primarily dictated by the uniformity of the second-phase dispersion in the matrix. The distribution is controlled by solidification and can be later modified during secondary processing. In particular, due to the addition of magnesium in the A359 alloy, the mechanical properties of this material can be greatly improved by heat treatment process. Furthermore, the A359 alloy composite contain an excess of Si required to form stoichiometric Mg_2Si precipitates. There are many different heat treatment sequences and each one can modify the microstructural behaviour as desired [59]. Precipitation

heat treatments generally are low temperature, long-term processes with ageing temperatures ranging from 110°C to 195°C for 5 to 48 hours.

The selection of the time temperature cycles for precipitation heat treatment should receive careful consideration. Larger precipitate particulates result from longer times and higher temperatures. On the other hand, the desired number of larger particles formed in the material in relation to their interparticle spacing is a crucial factor for optimising the strengthening behaviour of the composite. The objective is to select the heat treatment cycle that produces the most favourable precipitate size and distribution pattern [60].

III.3 Segregation

The satisfactory performance of metal matrix composites depends critically on their integrity, the heart of which is the quality of the matrix-reinforcement interface. The nature of the interface depends in turn on the processing of the MMC component. At the micro-level, the development of local concentration gradients around the reinforcement can be very different to the nominal conditions. The latter is due to the metal matrix attempt to deform during processing. This plays a crucial role in the micro-structural events of segregation and precipitation at the matrix-reinforcement interface. Equilibrium segregation occurs as a result of impurity atoms relaxing in disordered sites found at interfaces such as grain boundaries whereas, non-equilibrium segregation arises because of imbalances in point defect concentrations set up around interfaces during non-equilibrium heat treatment processing.

III.4 Heat treatment processing

The microstructural modification of particulate metal matrix composites is primarily affected by the uniformity of the second-phase dispersion in the matrix. The mechanical properties are also influenced by the heat treatment processing.

The important factors affecting the heat treatment process are the temperature, the cooling rate, the concentration of solute atoms and the binding energy between solute atoms and vacancies.

A good bond can be formed by proper and adequate interaction between the reinforcement and the matrix. Inadequate interaction results in lack of proper bonding, whereas excessive interaction leads to the loss of the desired properties and inferior performance of the MMC. The thermal conditions for this reaction depend on the composition of the MMC and its processing method. As the reaction progresses, the activity of silicon in liquid aluminium increases and the reaction tends to saturate. The presence of free silicon in an aluminium alloy has been shown to inhibit the formation of Al_4C_3. Temperature control is extremely important during the fabrication process. If the melt temperature of SiC/Al composite materials rises above a critical value, Al_4C_3 is formed, increasing the viscosity of the molten material, which can result in severe loss of corrosion resistance and degradation of mechanical properties in the cast composite; excessive formation of Al_4C_3 make the melt unsuitable for casting.

Heat treatment of composites though has another aspect to consider, which is the particles introduced that may alter the alloys surface characteristics and increase the surface energies. The process variables affecting the dispersion of the particulate is very important, including temperature and time of heat treatment of the particles, particle size and shape, melt temperature at the introduction of the particulate, feed rate of the particulate, volume percent of the dispersoid and melt degassing [62].

One of the most used heat treatments for the specific composite, T6 heat treatment consists of the following steps: solution heat treatment, quench and age hardening. In the solution heat treatment, the alloy is heated to a temperature just below the initial melting point of the alloy, where all the solute atoms are allowed to dissolve to form a single phase solid solution. The alloy is then quenched to room temperature at a rate sufficient to inhibit the formation of Mg-Si precipitates, resulting in a non-equilibrium solid solution which is supersaturated. In age hardening, the alloy is heated to an intermediate temperature where nucleation and growth of the Mg-Si precipitates can occur. The precipitate phase nucleates within grains and at grain boundaries, as uniformly dispersed particles. The holding time plays the key role in promoting precipitation and growth which results in higher mechanical deformation response of the composite. The material is then cooled to room temperature, where it may receive further processing.

It is known that molten aluminium does not wet silicon carbide readily, which is one of the major concerns which needs to be overcome to prevent silicon carbide particles being displaced from molten aluminium and to ensure Al/SiC bonding. In addition, as mentioned, heating above a critical temperature can lead to the undesirable formation of Al_4C_3 flakes. MC-21, Inc. patented melt stirring, a method of satisfying these requirements and producing high quality composites. SiC particulates are added to Al-Si casting alloys, where Si in the alloy slows down the formation of Al_4C_3. The process yields material with a uniform distribution of particles in a 95-98% dense aluminium matrix. The rapid solidification, inherent in the process, ensures minimal reaction between reinforcing material and the matrix [63].

III.4.1 T6 and HT1 Heat Treatments

There were two different heat treatments used in this research work; T6 and modified-T6 (HT-1) [59]. The T6 heat treatment process consists of the following steps: solution heat treatment, quench and age hardening (Figure III.1). In the solution heat treatment, the alloys have been heated to a temperature just below the initial melting point of the alloy for 2 hours at 530±5 ºC where all the solute atoms are allowed to dissolve to form a single-phase solid solution then quenched in water. Next, the composites were heated to a temperature of 155 ºC for 5 hours then cooled in air. The second heat treatment process was the HT-1 heat treatment, where the alloys in the solution treatment were heated to a temperature lower than the T6 heat treatment, at 450±5 ºC for 1 hour, and then quenched in water. Subsequently, the alloys were heated to an intermediate temperature of 170 ºC for 24 hours in the age hardened stage and then cooled in air (Figure III.2).

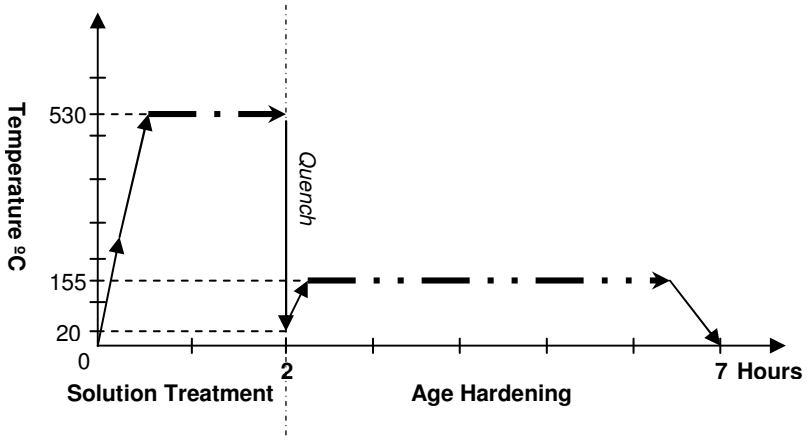

Figure III.1. T6 Heat treatment diagram showing the stages of the solution treatment for 2 hours and artificial ageing for 5 hours.

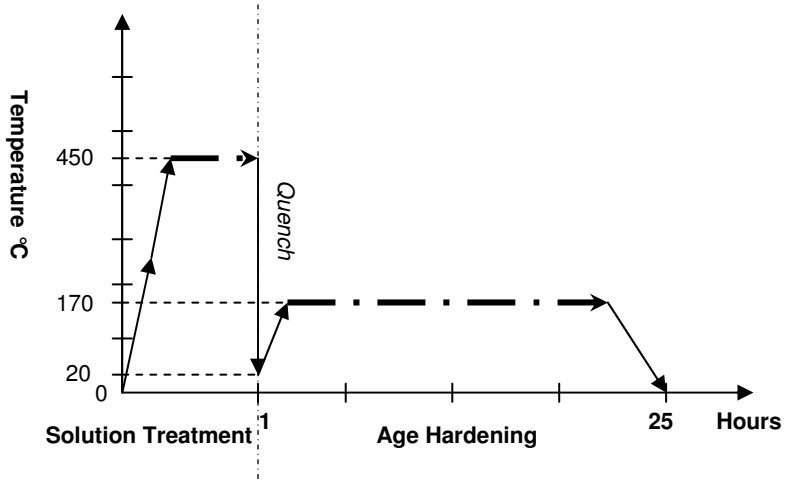

Figure III.2. HT-1 showing stages of solution treatment for 1 hour and artificial ageing for 24 hours.

III.5 Materials

The metal matrix composites studied were aluminium – silicon – magnesium alloy matrix (A359) reinforced with varying amounts of silicon carbide particles. Aluminium alloys A359 are important materials in many industrial applications, including aerospace and automotive applications.

For the investigation, four types of material were used: 1) Ingot as received A359/40%SiC, with an average particle size of 19±1 micron, 2) Ingot as received A359/25%SiC, with an average particle size of 17±1 micron, 3) Hot rolled as received A359/31%SiC with an average particle size of 17±1 micron, 4) Hot rolled as received A359/20%SiC with an average particle size of 17±1 micron and 5) Cast alloy as received A359/30%SiC with an average particle size of 17±1 micron. All the above mentioned materials have been thermally modified by the two heat treatments discussed in III.4.1 section. Table III.1, contains the details of the chemical composition of the matrix alloy as well as the amount of silicon carbide particles in the metal matrix

composites according to the manufacturer [63]. The alloys from the Al-Si-Mg system are the most widely used in the foundry industry thanks to their good castability and high strength to weight ratio.

TYPES	Si	Mg	Mn	Cu	Fe	Zn	SiC
INGOT A359	9.5	0.5	0.1	0.2	0.2	0.1	40
INGOT A359	9.5	0.5	0.1	0.2	0.2	0.1	25
CAST A359	9.5	0.5	0.1	0.2	0.2	0.1	30
ROLLED A359	9.5	0.5	0.1	0.2	0.2	0.1	31
ROLLED A359	9.5	0.5	0.1	0.2	0.2	0.1	20

Table III.1. The chemical composition of the matrix alloy and the amount of SiCp.

The above mentioned composites were used for this work according to the experiment that was performed. The ingot and cast type of composites were used for the metallographic, microhardness and microstructural investigation. The hot rolled type of composite was used mainly for mechanical testing experiments due to the fact that coupons could be easily produced form the raw material without much machining processing (cutting), whereas machining coupons coming from the ingot or cast raw material was difficult.

The materials used were kindly supplied by MC-21, Inc located in Carson City, NV, USA, which developed, patented, and demonstrated at commercial scale a proprietary process improvement that achieves much greater efficiency in the mixing operation (Figure III.2a, Figure III.2b). This increased efficiency allows SiC particles to be mixed into molten aluminium much more rapidly. This rapid mixing process is discussed in detail in section II.6.2.1. In addition, lower cost SiC particles possessing

wider size distributions could be used and higher amounts of SiC particles included into the molten mixture, up to 45 vol. % SiC could be achieved.

2(a) 2(b)

Figure III.2. MC-21 MMC fabrication setup. (a) MMC mixer. (b) MMC holding furnace.

The benefits of the rapid mixing process developed by MC-21, Inc. include its demonstrated ability to produce a much wider range of reinforcement size and volume fraction combinations. For example, materials with twice the stiffness of aluminium at comparable density greatly reduced thermal expansion coefficient and orders of magnitude improvement in wear resistance are achievable in the higher reinforcement volume fraction composites.

III.6 Microstructure of Al/SiCp

The microstructure of such materials consists of a major phase, aluminium or silicon and the eutectic mixture of these two elements. In this system, each element plays a role in the material's overall behaviour. In particular, Si improves the fluidity of Al and also Si particles are hard and improve the wear resistance of Al. By adding Mg, Al – Si alloy become age hardenable through the precipitation of Mg_2Si particulates.

One can refer to article by Strangwood et al. [64] that quantifies the segregation to Al /SiC interfaces using TEM and in-situ analyses to show Mg segregation to interfaces.

An additional advantage of Al-Si alloys for casting applications is that Si expands on solidification. Silicon and magnesium are often added in balance to form the quasi-binary Al-Mg_2Si, although sometimes Si is added in excess of that needed to form Mg_2Si. The phase diagram of the Al-Si system in Figure III.3 [65] shows a eutectic with some solubility of Si in Al, but negligible solubility of Al in Si. The precipitation sequence is supersaturated solid solution → GP zones → β´ → β (Mg2Si). The GP zones are needled-shaped along the aluminium matrix and the β´ phase is rod-shaped along the matrix. The equilibrium phase β is face centered cubic and forms platelets on the matrix [66].

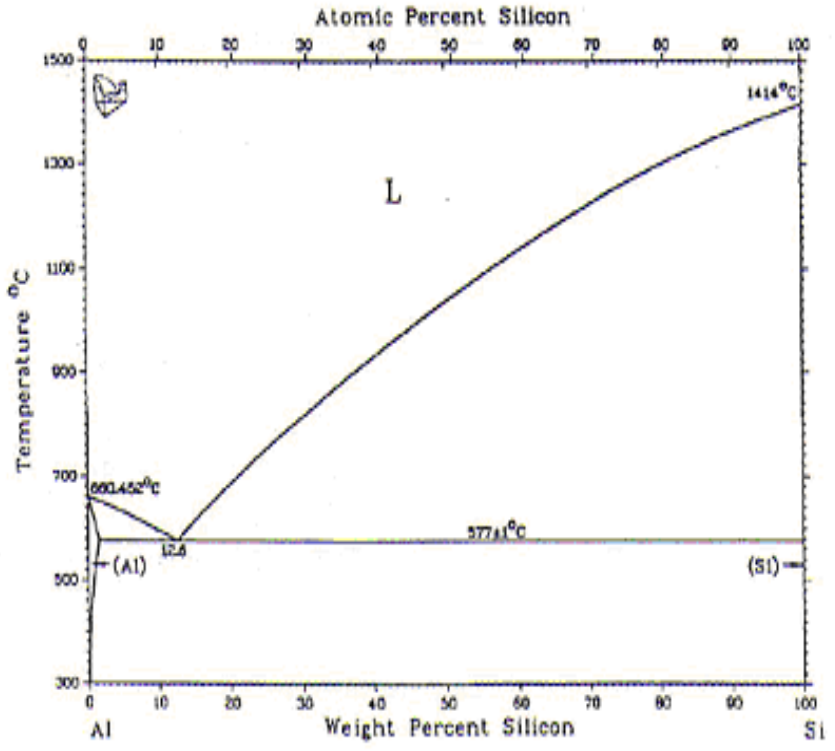

Figure III.3. The phase diagram of the Al–Si system shows an eutectic with some solubility of Si in Al, but negligible solubility of Al in Si.

III.6.1 Metallographic Examination

In order to analyse the microstructure, a series of sample preparation exercises were carried out, consisted of the cutting, mounting, grinding and polishing of the samples. The microstructures were investigated by using an optical microscope Leica DM 4000M, image analysis software, a Philips XL40 Scanning Electron Microscope with a link 860 EDAX, a Philips FEI Nova Nano – Scanning Electron Microscope, a Philips X-ray fluorescence spectrometry (XRF) and X-ray diffraction (XRD) techniques with a link to Philips X'Pert High Scores software 2000. Furthermore, the microhardness was determined by a Mitutoyo Muk-H1 Hardness tester.

In particular, Struers Accutom-5 was used to cut the specimens in the desired size, a Struers SpeciFix-20, epoxy cold mounting system was used to mount the specimens in order to prevent thermal damages of the mounting specimen and also a Struers RotoPol-25 grinding machine was used for the grinding and polishing operations. The grinding was performed with Struers Silicon Carbide grinding papers with water lubrication. This grinding was done manually and light pressure was applied. This was followed by polishing, using the DP-Dac polishing cloth with DialPro Dac stable diamond suspension containing a mixture of diamonds and cooling lubricant with 6, 3 and 1 μm particulate size. Furthermore, Colloidal Silica was used for the final polishing to ensure an optimum surface [61].

III.6.2 SEM (Scanning Electron Microscopy) -EDAX-Mapping

Microstructural Analysis

III.6.2.1 T1 Condition

The microstructures were investigated by SEM, EDAX, XRD and image analysis pro software, to determine the Al/SiC area percentage, size and count of particulates. The area percentage of SiC was measured as the area of a particular microstructure image, divided by the area of the SiC represented in that image, by using the autobeam feature of the SEM microscope (Figure III.4).

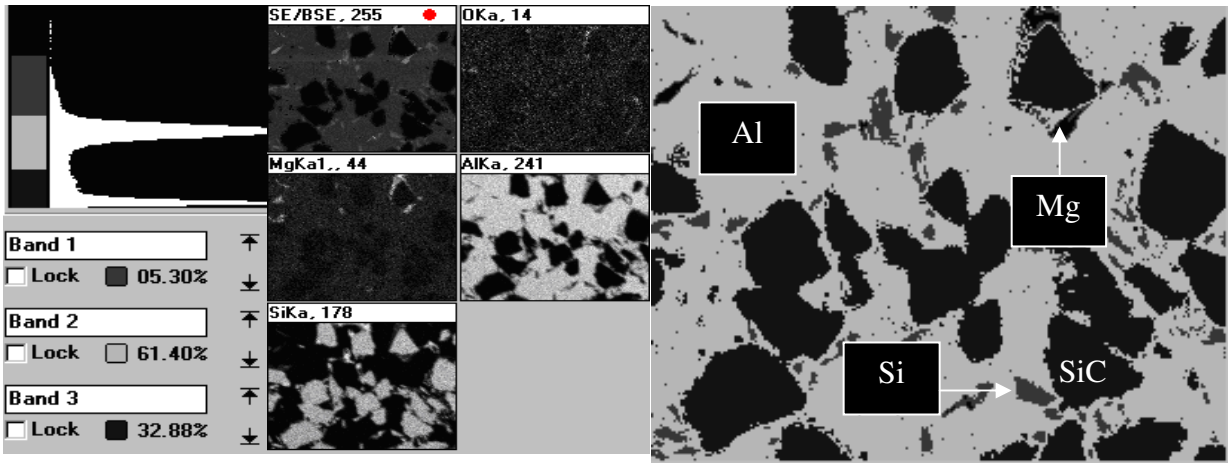

Figure III.4. SEM-Mapping Analysis of Cast A359/30%SiC microstructure showing four distinct phases-Al, Sic, Silicon and Magnesium

The results show the existence of Aluminium, Silicon Carbide, Silicon, Magnesium as well as a small percentage of Oxygen phases. Apart from the major elements, traces of Fe, Mn, Zn, and Cu were also identified (Figure III.5a). By using EDAX technique and quantitative analysis, percentages of the alloying elements were also obtained and found similar to the manufacturers' values (see Table III.1) and (Figure III.5b).

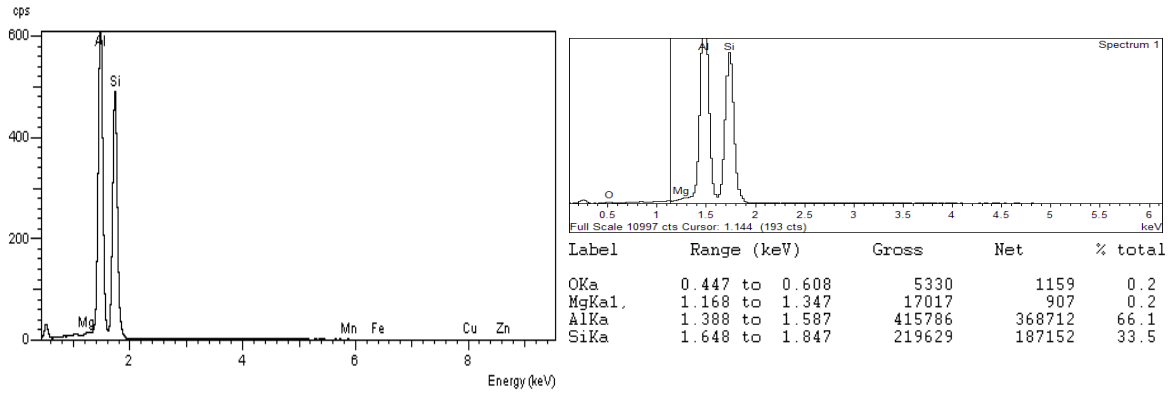

(a) (b)

Figure III.5a. Hot Rolled A359/31%SiC - EDAX Analysis showing traces of Mn, Fe, Cu and Zn identified. Figure III.5b. EDAX- Ingot A359/25% SiC elemental quantitative analysis showing percentage of Al, Si, Mg and Oxygen elements present.

The microstructures of the examined MMCs have four distinct micro phases, (as marked) which are as follows: the aluminium matrix (grey area), the SiC particles (dark area), the eutectic region of aluminium and silicon (white area and grey area) and the Mg_2Si phase (white area) (Figure III.6a, III.6b and III.6c).

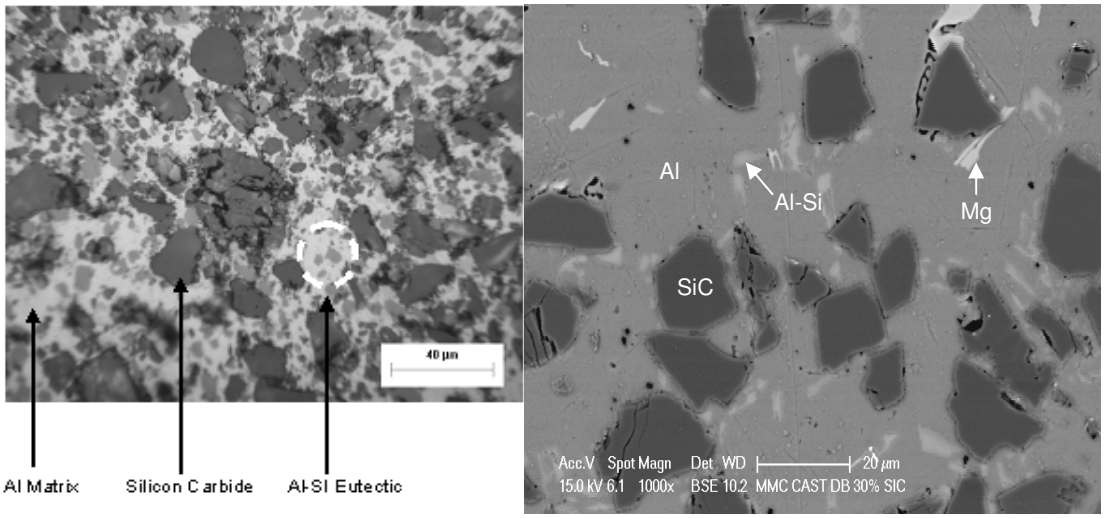

(a) (b)

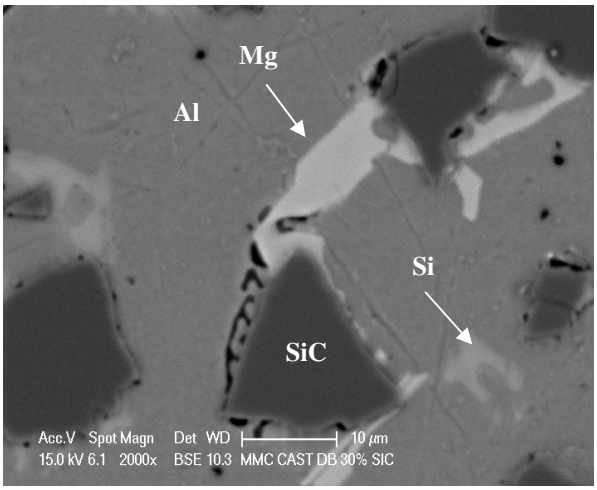

(c)

Figure III.6a Hot-Rolled A359/31%SiC showing microstructure distinct phases. Figure III.6b and c. Cast A359/30%SiC showing phases. Dark objects-SiC, Grey area-Al, Light white area-Si, white area-Mg.

The SiC particles were found to lay in the eutectic region. This is because, in MMCs, the SiC particles tend to aggregate in the eutectic region at the end of the solidification process. The distribution of SiC particles was found to be more or less uniform, however, instances of particle free zones and particle clustered zones were found. Furthermore, in the ingot samples examined, the dendritic microstructures of Al-Si clearly satisfy the process of homogenisation due to the nature of equilibrium segregation (Figure III.7).

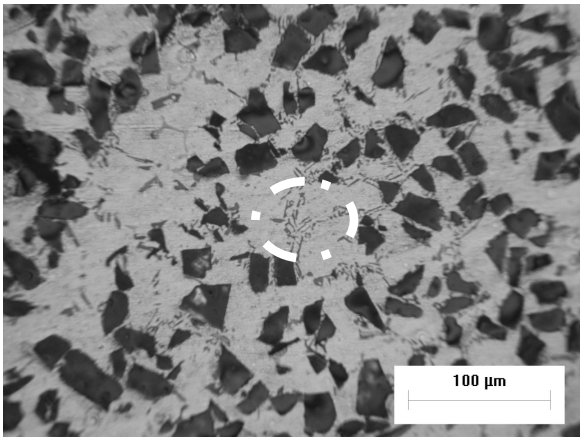

Figure III.7. Ingot A359/25% SiC- Showing Dendritic Al-Si arms and homogeneous distribution of SiC reinforcement.

Matrix-reinforcement interfaces were identified by using high magnification Nano-SEM microscope. In the as received hot rolled images the Al matrix/ SiC reinforcement interface is clearly identified (Figure III.8). These interfaces attain properties coming from both individual phases of constituents and facilitate the strengthening behaviour of the composite material.

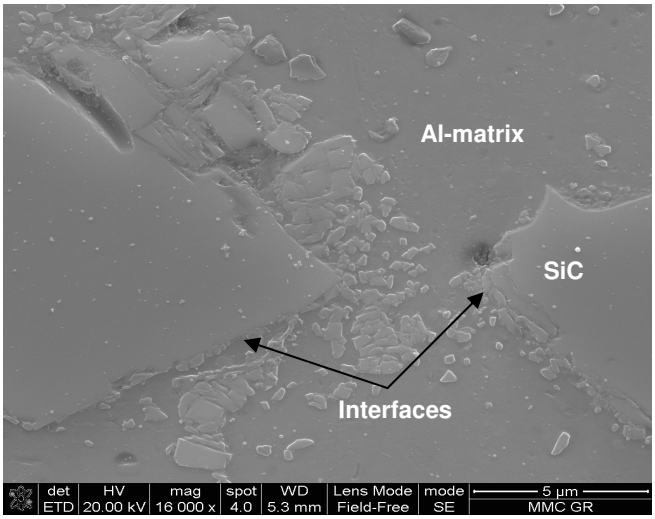

Figure III.8. Microstructure of rolled 31% SiC in the as received condition showing matrix-reinforcement interfaces.

In the hot rolled images, interfaces of Al matrix/ SiC reinforcement are clearly shown, and also Si phase area is identified close to the interface creating an Al - Si interphase (Figure III.9a). This interphase attains properties coming from both individual phases and facilitates the strengthening behaviour of the matrix/reinforcement interface. Furthermore, silicon particles identified in round form close to the interface of Al/SiC in a size of approximately 100nm (Figure III.9b). These silicons could form the SiO_2 layer when magnesium and oxygen are present and this will lead to the formation of $MgAl_2O_4$ phase.

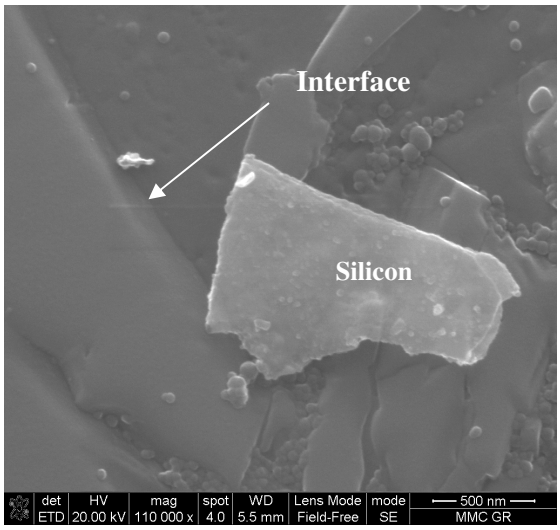

(a)

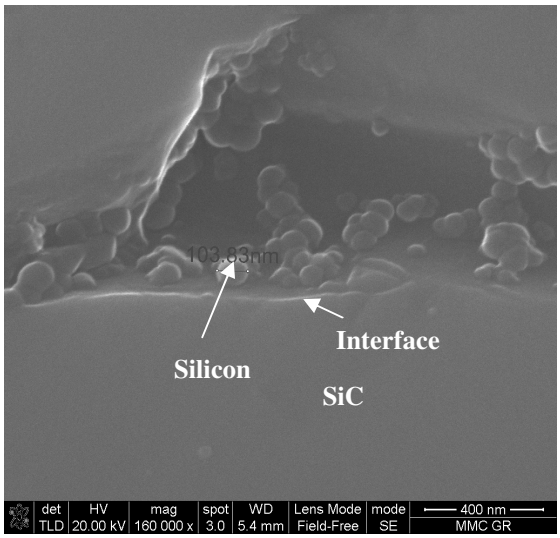

(b)

Figure III.9a. Hot Rolled A359/31%SiC showing Interface close to a large Silicon.

Figure III.9b. Nano -SEM image of Al-SiC Interface. Round particles measured 103.83nm are Silicon.

III.6.2.2 HT-1 Condition

In the HT-1 condition the microstructure of the cast 30% SiC has the same phases as in the as received state, plus one rod-shape phase (Figure III.10a, 10b) along the matrix and at the matrix-reinforcement interface has been identified to be Mg_2Si

precipitates in an early stage which are not fully grown. This evidence shows that β' phase has been formed with magnesium and silicon reacting together but β phases forming platelets of precipitates have not been formed in this HT-1 heat treatment, and this is probably due to the solution treatment temperature that did not allow enough reactivity time between the main alloying elements.

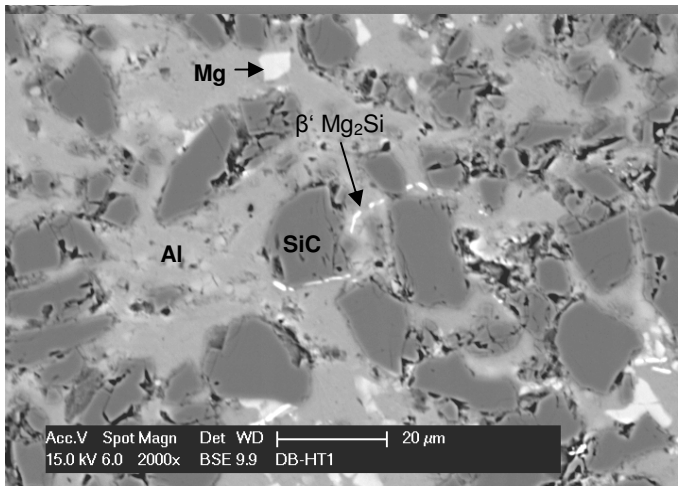

Figure III.10a. Microstructure of cast 30% SiC in the HT-1 condition showing rod shape β' phases of Mg_2Si around the matrix and the interface of the reinforcement.

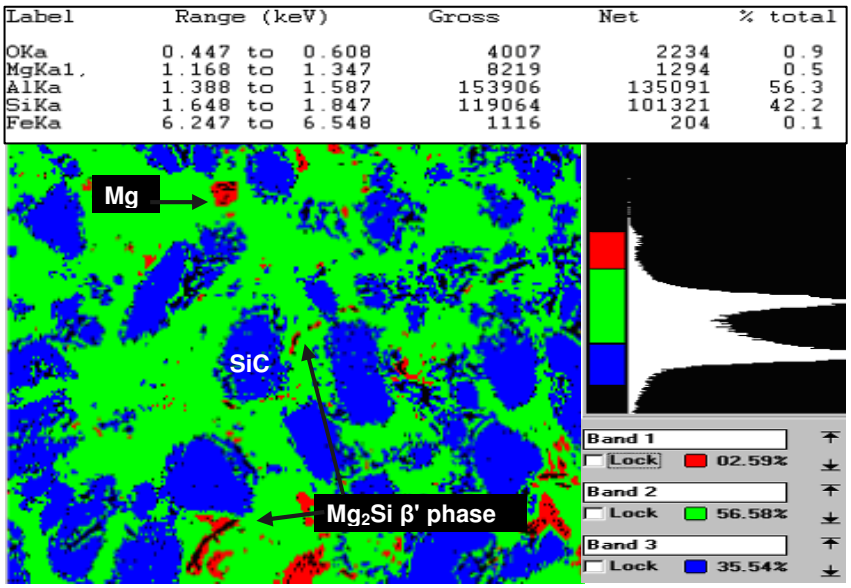

Figure III.10b. Cast 30% SiC - HT-1 sample showing phases and percentages. Aluminium (green), SiC (blue), Mg_2Si phase (red and dark as pointed in the image). Oxygen and Fe is also present in small percentages.

In the rolled 20% SiC the microstructure of HT-1 heat treatment shows an increase of the Silicon phase as shown in Figure III.11a. Silicon has been expanded during solidification and subsequent ageing. This formed round areas around the whole area of the composite.

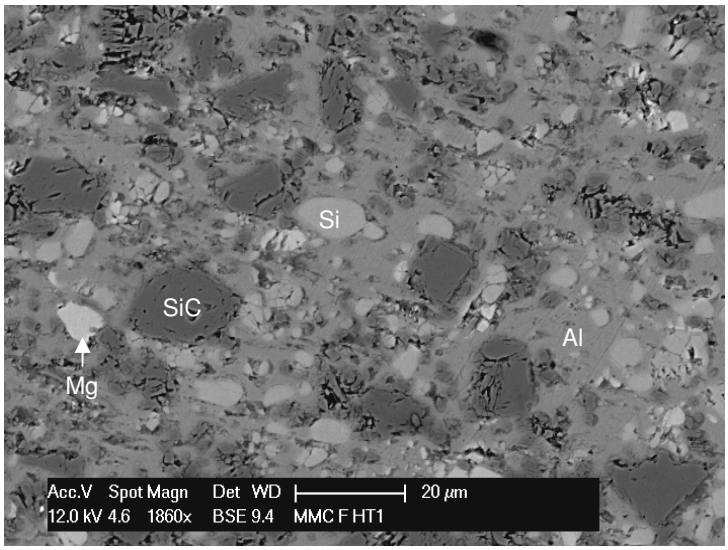

Figure III.11a Hot rolled 20 %SiC HT-1 sample showing phases of Aluminium, SiC, Silicon, Mg.

Comparing with the cast 30% SiC sample, in the rolled material the silicon phase is increased by ≈5%, as shown in (Figure III.11b and Figure III.4). This increase under the same heat treatment conditions is explained by the difference in the percentage of reinforcement in the material.

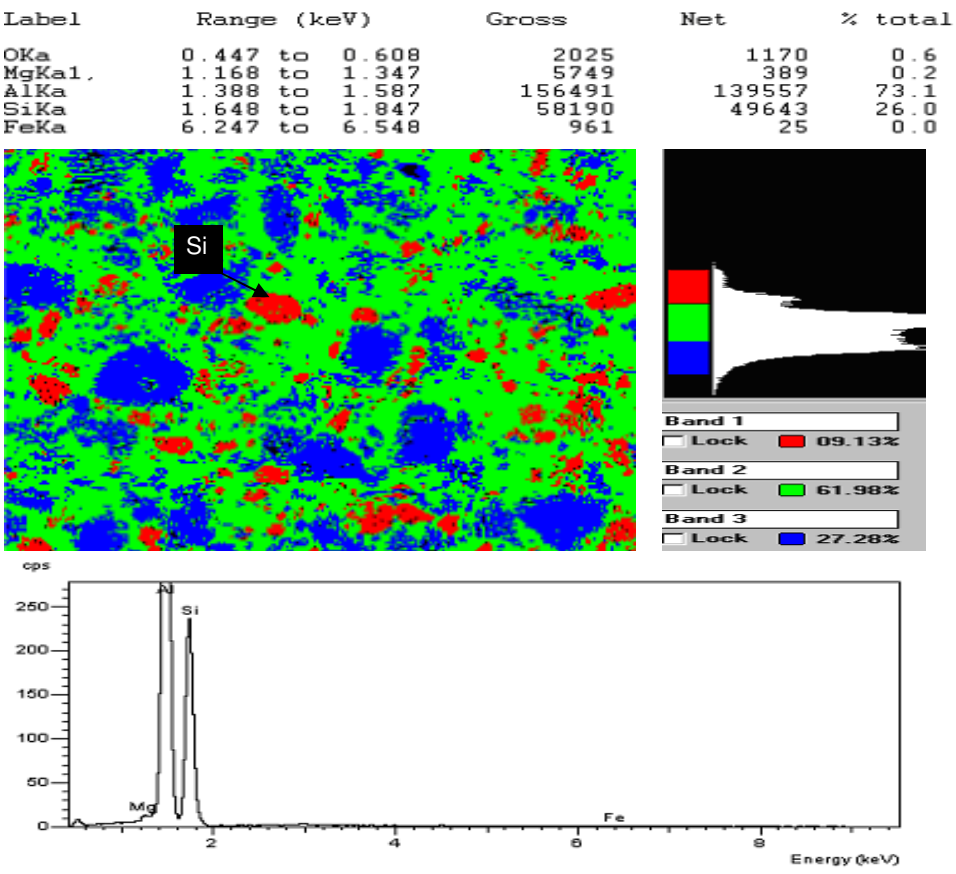

Figure III.11b Hot rolled 20% SiC - HT-1 microstructural analysis showing phases and elemental percentages. Silicon phase (red) has been expanded.

It becomes evident that the introduction of SiC reinforcement promotes zone kinetics and phase formation reactions during heat treatment process. The reinforcement, depending on its percentage in the matrix material, accelerates or restrains events such as precipitation and segregation. This is further supported by the fact that precipitation has not been observed in the HT-1 heat treated 20% SiC rolled material, where lower percentage of SiC reinforcement slowed-down the precipitation kinetics and β' phases could not be created in a similar manner as the 30% SiC cast sample.

III.6.2.3 T6 Condition

In the T6 condition the microstructural results showed that in the rolled 31% SiC sample precipitates of Mg_2Si have been formed in a platelet shape in the matrix as well as in areas close to the interface (Figure III.12a, 12b and 12c). The higher solution temperature and lower age hardening holding time that exist in the T6 heat treatment process, promoted the forming of this type of precipitates, which act as support to strengthening mechanisms of the reinforcement-matrix interface. In the case of presence of a crack in the matrix, these precipitates act as strengthening aids promoting crack deflection at the interface resulting in an increase of the composite's fracture toughness [67-72].

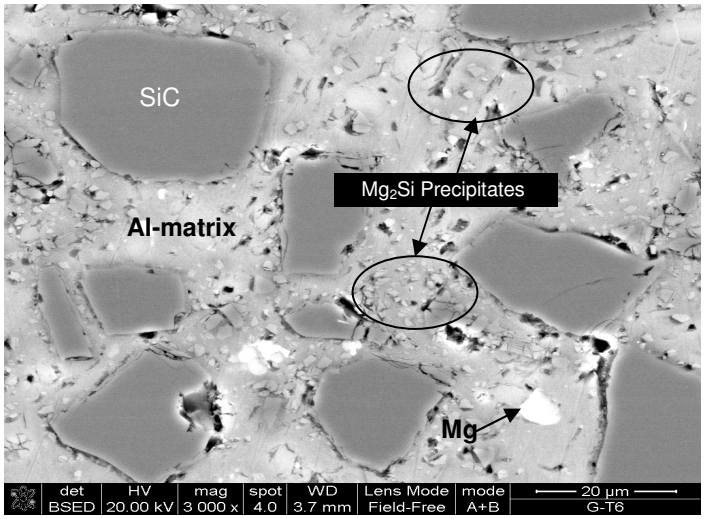

Figure III.12a. Hot rolled 31% SiC –T6 showing precipitates formed around the reinforcement.

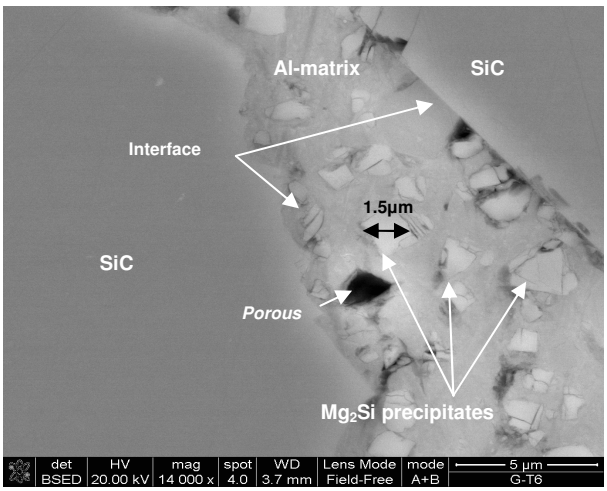

Figure III.12b. Hot rolled 31% SiC – T6 showing Mg_2Si precipitates formed between the SiC reinforcement interface in a platelet shape of around 1-3 µm. A porous close to the interface has been identified in a similar size.

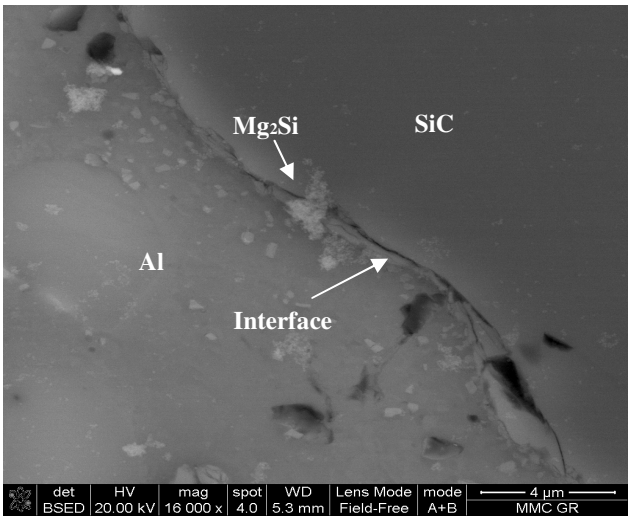

Figure III.12c. Hot Rolled – T6 A359/31%SiC showing interface of Al/SiC and also small precipitates of Mg2Si (white areas close to the interface). Mg2Si precipitate formed close to interface.

Furthermore, in the T6 condition, Fe elements have been identified by EDAX-mapping technique, therefore, demonstrating the existence of a new phase in the composite due to the reaction of Fe with other major alloying elements.

In addition, the presence of $MgAl_2O_4$ shows that magnesium reacted with SiO_2 at the surface of SiC and formed this layer in the interfacial region between the matrix and the reinforcement. The layers of $MgAl_2O_4$ protect the SiC particles form the liquid aluminium during production or remelting of the composites. This layer provides more than twice bonding strength compared to Al_4C_3 [60]. The presence of Al_4C_3 could not be identified by XRD (section III.6.3); something that verifies that high percentage of Si added in the composite during manufacturing and also existence of Al_2O_3 retards Al_4C_3 formation in the composite.

III.6.3 XRD Analysis

The X-ray diffraction was carried out on the MMCs in the as received, as well as, in the heat treatment conditions, in samples with 20% and 31% of SiC particulates. Even though some peaks were superimposed, the results clearly showed the phases present in the microstructures. In particular, in the as received condition and in the heat treatment conditions the results showed existence of aluminium matrix material, eutectic silicon, SiC, Mg_2Si, SiO_2 phases as the distinct ones, and also $MgAl_2O_4$ and Al_2O_3 phases (Figure III.13).

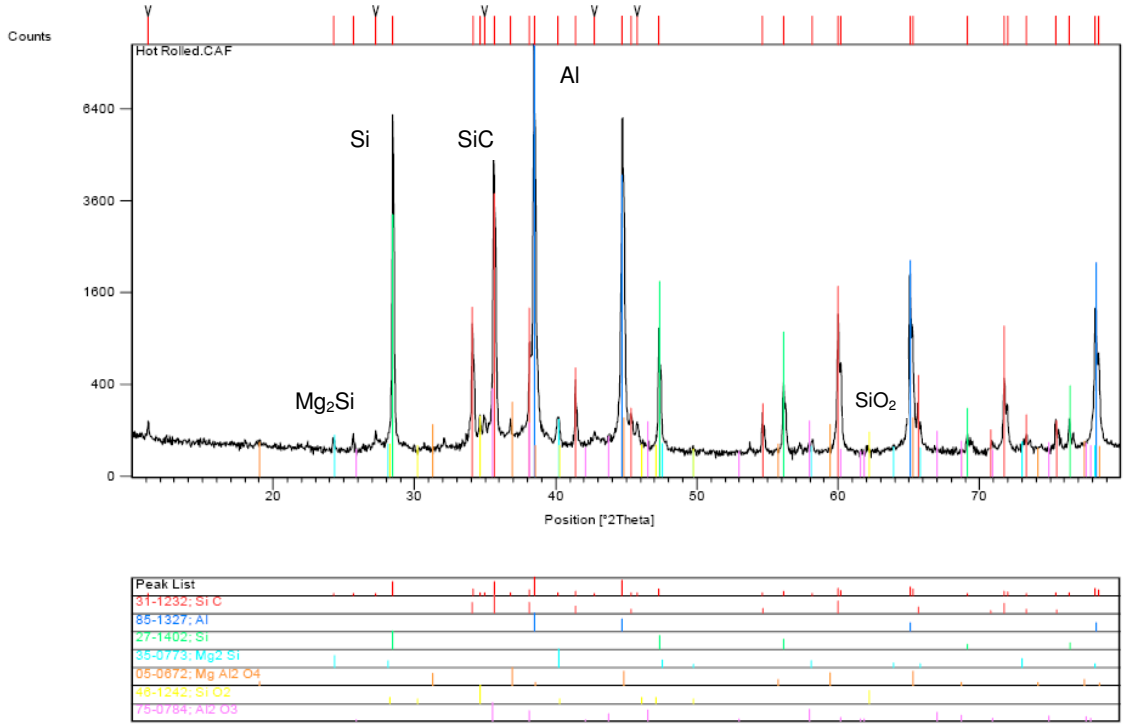

Figure III.13. XRD of hot rolled 31% SiC as received sample showing phases present and some superimposed oxides ($MgAl_2O_4$ and Al_2O_3).

$MgAl_2O_4$ and Al_2O_3 oxides give good cohesion between matrix and reinforcement when forming a continuous film at the interface. The presence of $MgAl_2O_4$ (spinel) shows that low percentage of magnesium reacted with SiO_2 at the surface of SiC and formed this layer in the interphacial region between the matrix and the reinforcement (Equation III.1). This layer has been identified by SEM-EDAX technique (Figure III.14).

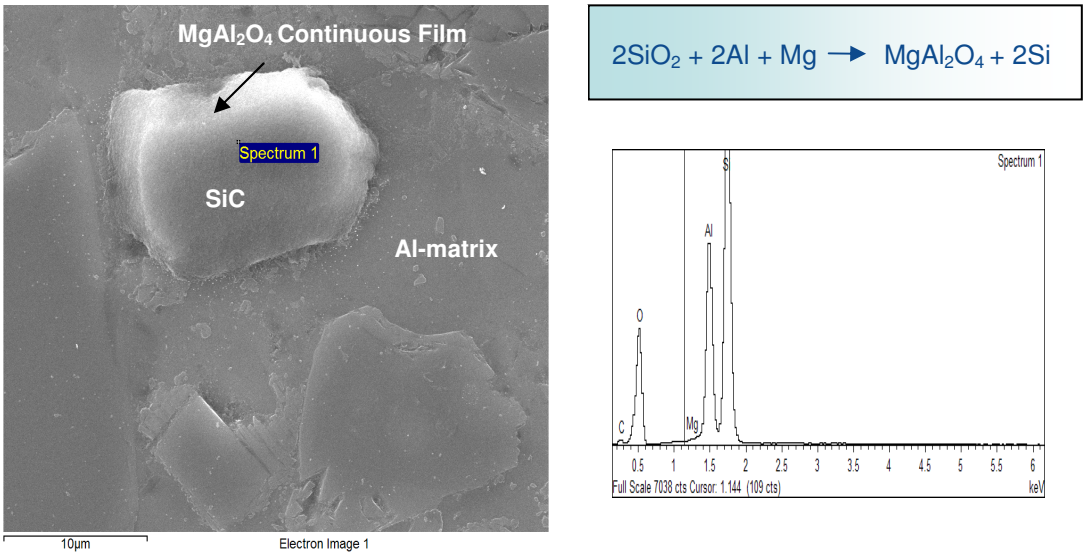

Figure III.14. $MgAl_2O_4$ phase observed to be a continuous film around the SiC particle. (white area)

$$2SiO_2 + 2Al + Mg \rightarrow MgAl_2O_4 + 2Si \qquad \text{III.1}$$

The layers of $MgAl_2O_4$ protect the SiC particles from the liquid aluminium during production or remelting of the composites. Furthermore, the layer of Al_2O_3 oxide is formed as a coating when SiO_2 is reacting with liquid Aluminium (Equation III.2).

$$3SiO_2 + 4Al \rightarrow 2Al_2O_3 + 3Si \qquad \text{III.2}$$

The presence of Al_4C_3 could not be identified by XRD in all samples in the as received or heat treated states, something that verifies that high percentage of Si added in the composite during manufacturing, leading to forming of Al_2O_3, retards Al_4C_3 formation in the composite [73].

The same phases have been identified in the HT-1 condition. In the T6 condition XRD results showed one more phase present which is the spinel-type mixed oxide

$MgFeAl0_4$ showing that Fe trace reacted with Mg and in the presence of aluminium and oxygen formed this oxide (Figure III.15a and b).

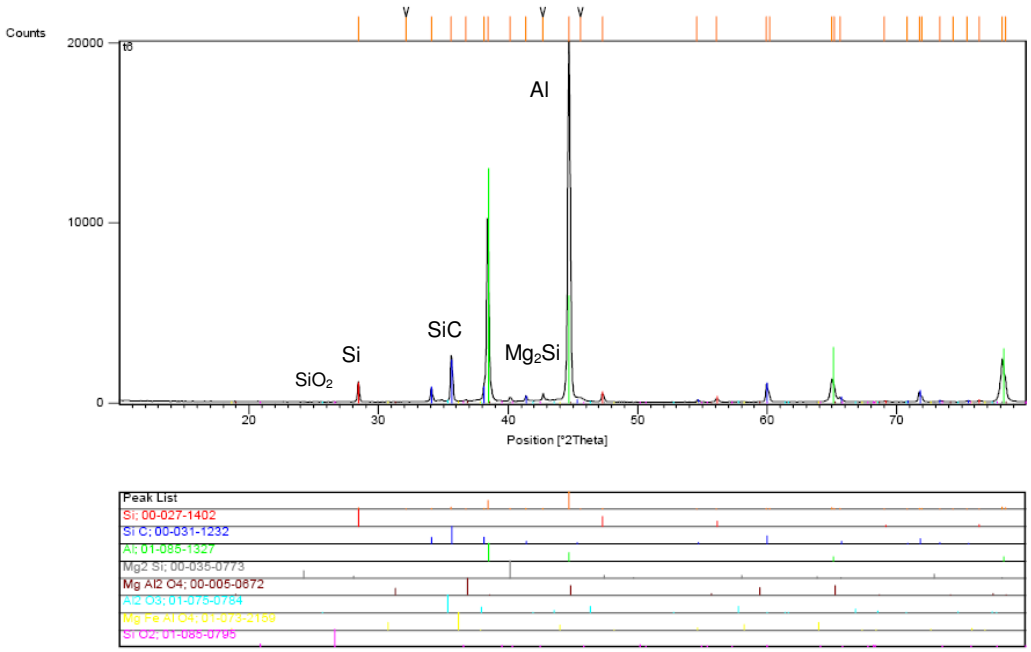

Figure III.15a. XRD of hot rolled 31% SiC - T6 sample showing phases present and $MgFeAl0_4$ phase.

The presence of Fe has also been identified in this study by microscopic analysis (Figure III.15 c).

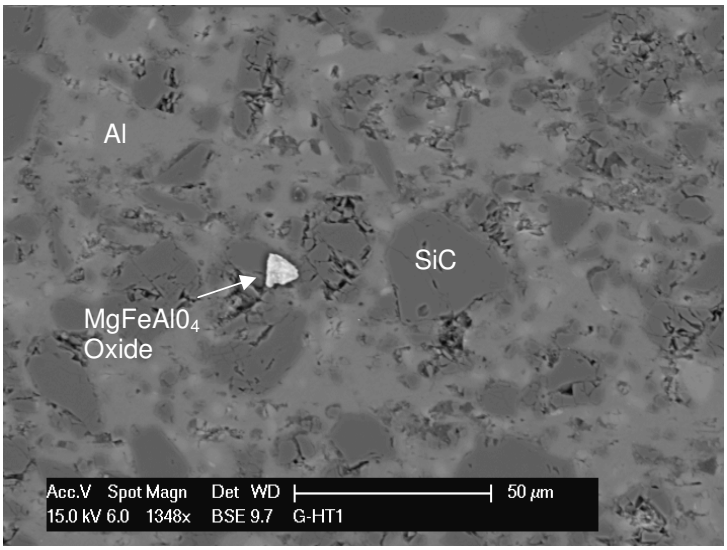

Figure III.15b. SEM image of rolled 31% SiC showing phase of $MgFeAl0_4$ formed in the composite.

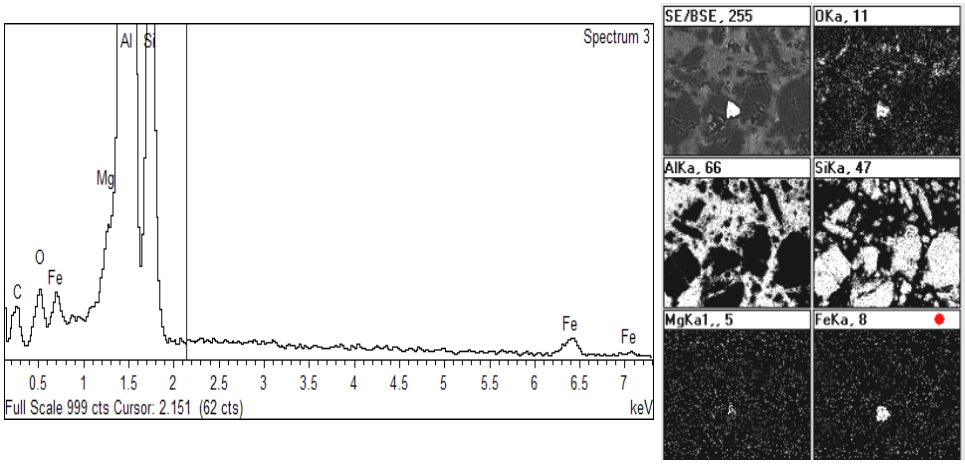

Figure III.15c EDAX-Mapping Techniques used showing Fe, O, Al, Mg, Si elements present.

As can be observed by the microscopic analysis porosities were present in some of the samples. A total avoidance of porosity is difficult to achieve, because the lower thermal conductivity of ceramic reinforcements requires them to be pushed to the solidifying front of a freezing melt in such way that shrinkage porosities appear around the particulate as the matrix shrinks during solidification. Also, as magnesium is surface active, it effectively reduces interfacial energies, resulting in the development of gas (due to air) and shrinkage porosity when an optimum amount of reinforcements is present [74].

Microscopic porosity was observed in specific areas of the reinforced and unreinforced regions of the composites in the as received as well in the heat treatment conditions. Porosities of 1-3 μm in size and ≈1 wt% were present in the materials examined. In the heat treated samples porosity was increased and found to be 1.5 wt% in the material. This is due to the treatment condition and these porosities may have been formed by solidification shrinkage, thus cannot be considered as major defects (Figure III.16a, b).

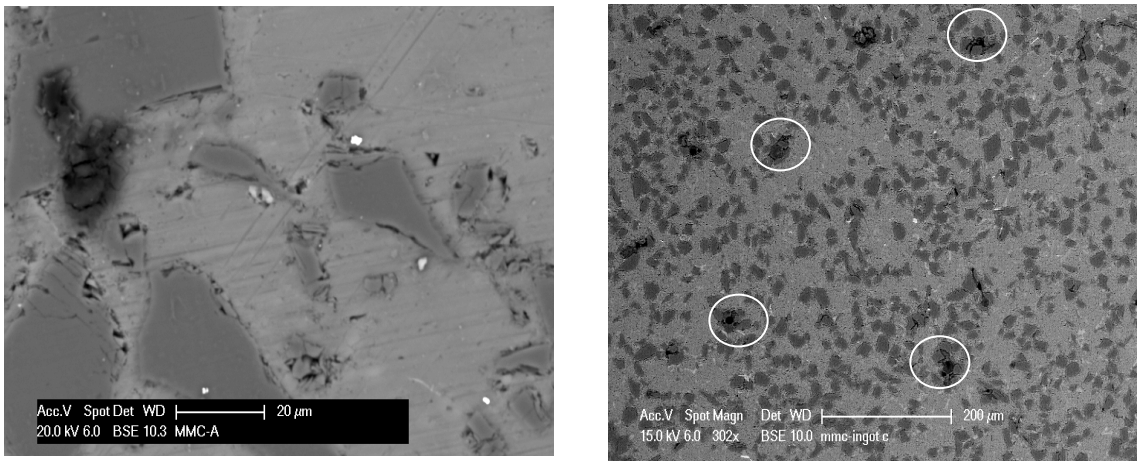

(a) (b)

Figure III.16a, b. Ingot A359/25%SiC and A359/40%SiC showing porosity of 10±5µm.

III.7 Microhardness Testing for T1, HT1 and T6 Conditions

The Al/SiCp samples have been compared in relation to their microhardness performance based on the reinforcement percentage, the heat treatment conditions and the different manufacturing forming processes. Microhardness of the composites has been measured in order to get the resistance of the material to indentation, under localized loading conditions. The microhardness test method, according to ASTM E-384, specifies a range of loads using a diamond indenter to make an indentation, which is measured and converted to a hardness value [75].

Measuring the different phases in the micro-level it is quite challenging, as the SiC reinforcement of ≈17µm in size was not easy to measure, due to small indentation mark left when a small load on the carbide is applied. When introducing higher values of load, the indentation was not localized in the carbide but covered some of the matrix area too. The load was set to 50 grams in order to obtain valid measurements coming from different areas of the samples: SiC, aluminium matrix, and the overall composite – MMC i.e. areas superimposing matrix and reinforcement.

There are many factors influencing the microhardness of a composite material, including the reinforcement percentage, interparticle spacing and also particle size. Moreover, manufacturing forming processes influence material's microhardness behaviour in relation to the reinforcement percentages in the composites [76].

The cast sample in the as received condition has the highest MMC microhardness, where the rolled 20% SiC with lower percentage of reinforcement has the lowest values. By altering the microstructure with modified T6 (HT-1) heat treatment all values of the three samples show an increase between 20-45% from the initial state (Figure III.17).

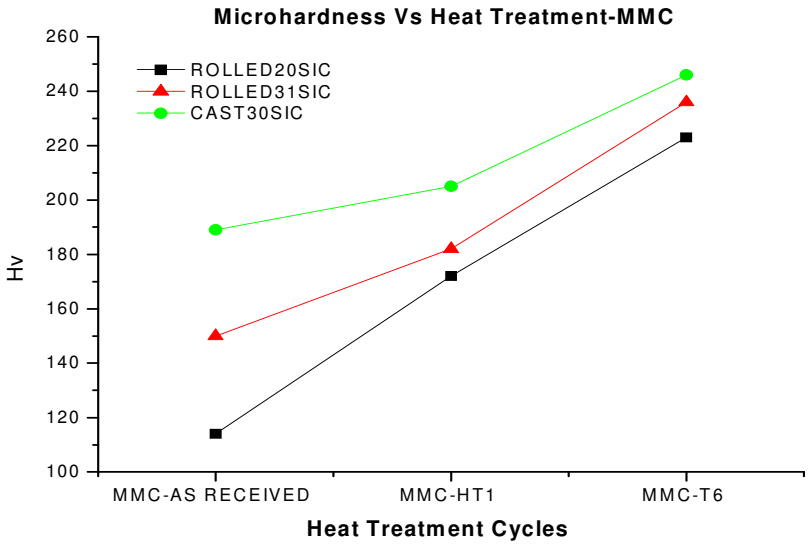

Figure III.17. Microhardness values Vs. Heat treatment cycles for the MMC areas.

This shows the effect of the heat treatment in the micro-deformation of the matrix-reinforcement interface due to the presence of precipitates and other phases and oxide layers.

As can be seen in Figure III.17 the T6 condition obtained the larger increase in microhardness values from the as received state, ranging from 20% to 90% depending on the reinforcement percentage and manufacturing process.

Furthermore, variability in microhardness values was observed when comparing cast and rolled materials with different percentage of SiC. However, this variability varied when samples processed at different heat treatment conditions were compared. Highest variability showed samples in the as received condition, whereas lowest variability showed samples in the T6 condition, with samples in the HT-1 condition in between. This can be explained by the fact that precipitates act as strengthening mechanisms and affect the micromechanical behaviour of the composite material.

In the absence of precipitates (in the as received condition), the volume percentage of SiC and the manufacturing processing play a significant role in micromechanical behaviour of the composite. As precipitates are formed due to heat treatment process they assume the main role in the micromechanical behaviour of the material. In the HT-1 heat treatment condition there is presence of β' precipitates which affect the micromechanical behaviour in a lesser degree than in the case of T6 heat treatment condition where fully grown β precipitates are formed. It becomes clear that after a critical stage, which if related to the formation of β precipitates in the composite the dominant strengthening mechanism is precipitation hardening.

While Figure III.17 shows results in areas that include the interface region (where precipitates are concentrated) Figure III.18, shows results on microhardness values in the aluminium matrix (where precipitates are dispersed). In Figure III.18 there is similar variability for all three materials processing states, as received, HT-1, and T6. This implies that in the matrix material the percentage of the reinforcements, the manufacturing processes, as well as the precipitation hardening, are strengthening mechanisms of equal importance.

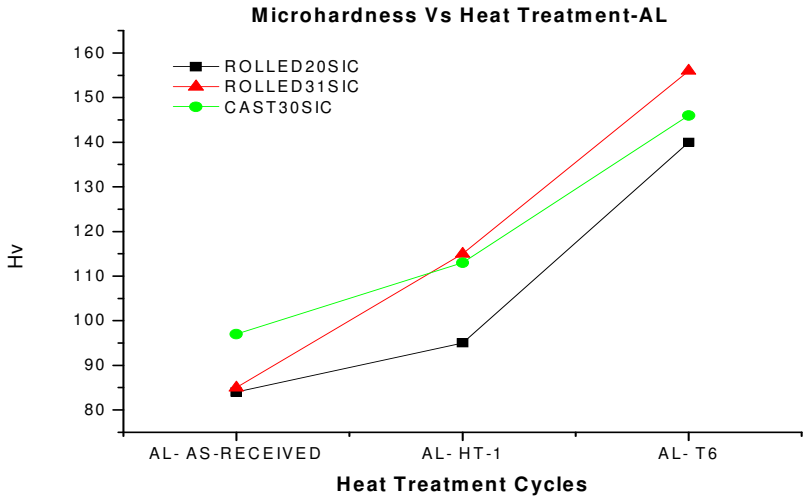

Figure III.18 Microhardness Vs. Heat treatment cycles for Aluminium areas.

Finally, Figure III.19 shows microhardness measurements obtained from areas around the matrix-reinforcement interface in a composite heat treated in the T6 condition. The microhardness values are higher in the close proximity of the interface. It is observed that cast material has higher values than the rolled material. In the case of rolled material, the microhardness raises as the percentage of reinforcement increases.

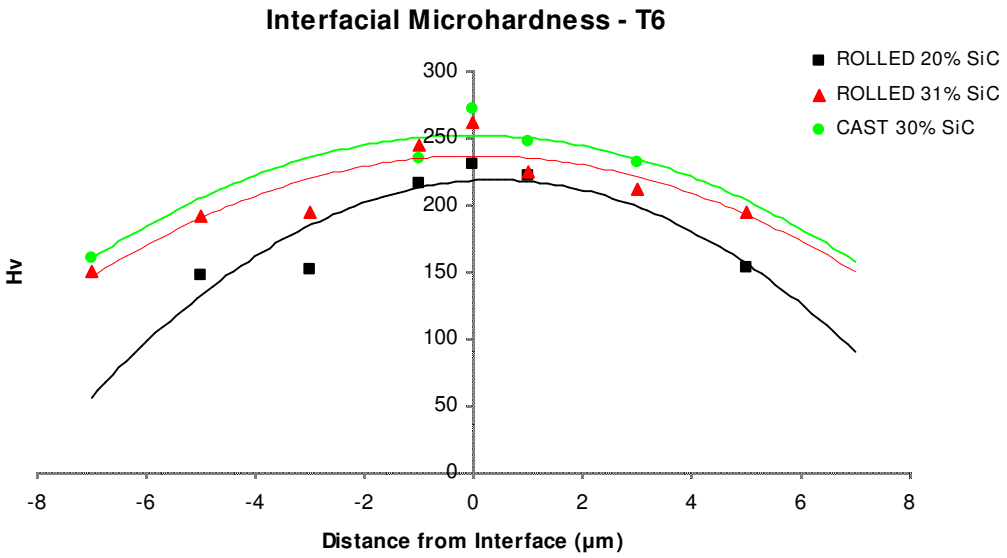

Figure III.19 Interfacial microhardness showing measurements obtained from areas close to the matrix- reinforcement interface in the T6 condition.

Furthermore, the size of the microhardness indentation mark was much smaller than the average spacing between SiC particles. The indentation mark was varying in size depending on the distance from the interface, as well as from the reinforcement percentage. By getting closer to the SiC particulates, the marks became smaller and the microhardness values higher. Furthermore, the 31% SiC composite left the smallest indentation marks verifying that with higher % of SiC the interparticle distance becomes smaller and therefore the microhardness increases in areas close to the interface (Figure III.20).

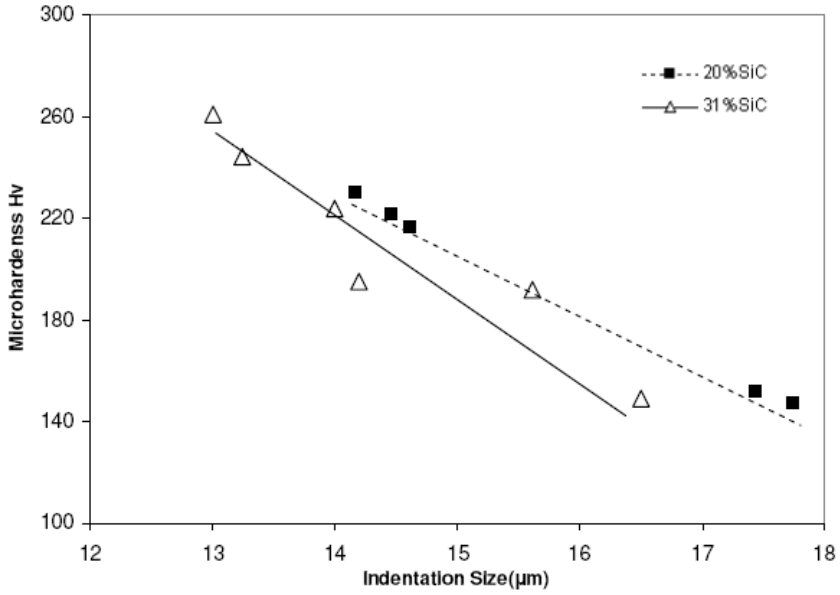

Figure III.20. Interfacial microhardness values vs. Microhardness indentation mark size in theT6 condition.

III.8 Discussion

Microstructure analysis of SiC particulate reinforced aluminium alloy composites shows the deformation that takes place in the material. Phase deformations in the hot-rolled samples create the Al-Si phase but Mg reaction produces Mg_2Si precipitates,

following the appropriate heat treatment. In the ingot samples, the dendritic microstructures of Al-Si clearly satisfy the process of homogenisation due to the nature of equilibrium segregation. Moreover, the general distribution and the size of the SiC particulates were satisfying.

In addition, the porosity observed shows that the material has some kind of imperfection in the 'as received' condition, something that may change by artificial ageing. In general, the porous percentage is low and the material can not be considered as defected.

Furthermore, the importance of the volume fraction of the precipitates and the reinforcement, as vital factors is observed. Dispersion of the particles, their mean size and the typical distance between them affects the microdeformation behaviour. Interaction mechanisms between particles and dislocations of precipitated particles can effectively impede the motion of dislocations in the matrix. If the particle is coherent with the matrix, i.e. if the glide planes of the matrix continue through the particle, a dislocation can intersect the particle.

From the microhardness testing it can be noticed that the percentage of reinforcement phase plays a crucial role in the overall composite hardness behaviour. Also, while segregation was identified as the principal strengthening mechanism of interfaces in SiC particulate reinforced aluminium alloy composites, other features also contribute to a lesser extent to the measured increase of microhardness near the interface compared to Al matrix. Such features are:

(a) Local chemistry changes due to Mg segregation and formation of spinel ($MgAl_2O_4$);

(b) Constraint effects provided by the SiC particles, which is harder than the deforming matrix;

(c) Potentially higher dislocation density near the SiC particles due to mismatch in the coefficient of thermal expansion; and

(d) Residual stresses near SiC particles due to mismatch in the coefficient of thermal expansion.

Moreover, with increasing volume fraction, the number of particles increases, whereas spacing between particles decreases. Consequent increase in the number of barriers to plastic deformation reduces the depth of plastically deformed by restraining the plastic flow of the matrix. This can lead to low fracture toughness of the composite, something that has to be avoided. Lower percentage showed in the hot rolled samples may be ideal as ductility of the matrix with a low % of SiC lead to the best composite behaviour, in relation to the application for the composite to be used.

Chapter IV-Tensile and Fatigue Behaviour of SiC particulate reinforced aluminium alloy composites

The main aim of this chapter is to investigate the Tensile and Fatigue behaviour of the SiC particulate reinforced aluminium alloy composites. Also, the understanding of the role of the heat treatment processing on the materials mechanical and interfacial properties are also being analysed so as to comprehend the importance of segregation the precipitation hardening phenomena. The data obtained from this chapter are used as input parameters in the model developed in the next chapter.

IV.1 Introduction

SiC particulate reinforced aluminium alloy composites are attractive engineering materials designed for a variety of structural applications, due to their superior strength, stiffness, low cycle fatigue and corrosion fatigue behaviour, creep and wear resistance, compared to the aluminium monolithic alloys.

The introduction of the reinforcement plays a key role in both the mechanical and thermal ageing behaviour of the composite material. Micro-compositional changes which occur during the thermo-mechanical forming process of these materials can cause substantial changes in mechanical properties, such as ductility, fracture toughness and stress corrosion resistance.

In the case of particulate-reinforced aluminium composites, the microstructure and mechanical properties can be altered by thermo-mechanical treatment, as well as by varying the reinforcement volume fraction. The strengthening of a monolithic metallic

material is carried out by alloying and supersaturating to the point that, on suitable heat treatment, the excess alloying additions precipitates out (ageing) [62].

IV.1.2 Interface in Metal Matrix Composites

In composites the role of interface is crucial. Stiffening and strengthening rely on load transfer across the interface, toughness is influenced by crack deflection, and ductility is affected by relaxation of peak stresses near the interface. However, the characterisation and optimisation of the mechanical response of the interface to stresses arising from an applied load is not well understood and needs further research.

In general, the interfacial properties are dependent on processing route and thermo-mechanical history. Among the relevant properties are the critical stress levels to cause interfacial debonding. Strain energy release rate critical value is another crucial factor that plays a critical role in the crack propagation along the interface. Also of interest are the conditions under which interfacial sliding can occur after debonding.

Metal matrix composites (MMCs) often behave asymmetrically in tension and in compression and have higher ultimate tensile strength, yet lower proportional limits, than monolithic alloys. Such behaviour lies with the factors governing matrix plasticity, which can be divided into two areas; those affecting the stress rate of the matrix, and those which alter the flow properties of the matrix through changes in microstructure induced by inclusion of the reinforcement. The characterisation of the mechanical response of the interface to stresses arising from an applied load in SiC-particle reinforced aluminium matrix composites is important in order to understand the MMCs overall behaviour [61].

IV.2 Tensile Behaviour of SiC particulate reinforced A359 aluminium alloy Composites

The tensile behaviour of the composites has been studied in the as received (T1) and in the T6 and modified T6 (HT1) conditions. In the non-equilibrium heat treatment processing of the composites, non-equilibrium segregation arises due to imbalances in point defect concentrations set up around interfaces. Stress-strain behaviour, of aluminum matrix composites containing various percentages of SiC particulate reinforcement has been investigated. The elastic modulus, the yield/tensile strengths and ductility of the composites were controlled primarily by the volume percentage of SiC reinforcement, the temper condition and the precipitation hardening.

To achieve good mechanical properties, a good globular microstructure must be obtained with very fine and homogeneous SiC distribution and with very low levels of voids produced during the solidification process. By using different heat treatments, the mechanical properties of metal matrix composites reinforced with SiC particulates can be strongly improved.

The objective is to observe whether or not, in the monotonic tensile testing, reinforcement with SiC particulates produces a substantial increase in the work hardening of the material. This increase can be related to a more significant way with increasing volume fraction of carbides.

Furthermore, investigation of the yield and ultimate tensile strength and the elastic modulus of the material need to be looked upon. The relationship of the microscopic and the macroscopic interfacial strength behaviour of the MMC will be the final objective to be investigated.

IV.2.1 Materials

For this investigation, two types of materials were used: 1) Hot Rolled A359/20%SiC, with an average particle size of 17±1 μm and 2) Hot rolled A359/31%SiC with an average particle size of 17±1 μm. Table IV.1, contains the details of the chemical composition of the matrix alloy, as well as the amount of silicon carbide particles in the metal matrix composites.

	Elements (wt %)					
Materials	**Si**	**Mg**	**Mn**	**Cu**	**Fe**	**Zn**
Rolled Al A359-SiC-20p	***9.5***	***0.5***	***0.1***	***0.2***	***0.2***	***0.1***
Rolled Al A359-SiC-31p	***9.5***	***0.5***	***0.1***	***0.2***	***0.2***	***0.1***

Table IV.1. The chemical composition of the Al/SiC composites.

The heat treatments were performed in Carbolite RHF 1200 furnaces with thermocouples attached, ensuring constant temperature inside the furnace. There were two different heat treatments used in the experiments, T6 and HT-1 (see section III.4.1).

IV.2.2 Tensile results

Aluminium – SiC particulate composite samples were tested in tension for two different volume fractions, 20% and 31%, in reinforcement. The dog-bone coupons were tested according to ASTM E8-04 [77] in the as received and, following two

different heat treatments, T6 and HT-1 heat treatment conditions. Tensile tests were conducted using a 100 KN Instron hydraulic universal testing machine and the strain was monitored using a clip gauge.

The mechanical properties of the composites are presented in Table IV.2. The engineering stress/strain curves of the composite are shown in Figure IV.1. As it can be clearly seen in this figure, the HT-1 heat treatment has improved both the strength and strain to failure in comparison with the untreated composites for both volume fractions. Furthermore, the failure strain for this temper is considerably higher than the one for the T6 heat treatment; this may be attributed either to the nucleation of the β` precipitate phases which is although not visible yet, may lead to the increase of the plastic deformation through crack deflection mechanisms and/or to annealing which acts competitively to the precipitation leading to the toughening of the composite. However, the T6 heat treatment exhibits the highest strength followed by the HT-1 and the as received state. Finally, as it was expected, the “as received” composites behaviour in tension deteriorates with increasing filler concentration.

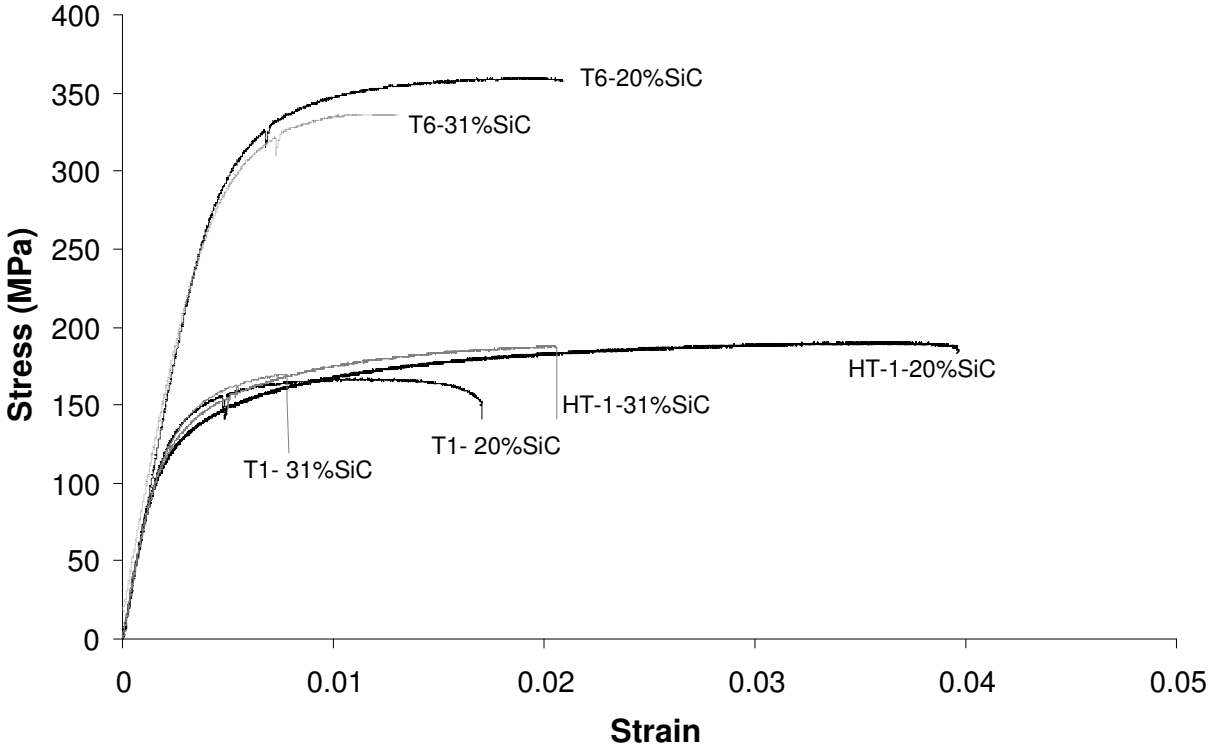

Figure IV.1. Stress / Strain curves of Al/SiC Composites.

The experiments showed that for the same range of conditions tested, the yield and the ultimate tensile strengths of the SiC/Al composites were mainly controlled by the percentage of reinforcement as well as by the intrinsic yield/tensile strengths of the matrix alloys. The addition of the SiC reinforcement created stress concentrations in the composite, and thus the aluminium alloy could not achieve its potential strength and ductility due to the induced embrittlement. Composites in the T1 condition failed in a brittle manner with increasing percentage of reinforcement. As a result, with increasing reinforcement content, the failure strain of the composites was reduced as shown in Figure IV.1.

From the above postulations it is obvious that the phase that dominates the mechanical behaviour of the composite is the precipitation phase created by age hardening while the reinforcement phase plays a secondary role.

The heat treatment affected the modulus of elasticity of the composites by altering the transition into plastic flow (see Table IV.2 and Figure IV.2). Composites in the T6 condition strained elastically and then passed into a normal decreasing-slope plastic flow. Composites tested in the HT-1 condition exhibit a greater amount of strain than the T1 and those heat treated in the T6 condition. The failure strain increasing from about 1.5% strain to about 4% but the greater influence was a sharper slope of the stress-strain curve at the inception of plastic flow.

Material	Condition	$\sigma_{0.2}$(MPa)	σ_{uts}(MPa)	ε (%)	E	$HV_{0.5}$
Rolled Al A359-SiC-20p	T1	**146**	**157**	**1.5**	**100**	**114**
	HT-1	**147**	**190**	**4**	**102**	**172**
	T6	**326**	**360**	**2.1**	**112**	**223**
Rolled Al A359-SiC-31p	T1	**158**	**168**	**1**	**108**	**150**
	HT-1	**155**	**187**	**2**	**110**	**182**
	T6	**321**	**336**	**1.3**	**116**	**236**

Table IV.2. The mechanical properties of Al/SiC Composites

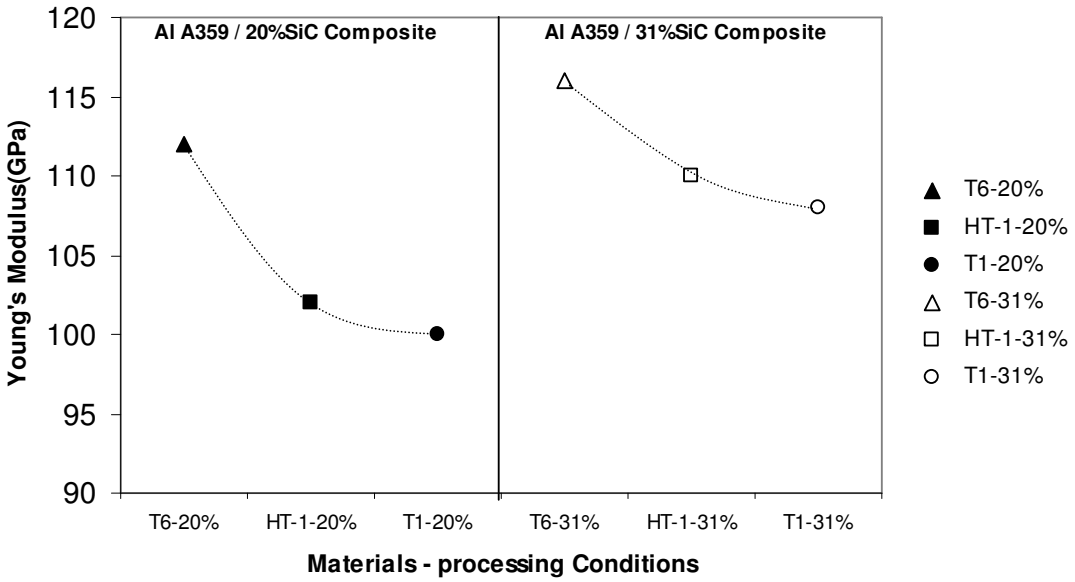

Figure IV.2. Young's Modulus vs. Processing Conditions curves showing T6 treated composites having the highest modulus.

This increase in elastic proportional strain limit and the steepening of the stress-strain curve were reflected by the higher yield and ultimate tensile strengths observed in the heat-treated composites. The increase in flow stress of composites with each heat-treatable matrix probably indicated the additive effects of dislocation interaction with both the alloy precipitates and the SiC reinforcement. The combination increased the strain in the matrix by increasing the number of dislocations and requiring higher flow stresses for deformation, resulting in the higher strengths observed. Ductility of Al/ SiC composites, as measured by strain to failure, is again a complex interaction of parameters. However, the prime factors affecting these properties are the reinforcement content, heat treatment and precipitation hardening.

IV.3 Fatigue behaviour of SiC particulate reinforced A359 aluminium alloy Composites

IV.3.1 Introduction

The fatigue behaviour of SiC particulate reinforced A359 aluminium alloy composites considering its microstructure and thermomechanical properties has been studied experimentally and analysed thoroughly. Three different heat treatment (T1, HT1 and T6) protocols on stripes of hot rolled Al/SiC_P 20% specimens with the aim of tailoring the fatigue properties of the composite have been examined. The fatigue behaviour was also monitored and the corresponding S-N curves were experimentally derived for all heat treatments. Fatigue tests were performed at three stress levels and microstructural analysis of the fractured surface was performed using Scanning Electron Microscopy (SEM). Simultaneously, the stress field on the sample was monitored non-destructively as imaged by the transient temperature gradient per fatigue cycle using lock-in thermography. The coefficient of thermo-elasticity allows the transformation of the temperature profiles into stress.

All the aforementioned techniques were employed with the aim to study the influence of microstructure which in its turn depends on the ageing conditions on the fatigue life and fracture behaviour of a SiC particulate reinforced A359 aluminium alloy composite. To this end, the cyclic fatigue life and fracture behaviour of the composite is going to be analysed related to the composite microstructural effects.

IV.3.2 Al/SiCp Fatigue behaviour considerations

The mechanical behaviour of the aforementioned composites is dominated by the interface between the Aluminium matrix and the SiC particles. While strengthening relies on the load transfer at the interface, toughness is influenced by the behaviour of the crack at the boundary between the matrix and the reinforcement and ductility is affected by the relaxation of peak stresses near the interface due to the plastic flow ahead of the crack tip. As a result, the non-elastic behaviour of the composite is dominated firstly by the time dependent stress field i.e. the imposed stress rate, and secondly by the induced changes in the microstructure because of the presence of the reinforcement. These changes consist of segregation and precipitation phenomena caused by the thermal treatment which in turn are expected to drastically affect the fatigue strength and the fatigue life behaviour of the Al/SiC composites.

The response of the structural element to fatigue is critical for many applications. In this case of MMCs the fatigue behaviour differs from the one of unreinforced metals in several ways. When referred to particle reinforced metals, numerous studies are based on understanding the influence of the reinforcing particle on the matrix microstructure and the corresponding effect on the fatigue behaviour of the MMCs [78-82]. It has been stated that the size and percentage of the reinforcement are affecting the fatigue life. In some cases, the fatigue strength may deteriorate by the addition of the reinforcement [83-84].

Furthermore, the fatigue strength of SiC particulate reinforced A359 aluminium alloy composites has been reported to be mainly influenced by the thermo mechanical processing history of the composite. Recent studies have discussed the influence of heat treatment on the interfacial strength and the mechanical properties of SiC particulate reinforced A359 aluminium alloy composite [68, 80, 85]. The results indicated the

interrelation between the heat treatment, the filler/matrix interface quality and the static failure mode of the composite. Further to the static properties, the heat treatment is expected to be of significant importance for the dynamic behaviour of these materials.

IV.3.3 Material

Hot rolled A359 Aluminium alloy with 20% SiC particles per weight with an average particle size of 17±1 μm was used (Figure IV.3). In Table IV.3, the chemical composition of the matrix alloy is shown.

Table IV.3. Chemical Composition of the silicon carbide (SiC_P) reinforced A359 aluminium alloy matrix composite.

Material	Elements (wt %)					
	Si	Mg	Mn	Cu	Fe	Zn
A359 /SiC_P-20%	9.5	0.5	0.1	0.2	0.2	0.1

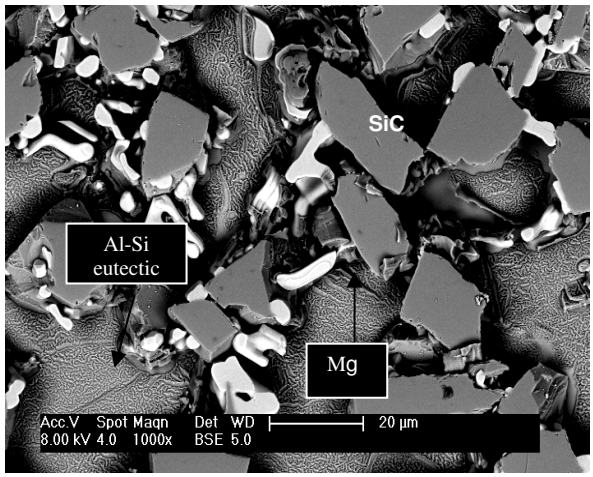

Figure IV.3.Aluminium/Silicon Carbide particulate Composite

IV.3.4 Fatigue Testing Parameters

Tension-tension fatigue tests were conducted using a 100KN Instron hydraulic universal testing machine with complementary data acquisition computer and software. The system was operated under load control, applying a harmonic tensile stress with constant amplitude. By specifying the maximum and the minimum stress levels, the other stress parameters could be easily determined. These were the stress range, σ_r, stress amplitude, σ_a, mean stress, σ_m, and fatigue stress ratio, R ($=\sigma_{min}/\sigma_{max}$).

Throughout this study, all fatigue tests were carried out at a frequency of 5 Hz and at a stress ratio R = 0.1. Three stress levels between the ultimate tensile strength (UTS) and the fatigue limit were selected, resulting in so-called Wöhler or S-N curves. Tests exceeding 10^6 cycles without specimen failure were terminated. Specimens that failed in or close to the grips were discarded. The geometry of the samples was the same as those used for the tensile characterisation, i.e. rectangular strips of 12.5mm width, and 1.55mm thickness.

IV.3.5 Real-time thermographic characterisation

Thermography is a non contact, non destructive technique which provides an image of the distribution of the temperature on the surface of the examined object proceeds by, Using an adapted detector, thermography records the two dimensional ‘‘temperature’’ field as it results from the infra-red radiation emitted by any object. The principal advantage of infrared thermography is its non-intrusive character.

The deformation of solid materials is almost always accompanied by heat release. When the material becomes deformed or is damaged and fractured, a part of energy necessary to initiate and propagate the damage is transformed in an irreversible

way into heat [86, 87]. The heat wave, generated by the thermo-mechanical coupling and the intrinsic dissipated energy during mechanical loading of the sample, is detected by the thermal camera. The stress field has been monitored in relation to the cycles undergone by the sample.

The important material property in radiation heat transfer is the emissivity ε of a test surface. The emissivity indicates the efficiency of a surface as a radiator of electromagnetic radiation. Blackbodies are the most efficient radiators and absorbers of electromagnetic radiation and have an emissivity of 1.0. All other bodies have an emissivity less than 1.0. In order to achieve an emissivity level as close as possible to that of a black body, a uniform coating of water soluble matt black paint was applied on the test samples. This allowed uniform heat transfer into (or from) the subject and produced a reasonably uniform emissivity [88]. All three fatigue stress levels were thermographically monitored for the 20% per weight Al/SiC composite. The thermographic image capture was set to 30 seconds per frame.

IV.3.6 Results

IV.3.6.1 Fatigue testing

In Figure IV.4a, the fatigue behaviour of all studied systems is depicted. All systems exhibit typical S-N behaviour, reaching the fatigue limit before 10^6 cycles, which was set as the run-out point for the fatigue experiments. While the HT1 system failed at approximately the same absolute stress level as the T1 system, the S-N curve of the T6 system was shifted to considerably higher stress values. In this context, the T6 heat treatment yielded higher fatigue strength than both the T1 and HT1 systems. As can be observed, the heat treatment had significant influence on the fatigue response of

Al/SiC composites. This is in agreement with previous observations [60], concluding that the heat treatment is strongly affected by both the static properties, as well as the failure mechanisms during quasi-static tensile loading.

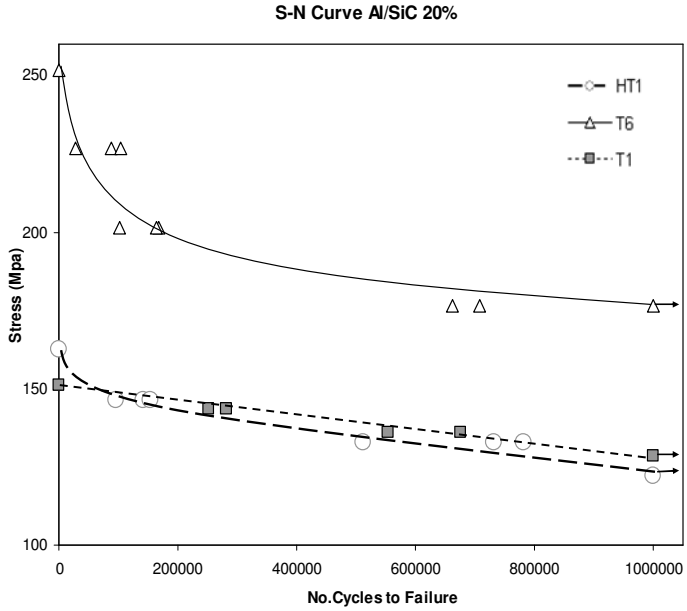

Figure IV.4a. S-N Curve of Al/SiC 20% Composite

In Figure IV.4b, the normalised "S-N" curves of the fatigue response of the Al/SiC composites are plotted for comparative purposes. The stress was normalised over the UTS of each material and plotted against the number of cycles to failure. As can be observed, the situation here was the reverse; whereas in the untreated T1 condition the composite retains at least 85% of its strength as fatigue strength, the corresponding value for the T6 heat treatment is falling to the 70% of UTS. The HT1 heat treatment is exhibiting an intermediate behaviour, with its fatigue strength falling to 75% of the corresponding UTS value. It can be concluded that aggressive heat treatment reduces the damage tolerance of the composites.

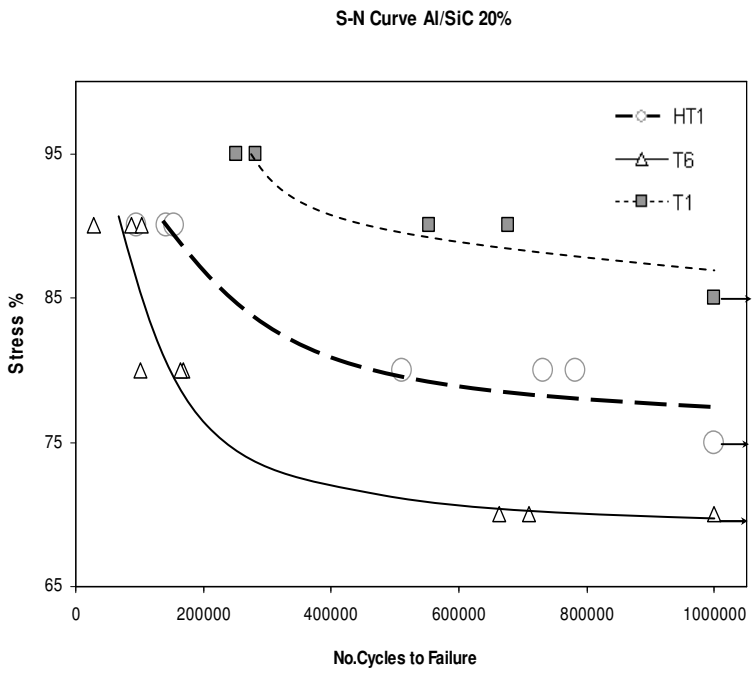

Figure IV.4b S-N Curve of Al/SiC 20% Composite

A direct comparison of the fatigue performance of the composite with the corresponding quasi static performance in tension reveals some interesting details (see Table IV.2). Undoubtedly, the T6 heat treatment improved the strength of the composite. This can be attributed to a dominant mechanism related to the changes in the microstructure of the composite. This mechanism relates to the precipitations appearing in the microstructure of the composite at the vicinity of the interphase area, which results to the composite hardening. The creation of the interphase together with the improved stress transfer may be regarded as the main contributing parameters to the improved mechanical properties of the particulate reinforced composite. The improved static strength is followed by a less spectacular performance in fatigue, with the fatigue limit of the material falling to the 70% of the UTS.

T6 specimens are quite brittle with low ductility compared to the HT1 specimens and therefore, crack initiation appears earlier at high stress levels, where the material's strain capability is not sufficient to impede crack initiation and propagation. This

behaviour can be explained by the presence of high stress concentrations which in their turn are due to the embritllement caused by the precipitates formed in the matrix and interphase areas during the age hardening process. The lower HT1 heat treatment temperatures render the composite substantially more ductile than both the untreated (T1 specimens) and the T6 specimens.

When a crack approaches a reinforcing particle, is either deflected by the hard reinforcement and continues around it, or propagates through the reinforcement by cracking it. In the T6 condition, due to the strengthening of the matrix and interphase region with hard precipitates of Mg_2Si phases, the interface is much stronger. As the crack approaches the interphase area, the crack energy tends to be absorbed by the SiC particles, leading them to fracture and an overall rapid failure. Thus the reinforcement no longer plays the role of stress relief site but behaves in a brittle manner, with the crack propagating through it. In lower stress levels the composite behaves in a different manner as the crack is arrested by the interphase.

IV.3.6.2 Fractography

IV.3.6.2.1 T6 Condition

Fractography has been employed in order to verify the aforementioned mechanisms. In the T6 condition, SiC particles seem to be cracked but not debonded (Figure IV.5a, b) indicating good interfacial bonding. It is usually the larger particles that break because of the higher probability of finding a flaw of critical size and because larger particles may have been cracked during fabrication. The extent of plastic zone ahead of the crack-tip depends on the stress intensity factor. As a result, the number of particles within the elevated stress zone increases, resulting in a larger number volume

of influence and finally to fracture. However, it is unclear that the breaking particles have much of an influence on the fatigue crack growth rate [89].

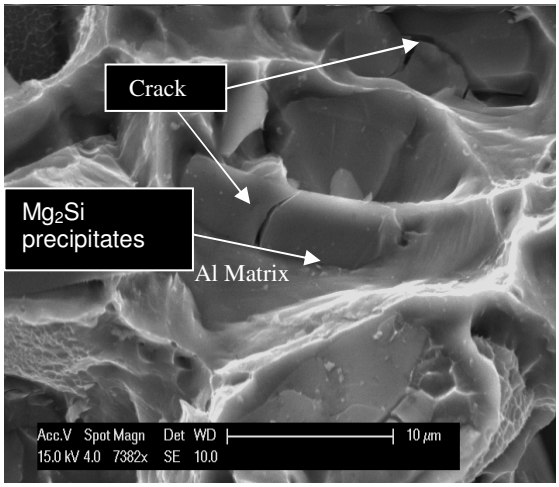

5a

5b

Figure IV.5a. T6 condition-SiC particles cracked but not debonded.

Figure IV.5b. Cracked SiC particles-Mg_2Si precipitates formation.

As the fractographic examination revealed for the T6 condition, the fractured surface at 28000 cycles at 95% of UTS fatigue (Figure IV.6a, b) showed striations formed in the aluminium matrix. This further supports the fact that high local stresses induce plastic flow of the matrix. As shown in Figure IV.6b, crack initiation occurred at the edge of the fractured surface. This was due to the higher defect concentration at the edge of the sample.

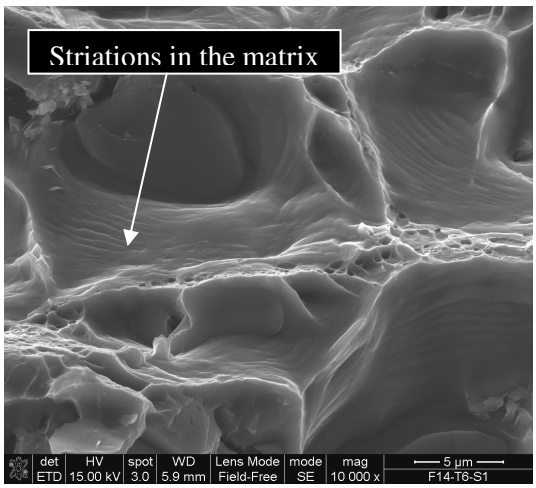

6a

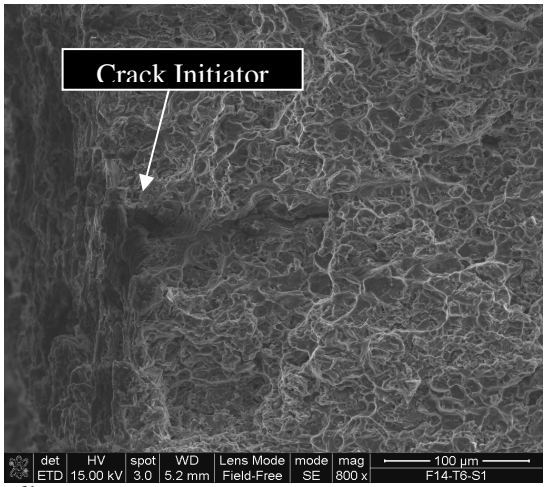

6b

Figure IV.6a. T6 condition sample fractured surface at 226MPa stress level fractures around 28000 cycles-Striations shown in Al matrix.

Figure IV.6b. Crack initiator at edge of fractured surface.

IV.3.6.2.2 HT1 Condition

On the other hand the HT1 specimen exhibited distinctly different behaviour. Fully grown precipitates were also observed, as it was in the case of T6 condition. However, the existence of other phases and especially β` phases, appeared to improve the strength of the composite and most importantly its strain to failure [60]. The composite became more ductile in comparison with the as received one. The fractographic examination revealed that the interface bonding is not as good as in case of the T6 condition. Therefore, both the static and the fatigue strength are lower than for the T6 condition. In this case, the crack is propagated mainly through the interphase region leaving the reinforcement intact (Figure IV.7a, b). The above postulation was validated by the clear evidence of debonded SiC reinforcement and the mark caused by the sliding of the reinforcement on the soft matrix (Figure IV.7b).

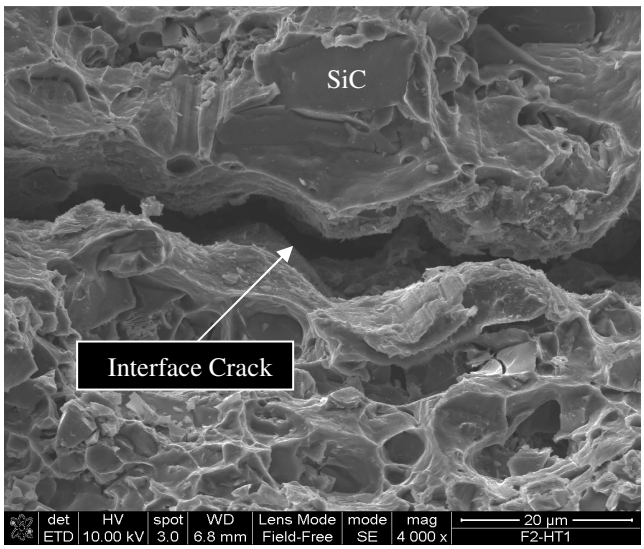

Figure IV.7a. Al/SiC -HT1 condition- cracking through interface.

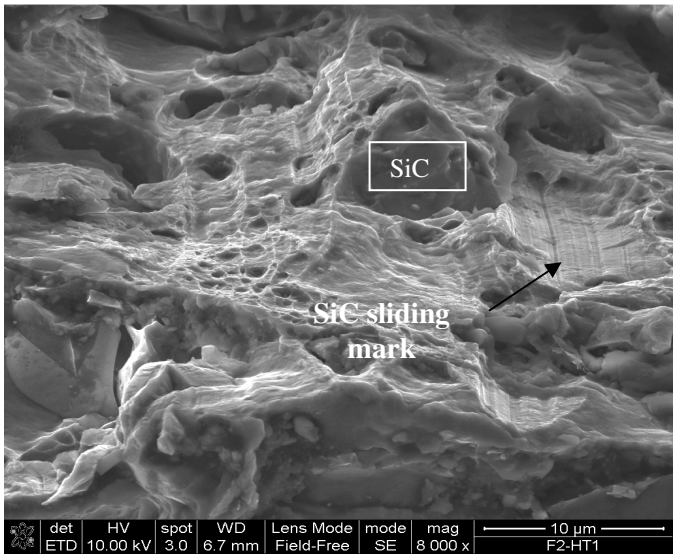

Figure IV.7b. Sliding of SiC on the Al matrix showing weak interface.

The matrix ductility is also clearly indicated by the rippling effect caused by extensive fatigue of the sample (Figure IV.8a). As in the case of the T6 specimen, crack initiation sites were observed at the edge of the specimen surface (Figure IV.8b). Although the ductile nature of the HT1 treatment was obvious in the quasi-static tensile tests, its fatigue behaviour was not improved compared to the untreated T1 condition. On the contrary, the normalized fatigue limit was slightly less for the HT1 condition falling to approximately 75% of the ultimate tensile strength.

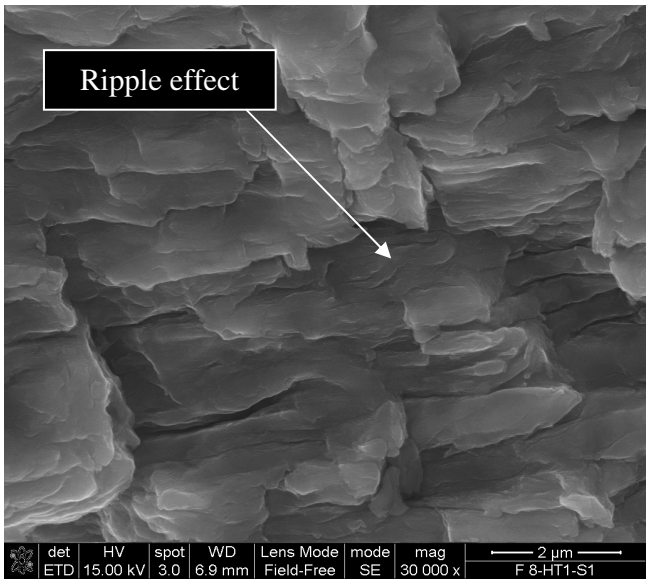

Figure IV.8a. HT1-Sample fractured surface at 133MPa stress level fractures around 782000 cycles-Rippling showing extensive fatigue.

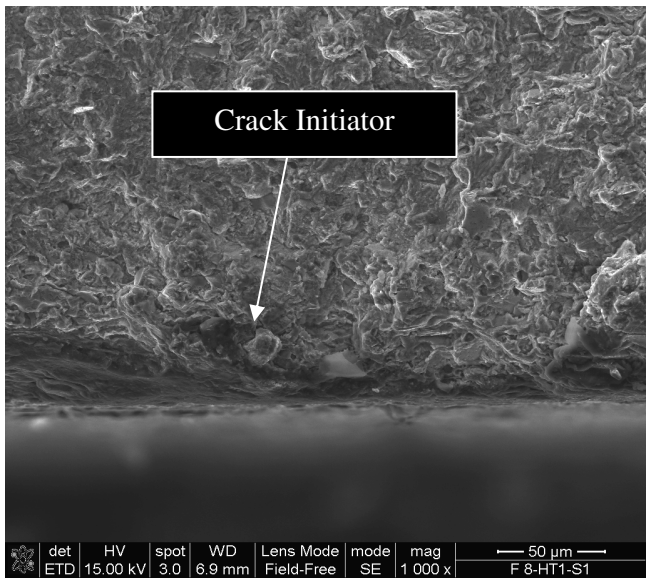

Figure IV.8b. Crack initiator close to surface edge.

IV.3.6.2.3 T1 Condition

The T1 condition composites were the least sensitive to fatigue testing. The T1 specimens exhibited a fatigue limit equal or higher to 85% of the ultimate tensile

strength. As can be seen in Figure IV.9 the composite is clearly dominated by its ductile matrix and the reinforcement plays a secondary role in the fatigue strength. The fractographic examination revealed the existence of coalescence which supports the aforementioned argument. Although the T1 specimens exhibited less ductile behaviour in quasi static tension, this is not mirrored in the fatigue performance of the composites, where the untreated T1 condition performed equally well to the HT1 condition.

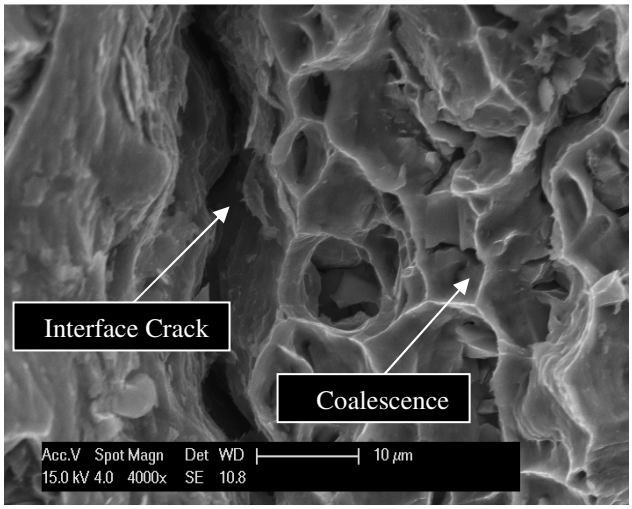

Figure IV.9. T1 condition fatigue sample at 125MPa stress level fractures around 10^6 cycles - Cracking through interface.

IV.3.6.3 Thermography

The thermographic characterisation revealed that the temperature/cycle slope rose more dramatically as the stress field increased. In Figure IV.10a, b, c, thermographic images are presented to demonstrate the development of damage close to the vicinity of the fracture area. As can be seen in Figure IV.10c, just prior to fracture, the plasticity area is clearly delineated on the specimen's surface as a round heated region which may be readily attributed to local plastic deformation.

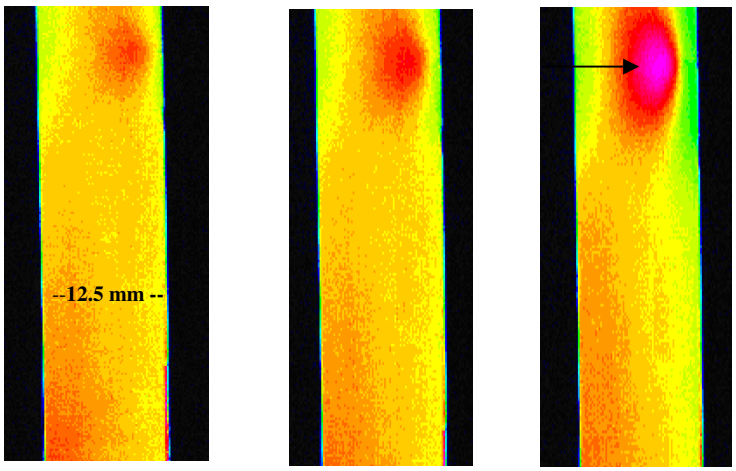

Figure IV.10. Thermographic images of fatigued Al/SiC composite specimen showing the formation of plasticity zone before fracture occurs, (a) at 246500 cycles, (b) at 248600 cycles, and (c) at 251000 cycles, which corresponds to the specimen's fracture point.

This real-time thermographic characterisation allowed the prediction of the fractured location of the specific sample approximately 25 minutes or 4493 cycles before failure. Therefore, thermography monitoring could play an important role in predicting fracture location and time before fracture occurs.

IV.3.7 Conclusions

The tension-tension fatigue properties of Al/SiC composites have been studied as a function of the heat treatment. The possible damage development mechanisms have been discussed. The composites exhibited endurance limits ranging from 70% to 85% of their UTS. The T6 composites performed significantly better in absolute values but their fatigue limit fell to the 70% of their ultimate tensile strength. This behaviour is linked to the microstructure and the good matrix-particulate interfacial properties. In the case of the HT1 condition, the weak interfacial strength led to particle/matrix debonding. In the T1 condition the fatigue behaviour is similar to the HT1 condition although the quasi

static tensile tests revealed a less ductile nature. Thermographic images delineated the plasticity areas in the case of the T6 condition well before the failure of the specimen.

IV.4 Fatigue crack growth behaviour of SiC particulate reinforced A359 aluminium alloy Composites

IV.4.1 Introduction

The investigation of the crack growth behavior of A359 aluminum alloy, reinforced with 31 wt. % SiC particulates is crucial in order to understand the different fatigue crack growth rate characteristics regarding the ageing conditions, and whether the crack propagation relies on microstructural strengthening mechanisms, i.e. precipitation hardening.

Fatigue crack growth tests were conducted in the as received T1 composite material as well as in the HT1 and T6 heat treatment conditions.

The objective is to investigate the influence of heat treatment on the crack growth rate in Al/SiCp composites. Correlation of the effect of heat treatment on the interphase microstructure with the crack growth rate is studied and a novel characterization method based on lock-in thermography has been developed to obtain the crack growth rate versus the range of stress intensity factor.

IV.4.2 Crack growth considerations in MMCs

In the case of particle-reinforced metals, numerous studies have focused on understanding the influence of crack growth rate [78-80] and the reinforcing particles on the matrix microstructure and the corresponding effect on the fatigue behavior of the

metal matrix composites (MMCs) [90]. There are three main mechanisms of fracture: (a) Crack propagation through the matrix without meeting reinforcing particles, (b) intergranular fracture, when the crack propagates through the reinforcement by cracking it, or (c) crack deflection by the hard reinforcement accompanied by interface failure. The different crack propagation mechanisms are illustrated in Figure IV.11.

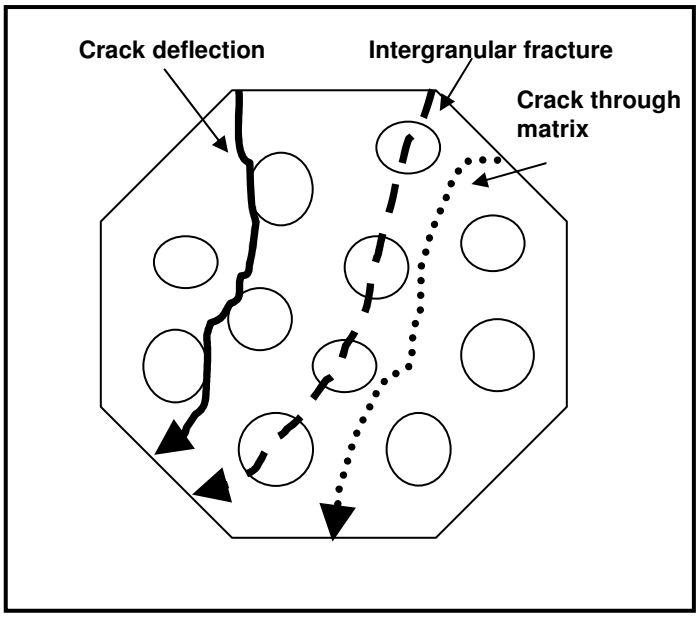

Figure IV.11. Crack propagation mechanisms for SiCp reinforced aluminum matrix composites.

It takes more energy for a crack to propagate through an interface and this is the ideal situation for a material to resist fracture. Stresses arising by the crack propagation are ideally sustained by the interface strength; therefore, the crack requires more energy in order to propagate (Figure IV.12). Precipitation hardening mechanisms can play an important role in strengthening mechanisms and in tailoring the A359/SiCp interface behaviour. The propagation of a crack through the matrix shows good interfacial strength, propagation by cracking the reinforcement indicates higher matrix strength, while propagation through the interface indicates weak interfacial strength.

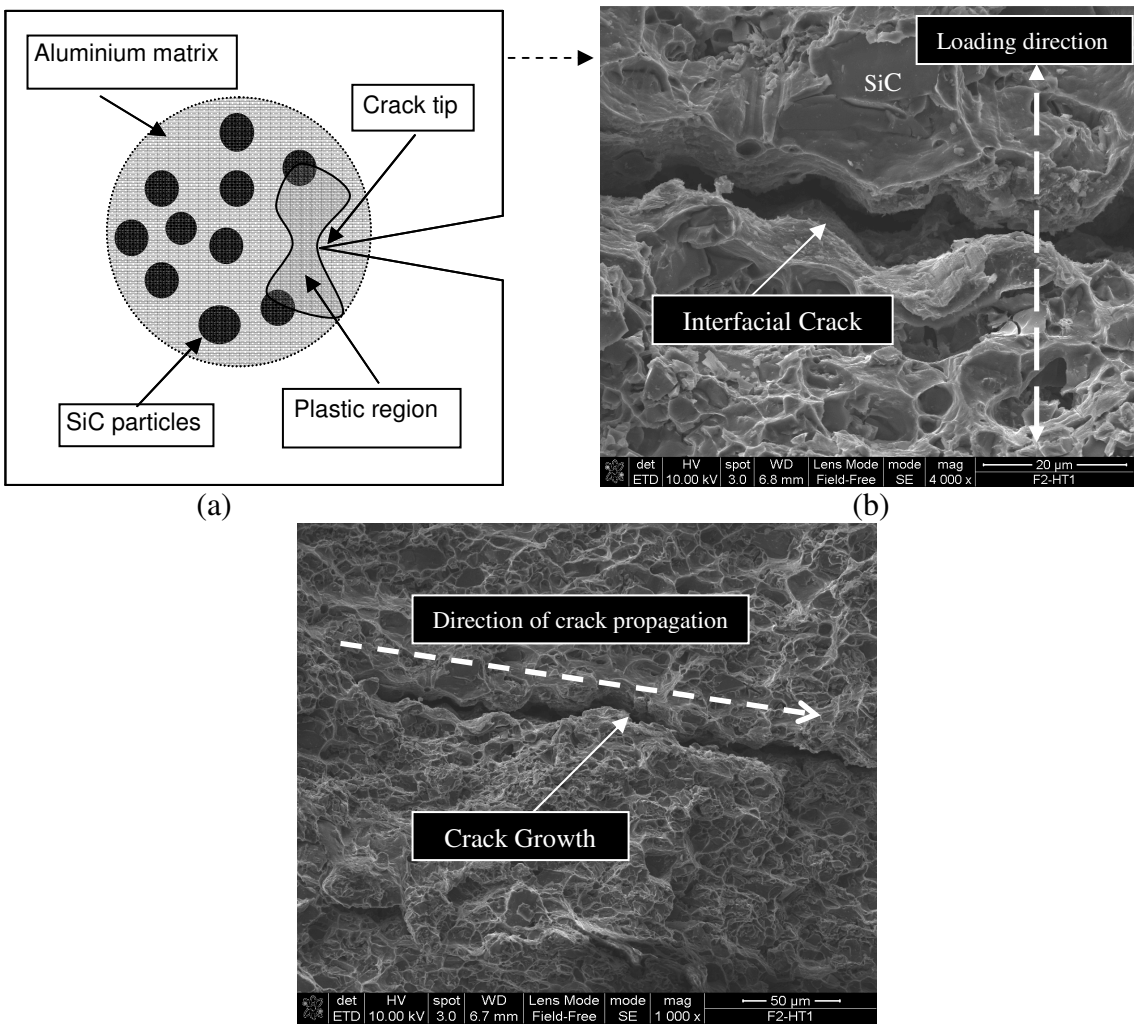

Figure IV.12. Crack propagation through an A359/SiCp -particulate composite: (a) Schematic of a crack propagation through the particulate-matrix interface, (b) SEM fractography image of an interfacial crack, and (c) SEM fractography image at a lower magnification showing crack growth in an A359/SiCp composite

Stress gradients within the matrix/reinforcement interphase region can cause varying levels of stress at which the crack becomes separated or trapped due to different levels of crack closure in the wake of the crack tip. The ideal solution is for the crack to be able to propagate through paths with the highest ductility and strength [91].

IV.4.2.1 Crack Growth Modeling

Fatigue crack growth prediction was recognized and developed into far more quantitative manner in the 1960's when Paris et al. [92] postulated that the range of stress intensity factor, K, might characterize sub-critical crack growth under fatigue loading in the same way that stress intensity factor characterized critical or fast fracture. He examined a number of alloys and realized that plots of crack growth rate against range of stress intensity factor gave straight lines on log-log scales.

This implies that:

$$\log\left(\frac{d\alpha}{dN}\right) = m\log(\Delta K) + \log C \qquad \text{IV.1}$$

Taking out the logarithms in Equation IV.1, it gives:

$$\frac{d\alpha}{dN} = C\Delta K^m \qquad \text{IV.2}$$

Using Paris law expressed in Equation IV.2, it becomes possible to make a quantitative prediction of residual life of a structure with a crack of a certain size. This simply required determining the limits of integration in terms of crack size, which could be done by estimating the final size, which caused fast fracture, from the relationship between the fracture toughness and the crack size (Equation IV.3):

$$K = Y\sigma\sqrt{\pi\alpha} \qquad \text{IV.3}$$

Separation of the variables *a* and *N*, and substitution for the range of stress intensity by the equivalent equation in terms of stress and crack size, gives Equation IV.4:

$$\frac{da}{dN} = C\Delta K^m = C(Y\Delta\sigma\sqrt{\pi\alpha})^m \qquad \text{IV.4}$$

This relationship is, however, applied to crack growth rates in the range of about

10^{-3} mm/cycle to 10^{-6} mm/cycle, and the fatigue crack growth rate curve exhibits a sigmoid shape outside the above range. The lower growth rate region is termed the threshold regime, because growth rates drop off steeply and the crack becomes essentially non-propagating. This represents a change in mechanism from double shear continuum growth to single shear non-continuum growth. The higher growth rate regime is where values of maximum stress intensity in the fatigue cycle are tending towards the fracture toughness and static modes of fracture (i.e. cleavage, intergranular) are adding to the fatigue induced growth rates.

Although Equation IV.4 does not cover the entire curve, it remains a very useful tool, because it covers the range of growth rates most useful to engineering structures, and also an extrapolation into the threshold regime gives a conservative estimate for the remaining life. This approach is crucial to the adoption of defect-tolerance concepts and the implementation of a retirement-for-cause philosophy [93-98].

IV.4.3 Fatigue crack propagation monitoring using infrared thermography

The fatigue crack propagation was monitored using infrared thermography and the crack-tip stress field has been mapped using thermoelasticity principles. The purpose is to develop a new nondestructive methodology based on lock-in thermography for studying the fracture behavior of A359/SiCp composites by determining the crack growth rate of the specimen undergoing fatigue. The new method is also applied for investigating the influence of heat treatment processing on the fracture properties of the material.

The technique is based on the fact that when a solid material is rapidly stressed by external or internal loads and adiabatically deformed, the phenomenon is accompanied by simultaneous variation of temperature. When the material is under tensile load, its

temperature decreases proportionally to the load, however, when it is under compressive load its temperature increases proportionally to the load. This behavior is known as the thermoelastic effect.

IV.4.3.1 Thermoelacticity theory

The thermoelastic effect refers to the thermodynamic relationship between the change of stress in a component under elastic loading and the corresponding change of temperature. It is simply proportional to the change in the sum of the principal stresses, if adiabatic conditions prevail. An experimental setup is used to map the distribution of the sum of principal stresses in the structure [99]. This setup includes a radiometric camera, which measures the infrared radiation produced on the surface of the material undergoing cyclic loading, and a real-time correlator called "lock-in module", which measures the slight change of temperature extracting it from the noise that is specified by the thermal resolution of the camera.

The relationship between the thermal stress and strain in an isotropic, elastic element is given by the following Equation IV.5:

$$\Delta\varepsilon = \frac{(1-2v)\cdot\Delta\sigma}{\mathrm{E}} + 3\ \alpha\ \Delta\mathrm{T} \qquad \text{IV.5}$$

where $\Delta\varepsilon$ and $\Delta\sigma$ represent the change in the sum of principal strains and stresses, respectively ($\Delta\varepsilon$ and $\Delta\sigma$ are invariants). E is the Young's modulus, ν the Poisson's ratio, α is the linear thermal expansion coefficient, and ΔT is the change in temperature in degrees Kelvin.

A thermodynamic analysis of reversible, adiabatic behavior of a stressed, elastic element produces the equation below (Equation IV.6):

$$\Delta T = \frac{-3T\ \alpha\ K\ \Delta\varepsilon}{\rho\ C_v} \qquad \text{IV.6}$$

where T is the absolute temperature, K is the bulk modulus, ρ is the density, and C_v is the specific heat at constant volume.

By using the known relationship between C_v and C_p, the specific heat at constant pressure, equations IV.5 and IV.6 may be combined to obtain the following basic equation describing the thermoelastic effect (Equation IV.7).

$$\Delta T = -\frac{\alpha}{\rho C_p} T \Delta\sigma \qquad \text{IV.7}$$

This relation is only valid if adiabatic conditions prevail. For thermoelastic stress analysis applications, an adiabatic condition is achieved by cyclic loading of the structure, in which case a dynamic equilibrium (i.e., reversibility) is maintained between mechanical and thermal forms of energy. Equation IV.7 is a general thermodynamic equation quantifying temperature changes produced by changes in the applied stress. The minus sign in the equation means that tension (i.e., Δσ positive) produces a decrease in temperature, while compression results in an increase in temperature. The change of temperature is proportional to the change in the sum of principal stresses, if adiabatic conditions exist. The thermoelastic coefficient is then given by Equation IV.8:

$$K_m = \frac{\alpha}{\rho C_p} \qquad \text{IV.8}$$

IV.4.3.2 Lock-in thermography

Thermography is an advanced NDE technique based on the detection of infrared radiation. Lock-in thermography is an active technique in which the sample is subjected to modulated heating. This technique makes use of thermal waves generated inside a specimen and detected remotely by an IR camera. Lock–in refers to the necessity to monitor the exact time-dependence between the output signal and the reference input signal [100]. This is done using a lock–in amplifier so that both phase and magnitude images become available (Figure IV.14).

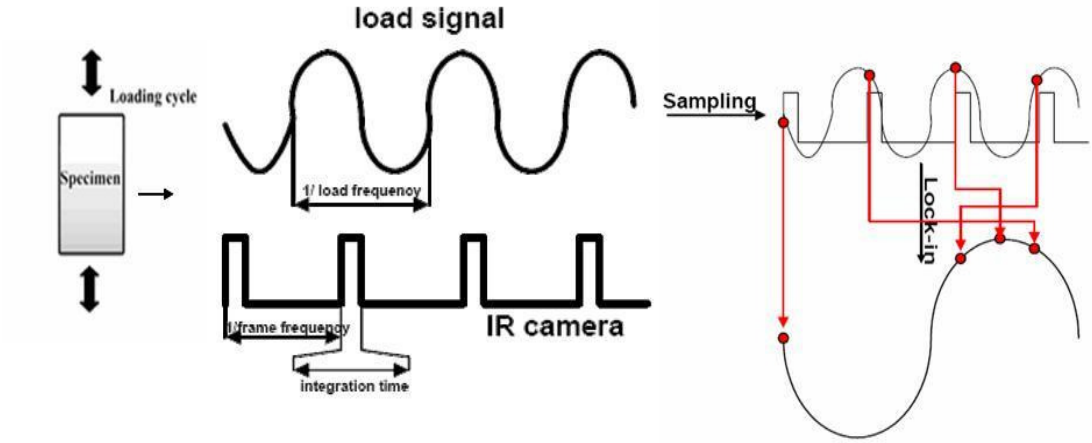

Figure IV.14. Principle of Lock-in Thermography

The principle of lock-in thermography is based on the synchronisation of the camera with the source of heating, which can be optical excitation, ultrasound, cyclic loading of the material, etc. In the case that a specimen undergoes cyclic loading, heat waves are generated and the resulting oscillating temperature field in the stationary regime is recorded remotely through thermal infrared emission. The frequency of modulation varies with the nature, size and shape of the defects to be detected. The IR radation emitted by the specimen during testing depends on the size and shape of the defects to be detected. Using this method, the influence of emissivity and non-uniform heating on the temperature measurement is reduced allowing inspection of large areas of

samples with high repeatability and sensitivity. The size of the area for thermographic imaging is 320x240 pixels with a pitch of 30μm x 30 μm. In the experiments the measurement temperature range was between 5°C - 40°C with a resolution of 20mK and integration time of 100ms. The capability of the camera's integration time is 1500 μs.

IV.4.4 Fatigue Crack Growth Test

To study the crack growth rate (da/dN) vs. stress intensity range (ΔK) data for SiC particulate reinforced aluminium alloy composite system the materials were subjected to cyclic loading. Fatigue crack growth tests were conducted according to the ASTM E647 standard, using a 100 KN servo hydraulic universal testing machine [101].

The tests were conducted under load control. Compact tension (CT) specimens were prepared for the fatigue crack growth experiments. The fatigue tests were conducted in a lower frequency of 1 Hz in order to minimise the effect of sudden failure due to the brittle nature of these materials. The experiments were performed at a load ratio R = 0.25 and maximum load ranges of 3.7 - 4.5 KN, keeping the maximum stress at about 70% of the material's ultimate tensile strength.

The technique used for determining the crack growth rate during the test is based on non-contact monitoring the crack propagation by lock-in thermography. For this reason, an infrared camera was placed at a distance close to the specimen. The model of infrared camera is Cedip Jade III MW (Mid wave) InSb. The camera was connected with the lock-in amplifier and the amplifier with the main servo hydraulic controller. Therefore, synchronization of the frequency through the lock-in amplifier (Cedip R-9902) and the testing machine could be achieved and lock-in images and data capture during the fatigue testing were enabled (Figure IV.15).

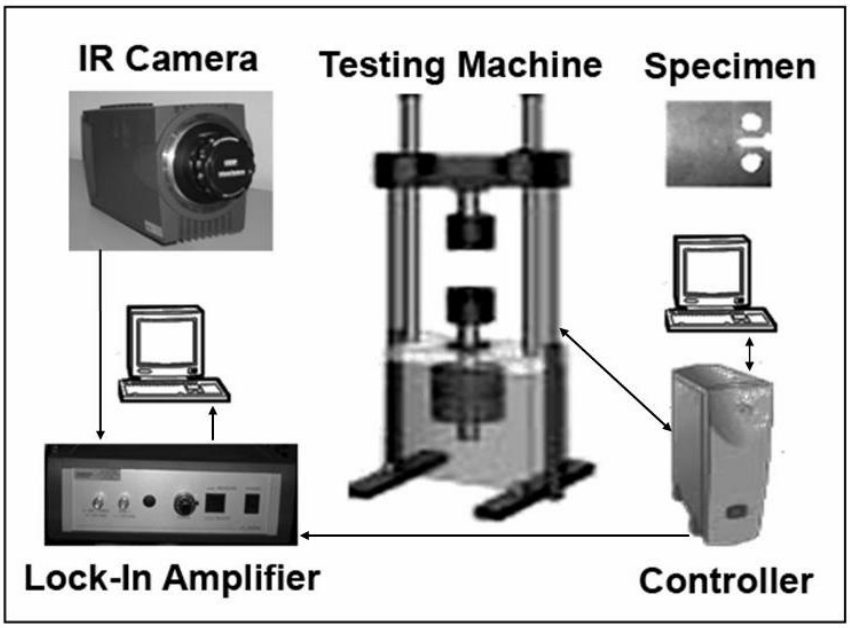

Figure IV.15. Experimental setup for fatigue crack growth monitoring using lock-in thermography

In order to determine crack growth rate using thermographic mapping of the material undergoing fatigue a simple procedure is used:

(a) The distribution of temperature and stresses at the surface of the specimen was monitored during the test. To this end, thermal images were obtained as a function of time and saved in the form of a movie.

(b) The stresses were evaluated in a post-processing mode, along a series of equally spaced reference lines of the same length, set in front of the crack-starting notch. The idea was that the stress monitored at the location of a line versus time (or fatigue cycles) would exhibit an increase while the crack approaches the line, then attain a maximum when the crack tip was on the line. Due to the fact that the crack growth path could not be predicted and was not expected to follow a straight line in front of the notch, the stresses were monitored along a series of lines of a certain length, instead of a series of

equally spaced points in front of the notch. The exact path of the crack could be easily determined by looking at the stress maxima along each of these reference lines.

Four lines of the same length, equally spaced at a distance of 1 mm, were set on the thermal images of the CT specimen, as shown in Figure IV.16a, b, and c. The length of each line is 10 mm long. Line A was set at a distance of 17 mm from the specimen's notch, line B at 18 mm, line C at 19 mm, and line D at 20 mm.

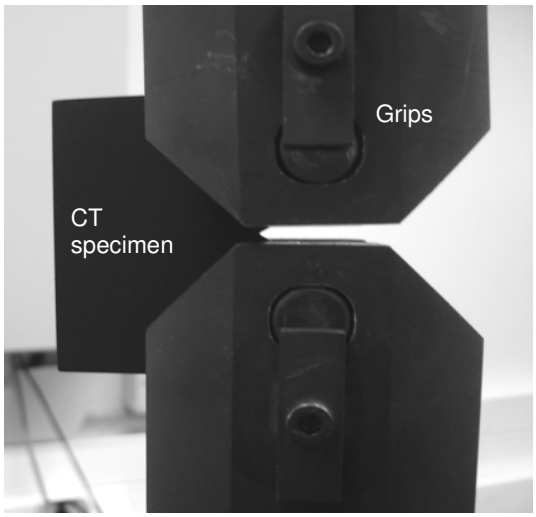

Figure IV.16a. Optical image of the CT specimen on the grips.

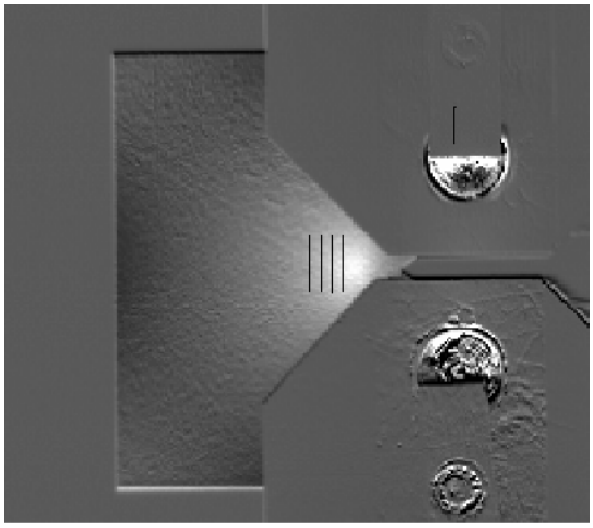

Figure IV.16b. Thermal image of the CT specimen with the four lines set.

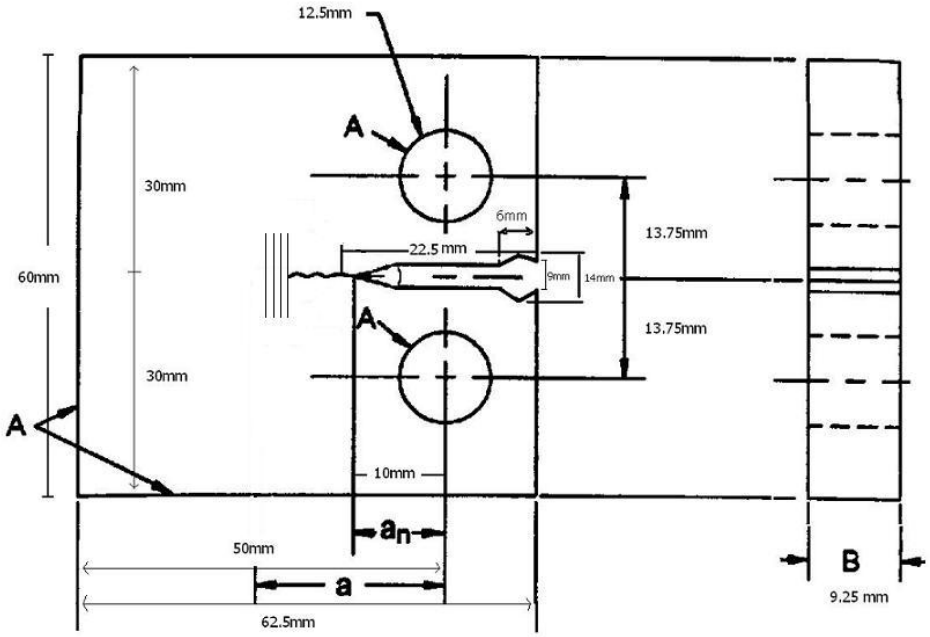

Figure IV.16c. Schematic of CT specimen showing 4 lines vertical to the crack's propagation direction, set at regular distances in front of the notch.

IV.4.5 Results

IV.4.5.1 Crack growth rate vs. range of stress intensity

In Figure IV.17, the crack growth rate for the heat treated composite specimens are plotted on a logarithmic scale as a function of the stress intensity range. Results, shown indicate the intermediate values of crack growth rate, which are between (10^{-2} to 10^{-5} mm/cycle). The results show that the heat treatment processing influences crack growth behaviour of the composite materials. Specimens subjected to T6 heat treatment condition exhibit the highest crack growth rate vs. stress intensity range slope compared to the other composite systems.

Moreover, the crack growth rate vs. stress intensity range line of specimens subjected to T6 heat treatment was shifted towards higher ΔK values compared to that

from specimens subjected the other two heat treatment conditions. This implies that in order to attain the same crack growth rate, higher stress intensity factor is required for specimens subjected to T6 condition compared to those subjected to T1 and HT-1 conditions. The need for higher stresses for a crack to propagate reveals the material's microstructural strength, where micro-mechanisms such as precipitation hardening promote high stress concentrations at the crack tip, resulting in the toughening of the crack path. The above postulations agree with previews results [61], where the T6 heat treated composites showed superior strength but the lowest ductility compared to T1 or HT-1 heat treated specimens.

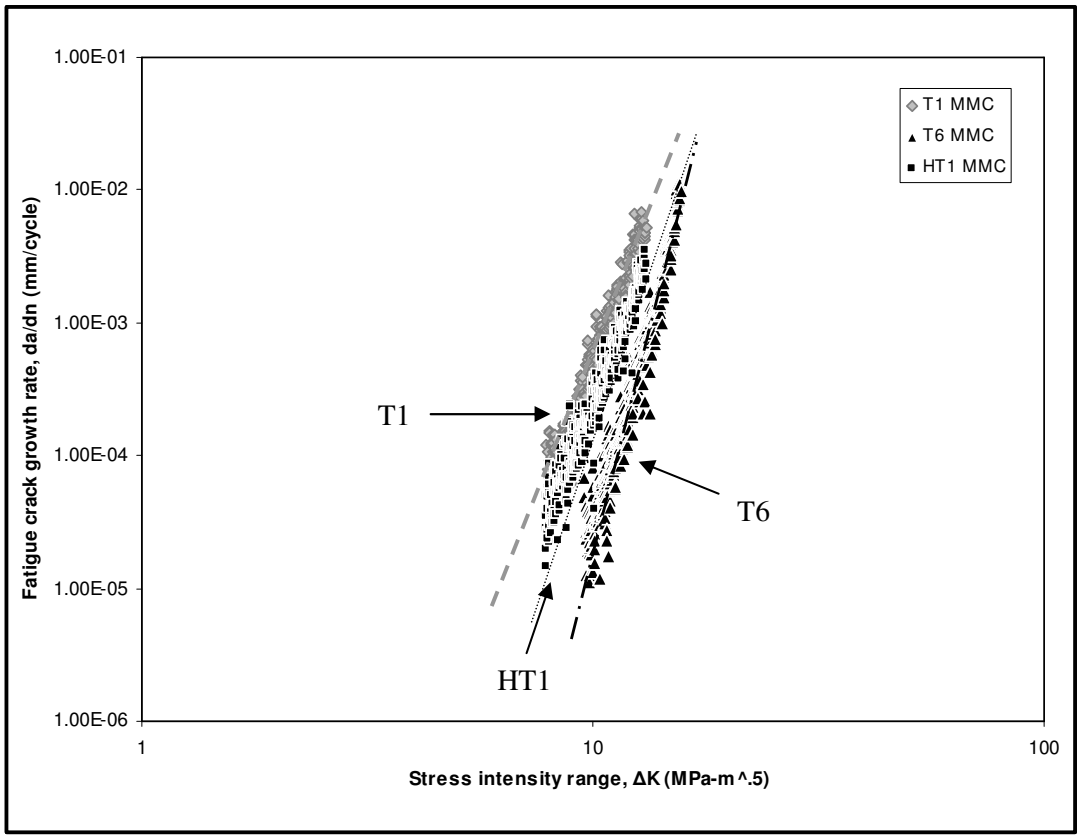

Figure IV.17. Da/dN vs. ΔK plots of Al/SiCp composite in three heat treatments.

IV.4.5.2 Non-contact crack growth rate monitoring using lock-in thermography

Using the procedure described in the previous section, the local stress versus time was measured along each of the four reference lines placed in front of the notch (Figure IV.17a). The maximum value of stress versus the number of fatigue cycles was then plotted for the four different lines (Figure IV.17b). As expected, Figure IV.17a shows that the local stress, monitored at the location of each line, increases while the crack is approaching that line, then attains a maximum when the crack tip is crossing the line. Finally, after the crack has crossed the line, the local stress measured at the location of the line decreases. This is also expected, since the stress values shown in Figure IV.17a are maximum stresses from all the locations along the particular line. At the exact position on a line where the crack has crossed, the local stress is off coarse null. Figure IV.17b shows an example of the maximum stress monitored along a reference line, in this case Line D, for a specific time, corresponding to a certain number of fatigue cycles of 13000 cycles. The total maximum values measured along a line for different number of cycles are plotted versus the number of cycles, as shown in Figure IV.17a for four different reference lines.

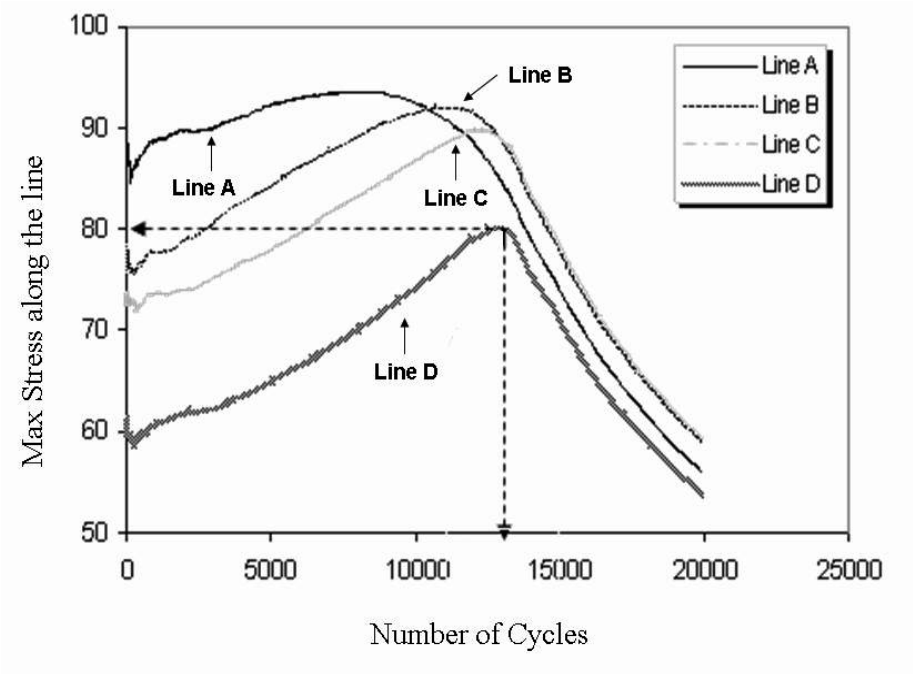

Figure IV.17a. Maximum Stress along the four reference lines vs. fatigue N cycles.

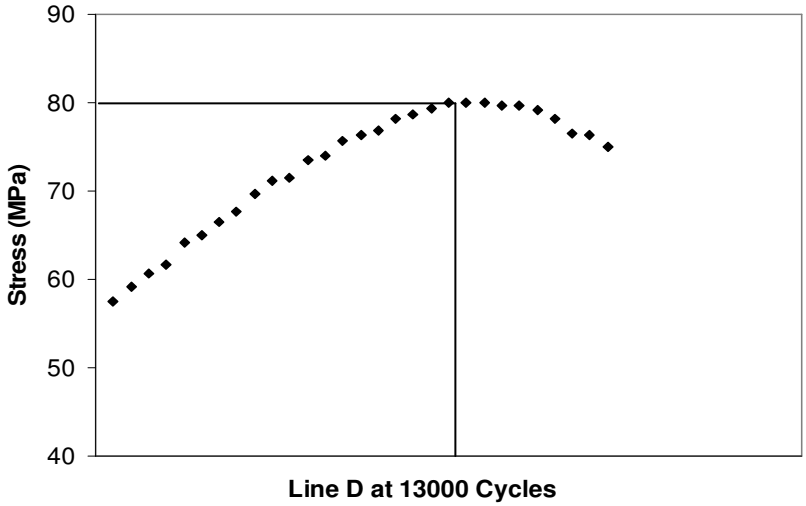

Figure IV.17b. Example of stress monitored along a reference line for a specific time, corresponding to a certain number of fatigue cycles.

The actual thermographic images shown in Figure IV.18. correspond to the 4 different reference lines showing the crack propagation length and the stress field for each of these lines. It can be clearly seen that as crack propagates the stress field

changes accordingly (clearly shown with white areas formed on the specimen) through each individual line.

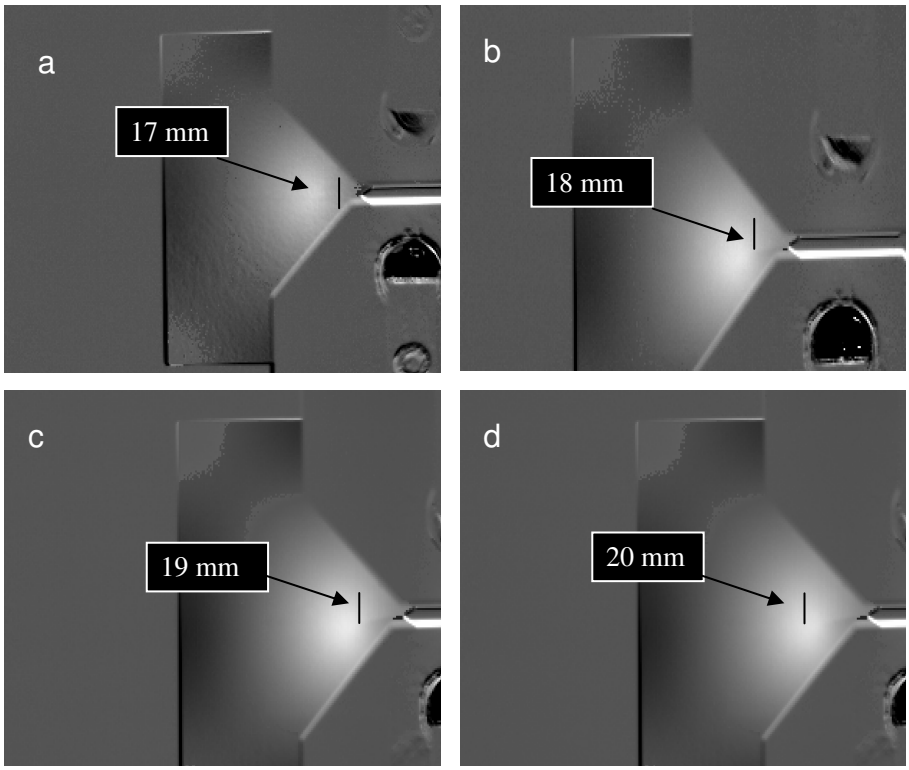

Figure IV.18. Thermographic images correspond to the 4 different reference lines showing the crack propagation length and the stress field for each of these lines

The moment the crack crosses a particular reference line, denotes the occurrence of a stress maximum, and corresponds to a specific fatigue cycle. In this way, the points on the line of crack crossing that particular reference line are determined, as well as the fatigue cycles for which the crack has crossed the specific reference line. Using these data, enabled estimation of the crack path as well as the crack growth rate.

From the maximum stress versus fatigue cycles curves for each reference line shown in Figure IV.17a, the crack lengths versus the number of fatigue cycles were determined for A359/SiCp composites heat treated in three different conditions; T1, T6, and HT-1 (Figure IV.19). As it is shown in Figure IV.19, the crack growth rate was

found to be rather linear for all heat treatments. It is shown that the crack growth linear slope in both systems T1 and T6 is similar, but for the T6 condition the number of cycles required for the crack to be initiated is less than the T1 condition. On the other hand, there is a small change of the linear slope for the HT-1 heat treated sample, showing increased ductility which indicates that it needs more time (i.e., number of cycles) for the crack to grow in this case. For the T6 heat treatment, the results depict a brittle behavior, as the crack starts to grow earlier than in the other two cases, supporting evidence of brittle behaviour [58].

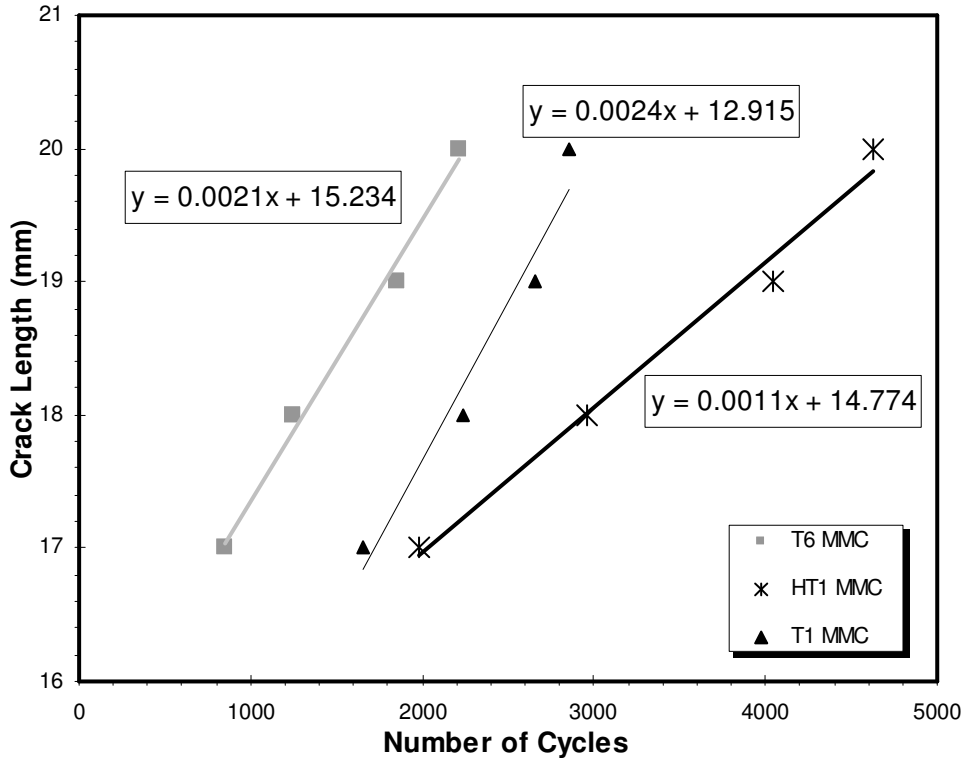

Figure IV.19. Crack length vs. cycles plots from lock-in thermography data for A359/SiCp composites subjected to three different heat treatment conditions

The data obtained using lock-in thermography, as shown in Figure IV.19, were correlated with crack growth rate values obtained by the conventional compliance method. Figure IV.20, show crack growth rates determined by the conventional

compliance method versus the lock-in thermography method for A359/SiCp composites, as received, T6 heat treated, and HT-1 heat treated, respectively. Looking at these figures, one can observe that that there is a good correlation between the two methods for determining crack growth rate.

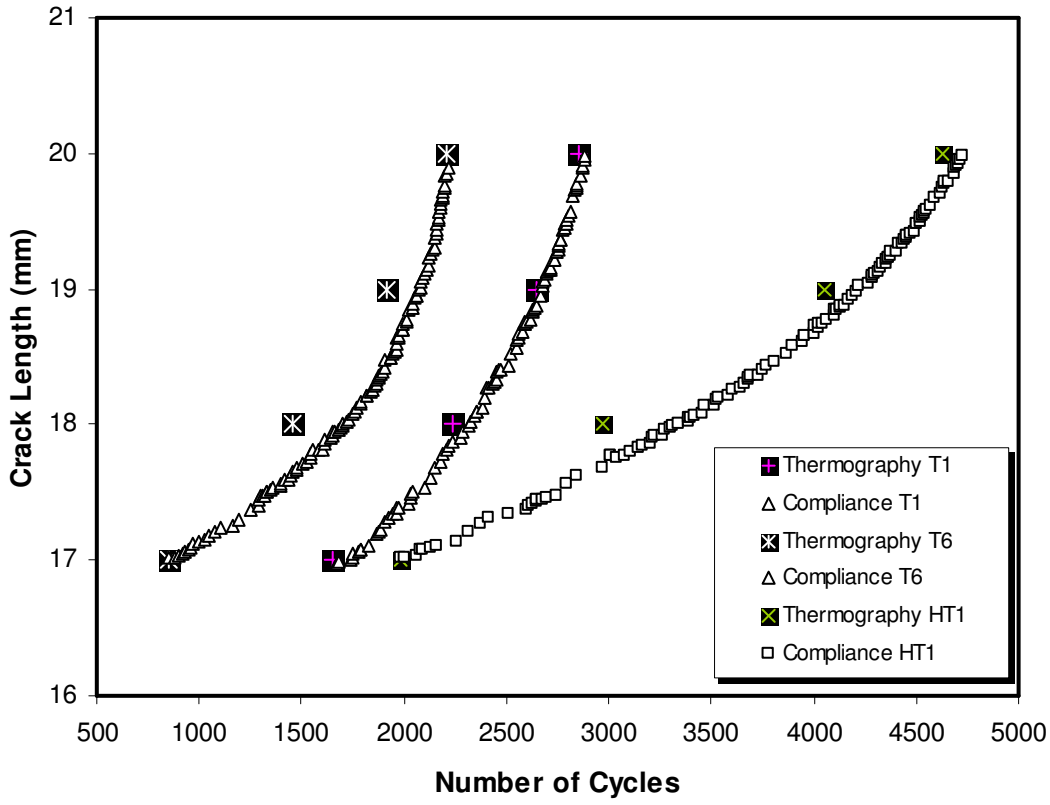

Figure IV.20. Crack growth rate determined by the compliance vs. thermography methods for A359/SiC_P composite in as received (T1), T6 and HT1 heat treatments

The actual difference between the values determined with the two methods is only of the order of about 50 cycles. Given the fact that the IR camera acquires a signal at a rate 20 times faster than the controller of the fatigue machine, it is expected that the thermographic measurement is more accurate in respect to the cycles, than the

compliance measurement made by the fatigue machine. At the center of the test this difference is more accentuated than at the beginning or the end of the experiment.

IV.4.5.3 Estimation of da/dN vs. ΔK relationship using thermography and compliance methods

Using the thermographic mapping procedure described in section IV.4.5 and IV.4.5.2, an estimation of da/dN vs. ΔK relationship using thermography and compliance methods is determined.

The stress intensity range was further calculated by the data shown in Figure IV.17a. ΔK values have been estimated from the stress maxima versus fatigue cycles curves for each reference line. Each of the four lines provides a stress intensity range and a da/dN value. The data obtained using lock-in thermography, were correlated with crack growth rate values obtained by the conventional compliance method and calculations based on the Paris law.

Furthermore, the da/dN vs. ΔK curves steaming from the compliance method were plotted in the same graph, for comparison purposes, with those obtained using lock-in thermography. It can be seen in Figure IV.21 that the two different methods are in agreement, demonstrating that lock-in thermography is a credible nondestructive method for noncontact evaluation of the fracture behavior of materials.

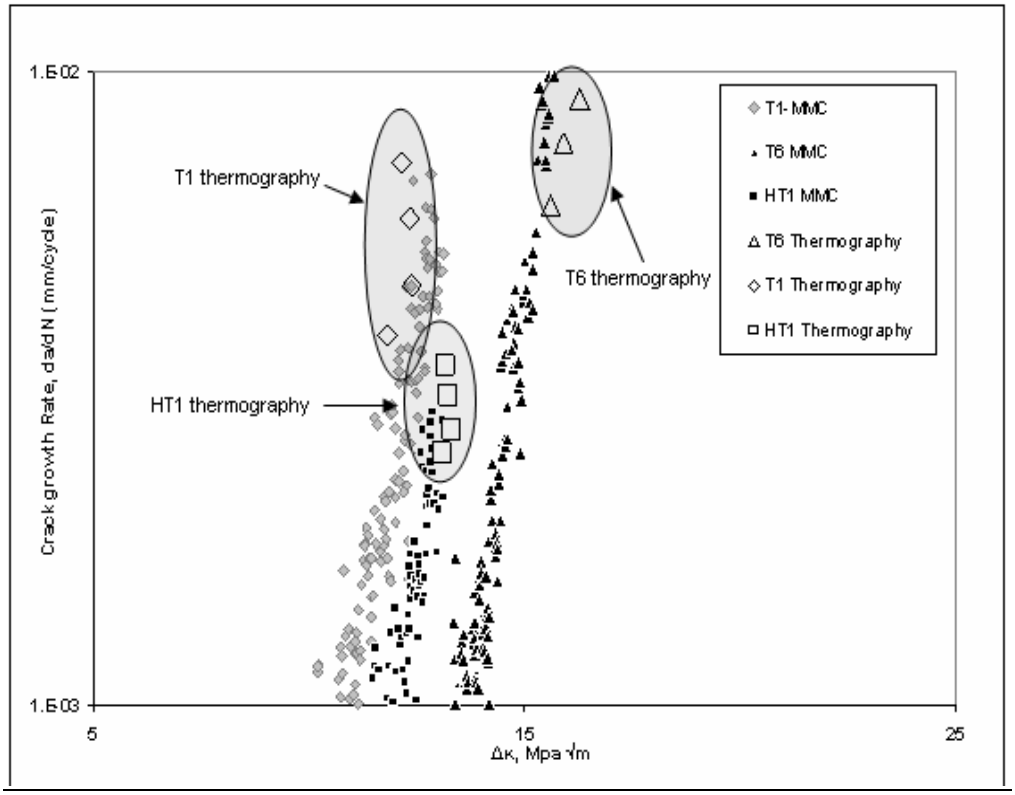

Figure IV.21. Da/dN vs. ΔK in Al/SiCp specimens: Thermography vs. Compliance method.

IV.4.5.4 Microstructural examination (Fractography)

The fractured surface of the CT samples was examined with the help of scanning electron microscopy in order to investigate the effect of microstructure on the fracture behavior of the tested materials. Fractography of the rapid overload fracture region in the Al/SiCp composites did show some particle fracture, mostly in the T6 heat treated specimens. This is in accordance with previous observations, where T6 heat treatment was found to enhance interfacial, as well as matrix, strength leading to crack propagation or relief though the reinforcement [102]. As shown in Figure IV.22a, in the T6 heat treatment condition, SiC particles seem to be cracked but not debonded, indicating good interfacial bonding. The cracking of the larger particles could be due to the fabrication process as well as to the higher probability of a flaw of critical size to

meet them. In the HT-1 heat treatment condition, shown in Figure IV.22b, cracking was identified through the interface region. This is not the desired propagation route since the interface has to remain uncracked to sustain the stresses arising from the approaching crack. The as-received condition T1, shown in Figure IV.22c, shows some coalescence microvoids, evidence of ductile behavior. The examination of the microstructure provides evidence that the heat treatment clearly improves the crack growth behavior of the composites. This is related to a precipitation hardening mechanism mainly due to the accumulation of precipitates at the interphase region.

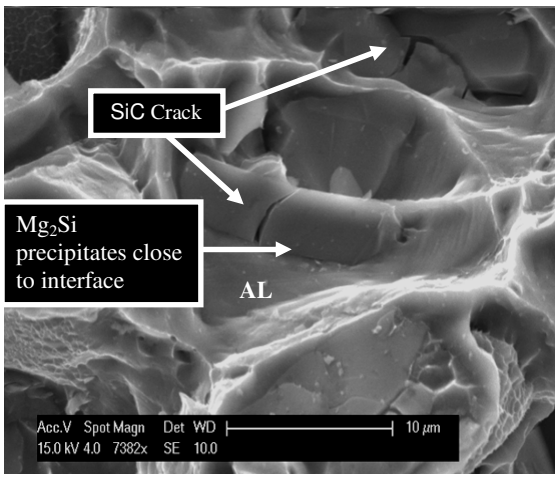

Figure IV.22a. T6 heat treatment condition: SiC particles cracked but not debonded.

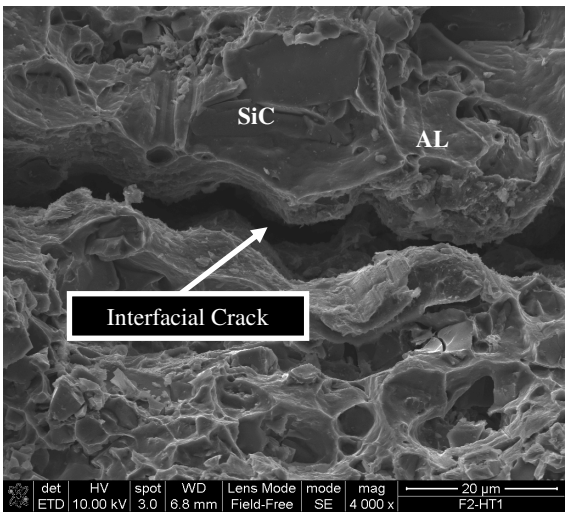

Figure IV.22b. HT-1 heat treatment condition: cracking through the interface.

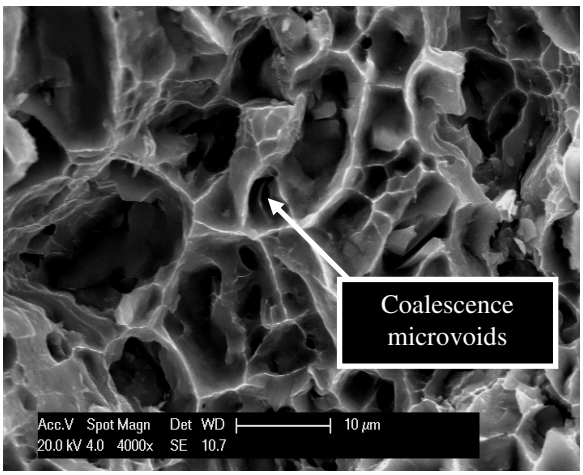

Figure IV.22c. As received condition: Presence of coalescence microvoids indicating ductile behavior.

IV.4.6 Discussion

The results on crack growth using this approach were found to be in agreement with those obtained by the conventional compliance method. The heat treatment, and especially the T6-aged condition, had a significant influence on the rate of crack propagation and the stress intensity factor. Furthermore, different fatigue crack growth rate characteristics were observed for the different heat-treated composite systems when compared to the base aluminum alloy. This is mainly due to the fact that the fatigue crack growth path depends on ageing conditions, and the crack propagation relies on microstructural strengthening mechanisms, i.e. precipitation hardening. Furthermore, interfacial decohesion and particle fracture phenomena have been observed by means of fractography.

The crack in these specific experiments was propagating in a straight line. However, the technique is equally applicable regardless the cracks propagating in a straight line or not because it is based on detecting the presence of cracks due to modifications of the stress fields ahead of the crack tip and not of optical observation of

the actual crack. This technique is capable of detecting surface as well as subsurface cracks in the material.

It has been demonstrated that heat treatment strongly influences the interfacial properties of the composite, which in turn have a considerable effect on the crack growth behavior. By appropriate heat treatment, the fracture behavior of the material can be tailored and the fatigue crack growth rate can become either faster or slower (i.e. the material can become less or more ductile). The microstructure of the interphase region was also found to play a significant role in the crack growth behavior of particulate-reinforced composites. In this sense, T6 heat treated Al/SiCp composite samples exhibited better interface bonding behavior than the other composite systems. The above observations have been further supported by metallographic examination of the fractured surfaces.

The fatigue crack growth curves revealed an approximately linear, or Paris law region, fitting the function $da/dN = C\ \Delta K$. Crack growth rate vs. stress intensity range curves have been obtained using lock-in thermography. These results were found to be in agreement with crack growth rate measurements using the conventional compliance method and calculations based on the Paris law. It became, therefore, evident that lock-in thermography has a great potential for evaluating non-destructively the fracture behavior of composite materials.

This new methodology can be dominant in situations when the compliance method cannot be used, e.g., crack growth in structures such as air wings and turbine engines during real-time applications, where nondestructive thermographic evaluation can be effective in monitoring crack propagation. The newly developed technique shows great potential in monitoring the crack growth rate of materials in regard to the crack depth, crack propagation time and path. The significant capability of this

technique is the detection and monitoring of crack growth, even if it is not visible on the specimen's surface and propagates inside the material.

IV.5 Effects of Heat Treatment on Microstructure and the Fracture of SiC particulate reinforced A359 aluminium alloy Composites

IV.5.1 Introduction

The fracture toughness behaviour of SiC particulate reinforced A359 aluminium alloy composite with 31 wt. % SiC particulates subjected to different heat treatment conditions has been examined. Unreinforced aluminium alloy fracture properties have been also determined for reference purposes. Infrared thermography was used to monitor the plane crack propagation behaviour of the materials and validate the fracture toughness testing. As expected, the obtained K_{IC} values were found to be lower than those of the unreinforced matrix alloy.

However, heat treatment considerably improved the fracture toughness of the composites. In particular, the specimens heat treated under the T6 condition exhibited enhanced fracture toughness compared to the other two conditions. This behaviour can be attributed to a mechanism related to alterations in the microstructure at the vicinity of the interface induced by the heat treatment. This mechanism was associated with precipitates accumulated at the interfacial region resulting in material hardening.

IV.5.2 Fracture Toughness considerations for SiC particulate reinforced aluminium alloy Composites

The major drawback of the inclusion of the ceramic reinforcement in aluminium matrix composites is their tendency to brittle behaviour, i.e. low fracture toughness

values. This is attributed to the brittle nature of the ceramic reinforcement in an otherwise ductile matrix [103-109]. In the case of particulate-reinforced metal matrix composites (MMCs), the microstructure-dependent fracture mechanisms and their correlation to the macroscopical mechanical behaviour are not yet well understood. Furthermore, while performing fracture mechanics studies in such materials, it is rather difficult to satisfy specific validity criteria. Therefore, the provisional fracture toughness, K_Q, is often quoted instead of the plain strain fracture toughness, K_{IC}.

The mode I plain strain fracture toughness, K_{IC}, is a material property characterising its resistance to fracture under the following conditions: i) a sharp crack is present under tensile loading, ii) in the vicinity of the crack's front triaxial plane strain conditions occur and iii) the plastic region at the crack-tip is small compared with the crack size and the specimen dimensions. A valid K_{IC} value provides a lower limit for fracture toughness, and is a key parameter for estimating the relationship between failure stress and defect size for a material under similar in service stress state [110].

At present, there are no standard fracture toughness testing methods specifically for MMCs. Therefore, conventional standards for metals such as the ASTM E399 are normally employed [111]. Some of the problems associated with interpreting toughness test results on MMCs have been considered by Goolsby and Austin [112] who concluded that very few results appearing the literature met the ASTM E399 validity criteria. The main reasons for failing to obtain valid K_{IC} values were largely due to excessive crack curvature, non-linearity of the load-displacement curve, or out-of-plane crack propagation.

To further understand the mechanisms involved in the fracture toughness of MMCs, microstructural strengthening mechanisms such as precipitation hardening, need to be considered. The strengthening micromechanical mechanisms of MMCs are very complicated due to the several parameters involved. The use of particulate

reinforcement is not always successful in improving antagonistic mechanical properties of the MMC and thus enhances the overall material mechanical behaviour of the composite. This is attributed to the brittle nature of the reinforcement which usually deteriorates properties, such as the fracture toughness.

Some of the factors affecting significantly the fracture properties of particulate MMCs, are the particle size, interparticle spacing, and volume fraction of the reinforcement [113-114]. Moreover, the fracture toughness values of particulate MMCs can be influenced by complex microstructural mechanisms such as precipitation hardening achieved by heat treatment processing. The appropriate heat treatment leads to the precipitation of distinct phases in the matrix material which lead to the improvement of interfacial strength of the composite, and subsequently the enhancement of the overall strength of the material [115].

The understanding of the influence of the microstructure at the vicinity of the interface on the fracture behaviour of particulate-reinforced aluminium alloy matrix composites is crucial, therefore experiments have been conducted. Furthermore, a novel approach was applied to characterise the fracture behaviour of the particulate composites. Infrared thermography was used to monitor the plane crack propagation behaviour of the materials.

IV.5.3 Fracture Toughness K_{IC} Testing

The plane strain fracture toughness test involves the loading to failure of fatigue pre-cracked, notched specimens in tension or in three-point bending. The calculation of a valid toughness value can only be determined after the test is completed, via examination of the load-displacement curve and measurement of the fatigue-crack

length. The provisional fracture toughness value, K_Q, is first calculated from the following equation IV.8:

$$K_Q = \left(\frac{P_Q}{BW^{1/2}} \right) \cdot f\left(\frac{a}{W} \right) \qquad \text{IV.8}$$

where P_Q is the load corresponding to a defined increment of crack length, B is the specimen's thickness, W is the width of the specimen, and f(α/W) is a geometry dependent factor that relates the compliance of the specimen to the ratio of the crack length and width, expressed as follows (Equation IV.9):

$$f\left(\frac{a}{W} \right) = \frac{(2 + a/W)(0.86 + 4.64a/W - 13.32a^2/W^2 + 14.72a^3/W^3 - 5.6a^4/W^4)}{(1 - a/W)^{3/2}} \qquad \text{IV.9}$$

Only when specific validity criteria are satisfied, the provisional fracture toughness, K_Q, can be quoted as the valid plane strain fracture toughness, K_{IC} [110].

The standard used for conducting this experiment, i.e. ASTM E399, imposes strict validity criteria to ensure that the plane strain conditions are satisfied during the test. These criteria include checks on the form and shape of the load versus displacement curve, requirements on specimen's size and crack geometry, and the 0.2% proof strength values at the test temperature. Essentially, these conditions are designed to ensure that the plastic zone size associated with the pre-crack is small enough so that plane strain conditions prevail, and that the linear elastic fracture mechanics approach is applicable.

Fracture toughness tests were conducted using a 100 KN servo-hydraulic universal testing machine with data acquisition controller. The system was operated on load control for the fatigue pre-cracking stage, and on position control for the crack opening displacement (COD) testing. The fatigue test for pre-cracking was conducted at

a frequency of 1 Hz, at a load ratio R = 0.25 and load range of 3.7 - 4.5 KN according to the materials' ultimate tensile strength. The COD was monitored by a clip gauge attached to the specimen with a testing rate set at 1 mm/min. Moreover, a thermal camera was set for thermographic monitoring of the crack opening displacement. Compact tension (CT) specimens were prepared for fracture toughness tests according to ASTM E399; the CT specimen geometry is shown in Figure IV.23. The thickness B of the specimens was 9.2 mm for the MMC, and 5 mm for the unreinforced aluminium alloys.

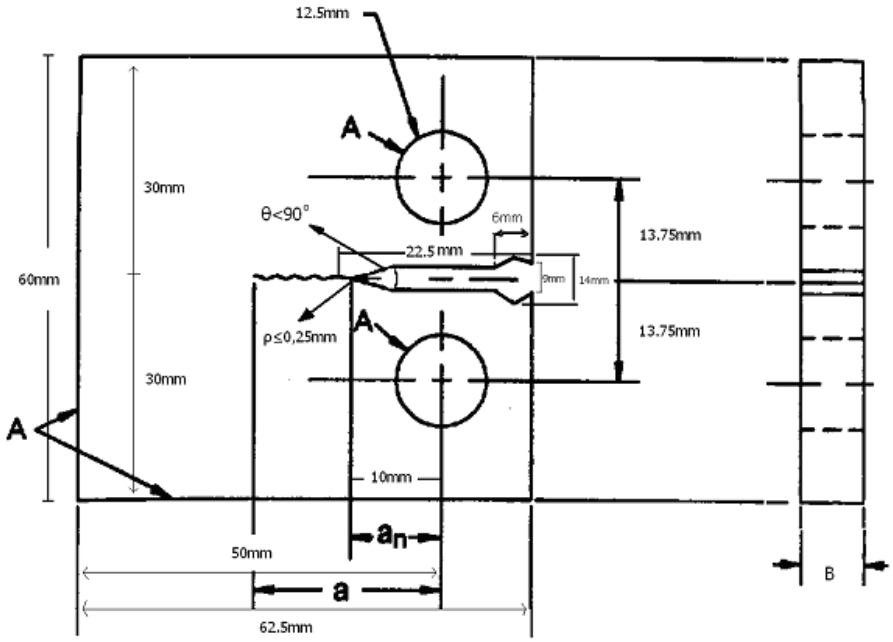

Figure IV.23. Fracture Toughness CT specimen geometry according to ASTM E399 standard.

IV.5.4 Results and discussion

IV.5.4.1 Fracture toughness, K_{IC}

Provisional K_Q values were calculated according to ASTM E399 standard for all specimens according to Equations (IV.8) and (IV.9), where $P_q = P_{max}$. Load versus displacement curves for Al/SiCp composites and unreinforced aluminium alloys are shown in Figure IV.24. Fracture toughness data for Al/SiC_p and unreinforced aluminium alloys are summarised in Table IV.4.

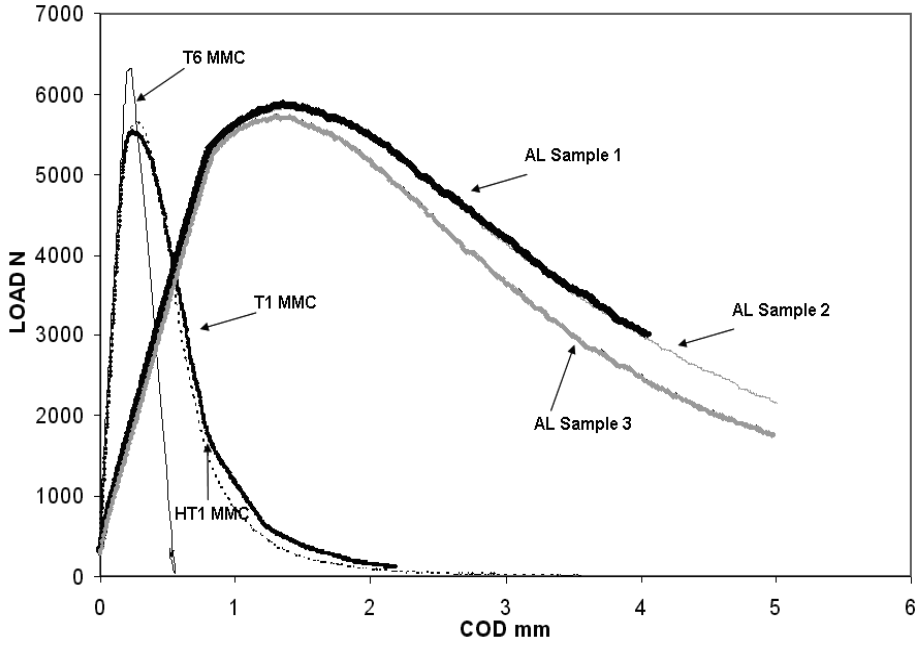

Figure IV.24. Load – Displacement curves for Al/SiCp composites subjected to T1, T6 and HT-1 heat treatment conditions and three unreinforced aluminium alloy samples.

Material	Heat Treatment	E (GPa)	$Rp_{0.2}$ (MPa)	B (mm)	a/W	α_{eff} (mm)	K_Q (MPa √m)	Valid	Reason
2000 series Al	AR	71	75	5.10	0.552	27.62	55,36	No	2**
2000 series Al	AR	71	78	5.13	0.555	26.76	56,00	No	2**
2000 series Al	AR	71	72	5.00	0.558	28.43	58,48	No	2**
A359/SIC/31p	T1	108	158	9.20	0.456	20.79	19,28	Yes	-
A359/SIC/31p	T6	116	290	9.21	0.462	20.12	22,05	Yes	-
A359/SIC/31p	HT1	110	155	9.20	0.467	21.33	20.75	Yes	-
A357/SIC/20p [16]	-	-	215	-	-	-	18.60	-	-
A359/SIC/10p [16]	-	-	300	-	-	-	17.40	-	-

1 Excessive crack curvature

2 Thickness criteria not satisfied

3 Excessive plasticity

4 a/W out of range

5 Non-symmetrical crack front

6 In plane crack propagation

Table IV.4. Fracture toughness data for Al/SiCp and Al alloys and test validity.

As is shown in Table IV.4, Al/SiC_p composites exhibited lower provisional K_Q values than the reference unreinforced aluminium alloys. In addition, heat treatment processing, and especially T6 treated specimen, had the highest K_Q values compared to the other two heat treatment conditions. According to the load-displacement curves in Figure IV.24, composites clearly showed more brittle behaviour than the unreinforced aluminium alloys. T6 heat treated composites have the highest strength, but the lowest ductility compared to the other materials. Although these results provide some insight regarding the fracture behaviour of the materials examined, specific validity criteria have to be satisfied in order to obtain K_{IC} values.

Particular attention was paid to the influence of the specimen's thickness and other validity criteria such as crack curvature and in-plane crack propagation, since these are the most common reasons for a test to be invalid. In this work the most

important validity criterion related to the crack curvature was found to be satisfied both for the Al/SiC_p composite specimens as well as for the unreinforced aluminium alloys.

In Figure IV.25, the macroscopic view of the crack curvature for various specimens tested having different thickness is shown. For CT specimens, the fracture toughness standard requires that the surface crack length should not differ from the effective crack length by more than 15%. The effective crack length a_{eff} was calculated as the mean value of the crack lengths at the centre and quarter thickness positions [110]. These validity criteria considerations are reflected in Table IV.4.

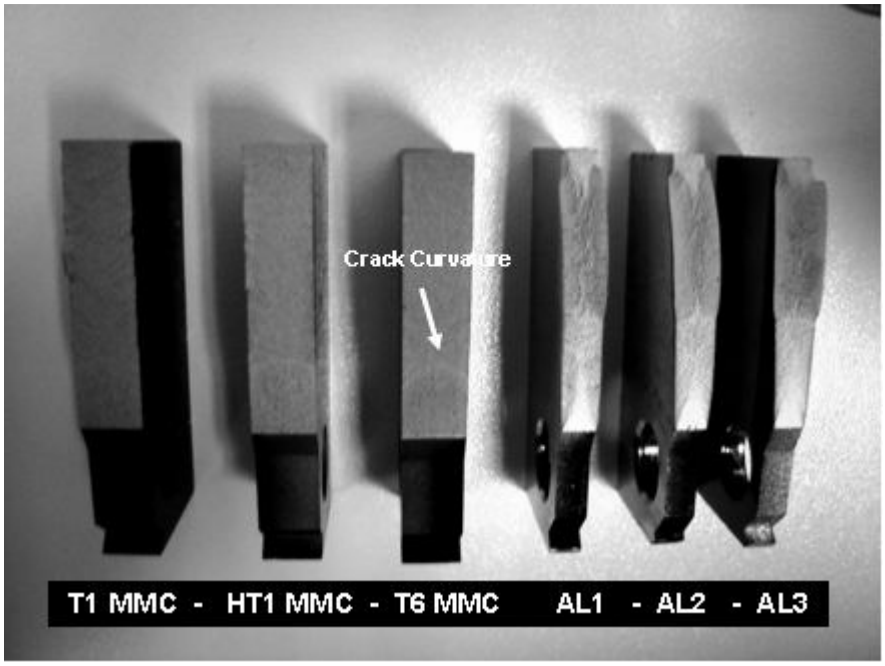

Figure IV.25.Variation in crack curvature with specimen thickness.

Next to the crack curvature, another important validity criterion is the plane crack propagation. It is very important to have a crack that propagates through the specimen in plane strain conditions with limited plasticity, preferably in a straight line. Especially for MMCs reinforced with brittle particles there is a high probability that a crack is deflected by the hard particles, and then propagates out of plane. However, in this study, all specimens satisfied the plane crack propagation criterion; thermographic evidence for this behaviour is shown in Figures IV.26b, c and d.

In summary, in the tests performed for the three different conditions for all MMC specimens, all validity criteria were met. Therefore, K_Q values could be considered as K_{IC} valid fracture toughness values. However, the aluminium alloy CT specimens did not meet the thickness validity criterion. Hence, in this case, the K_Q values were kept for comparison purposes. As expected, fracture toughness values of the composites were lower than those of unreinforced aluminium alloys. However, heat treatment significantly improved K_{IC} of the composites; The T6 condition was more effective in improving the fracture toughness values than the HT-1 condition. Additionally, the K_{IC} values for all heat treatment conditions were higher than values documented in the literature [110], even for lower weight percentage of silicon carbide particles.

IV.5.4.2 Thermography

A rectangular area on the specimen, located just in front of the initial pre-cracking region, was selected, as shown in Figure IV.26a. The development of fracture was monitored in that area using infrared thermography [116].

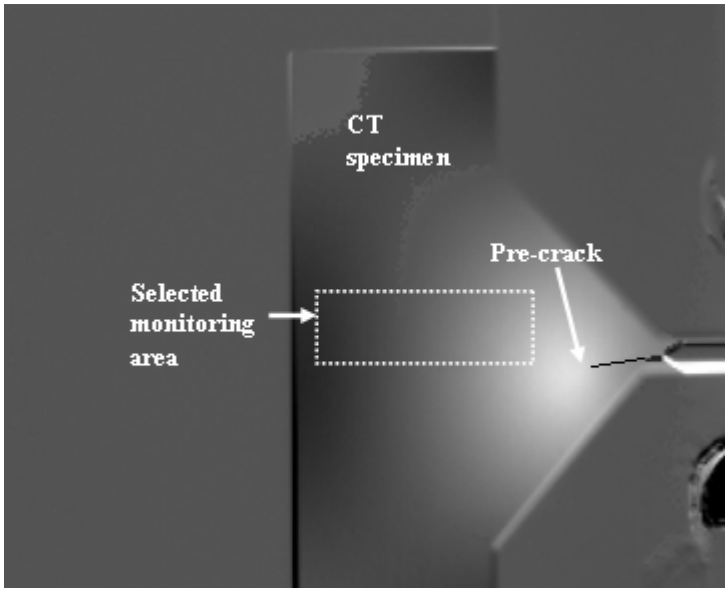

Figure IV.26a. CT specimen showing the selected area for thermographic monitoring.

The mean temperature in this area versus time during crack growth was calculated using the recorded thermal imprint. As the specimen was stretched in tension, stresses were accumulating in the specimen, and the temperature increased as a function of time.

A comparison of the thermography graphs in Figures IV.26b, 26c, 26d and 26e leads to the conclusion that the aluminium alloy exhibited different crack propagation behaviour than the Al/SiC_p composites. In these figures the thermographic monitoring of Aluminium 2xxx alloy, Al/SiCp T6 composite, and Al/SiCp HT1 composite samples is presented correspondingly. The different stages of crack growth for each material up to the final fracture of the specimen can be clearly observed. Just prior to fracture, the plasticity zone was clearly delineated on the specimen's surface as a heated region, which may be readily attributed to local plastic deformation. Furthermore, as seen in all figures, the crack was propagated in-plane throughout the experiment.

For the aluminium alloy, the temperature versus time curve in Figure IV.26b showed extended plasticity behaviour before final fracture occurred. However, for the T6 heat treated composite material in Figure IV.26c, multiple temperature peaks indicated a confinement of the plasticity zone. It was also observed that T6 heat treated composites exhibited fewer, but larger peaks compared to the HT1 heat treated specimens, (Figure IV.26d) where multiple small temperature peaks, indicate less plasticity and steadier crack growth propagation. Furthermore, for T6 composite, large ($\Delta T/\Delta A$) peaks, indicate that crack propagation exhibits higher stress concentrations followed by multiple stress relieves.

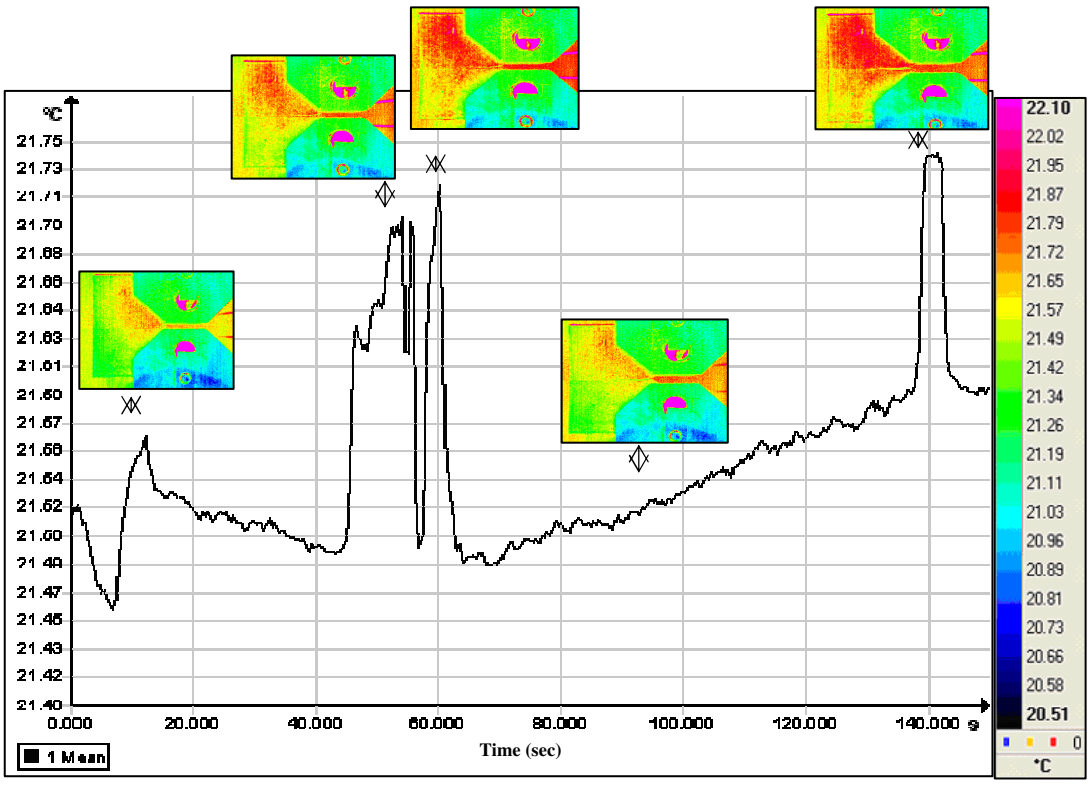

Figure IV.26b. Thermographic monitoring of Aluminium 2xxx CT sample showing the different stages of crack growth up to the specimen's final fracture.

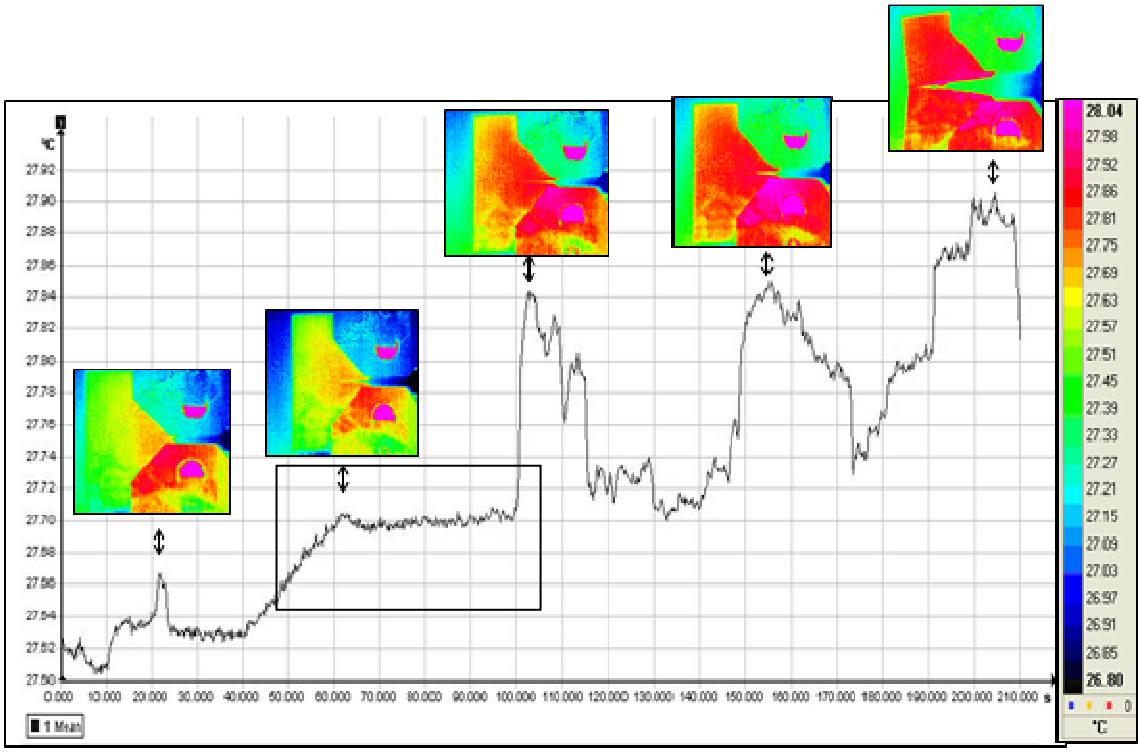

Figure IV.26c. Thermographic monitoring of Al/SiCp T6 composite CT specimen showing the different stages of crack growth up to the sample's final fracture.

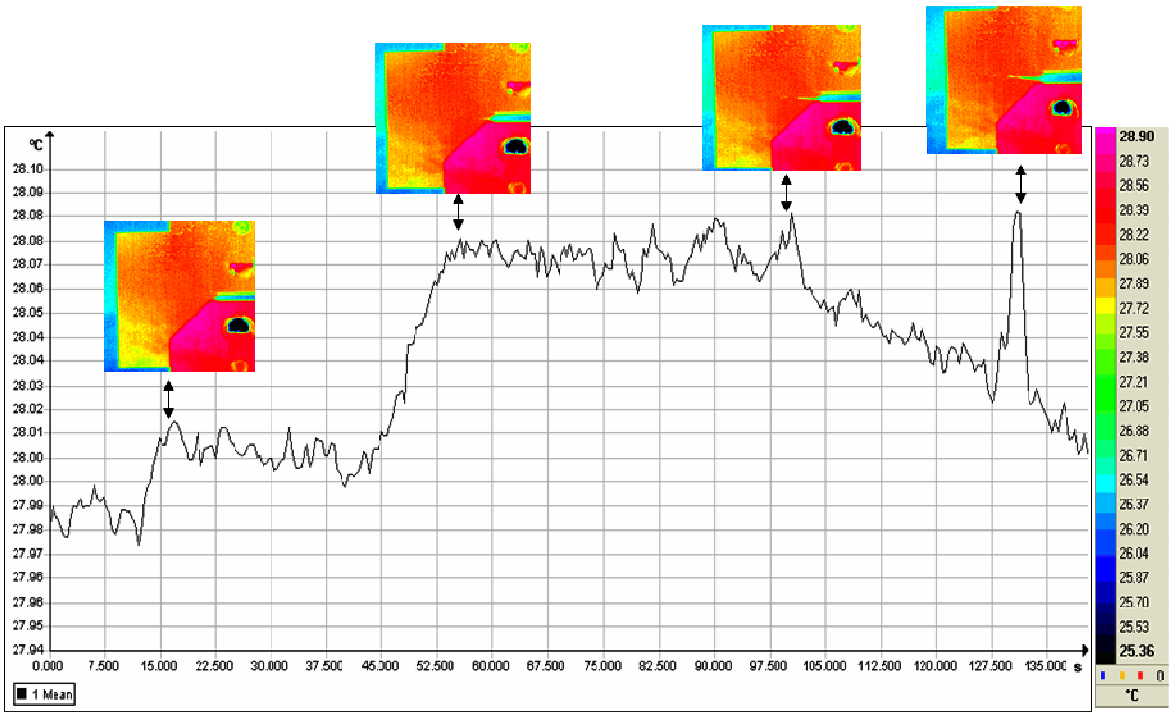

Figure IV.26d. Thermographic monitoring of Al/SiCp HT1 composite CT specimen showing the different stages of crack growth up to the sample's final fracture.

The selected area shown in Figure IV.26e point out the crack propagation stages: (i) Plasticity region as a function of temperature increase, shows that crack is close to be formed (ii) Steady crack growth region where crack is propagating, indicated by constant temperature rate (ΔT=constant) (iii) crack arrest and stress relief stage, where crack is arresting either by deflecting in a hard obstacle or crack bridged. During this last stage stress is increasing throughout the crack propagation and finally reaches a maximum value just before crack arrest occurs. After stress is relieved the crack continues this loop until the final fracture occurs.

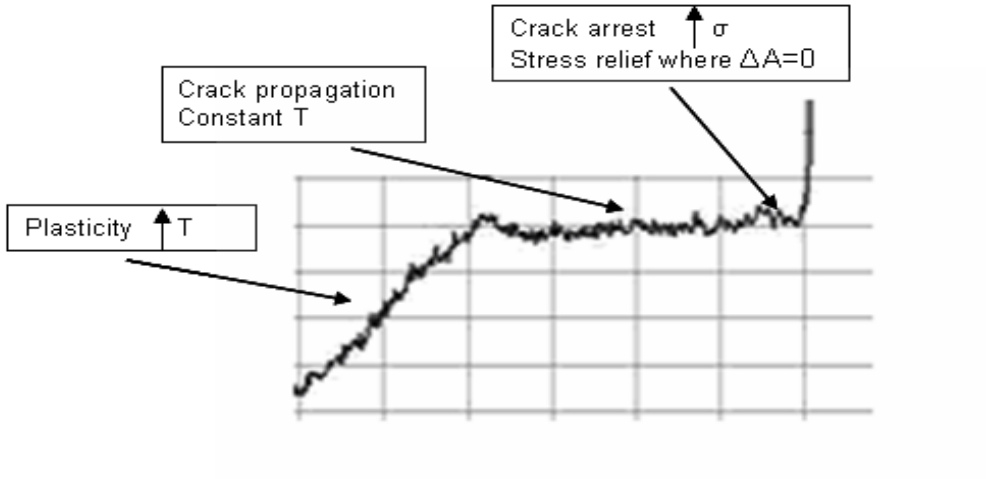

Figure IV.26e.Thermographic analysis of crack growth stages. (i) Plasticity (ii) Steady crack growth (iii) crack arrest and stress relief where ΔA=0.

IV.5.4.3 Microstructural examination

As it was also reported in previous section (IV.4.5.5), the fractographic examination of the rapid overload fracture region of tested MMC specimens revealed some particle fracture, especially for the T6 heat treatment. In the T6 condition, SiC particles seem to be cracked but not debonded (Figure IV.27a) indicating strong interfacial bonding.

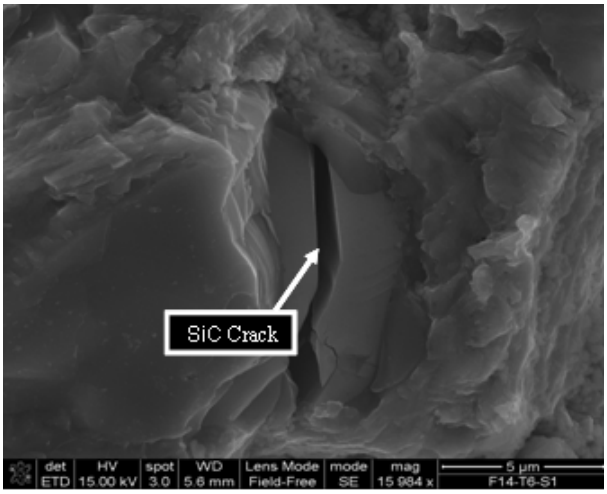

Figure IV.27a. T6 heat treatment condition: SiC particles cracked but not debonded.

Larger particles were more prone to fracture, as there was a higher probability of a critical flaw size to exist in the particle volume. Additional flaws in those particles could have been created during fabrication. As shown in Figure IV.27b, in the HT-1 heat treatment condition, sliding of reinforcement particles has been observed, evidence of a weak interface.

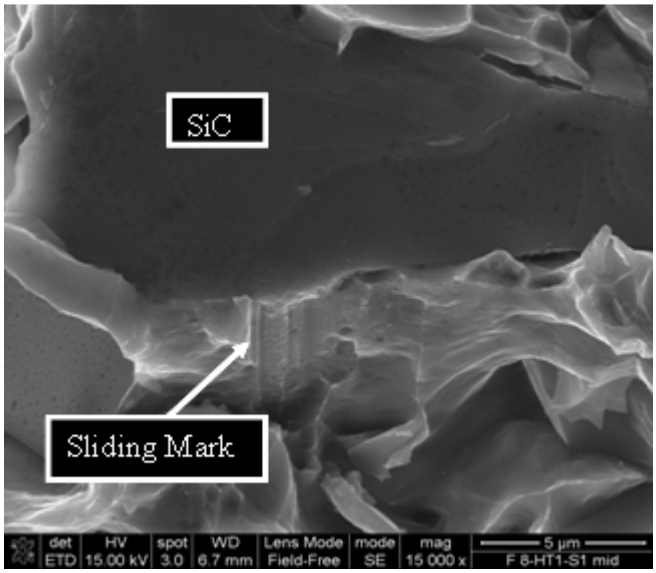

Figure IV.27b. HT-1 heat treatment condition: SiC Sliding mark indicates weak interface.

The T1 condition, (Figure IV.27c), showed some coalescence microvoids, which are characteristic of ductile behaviour.

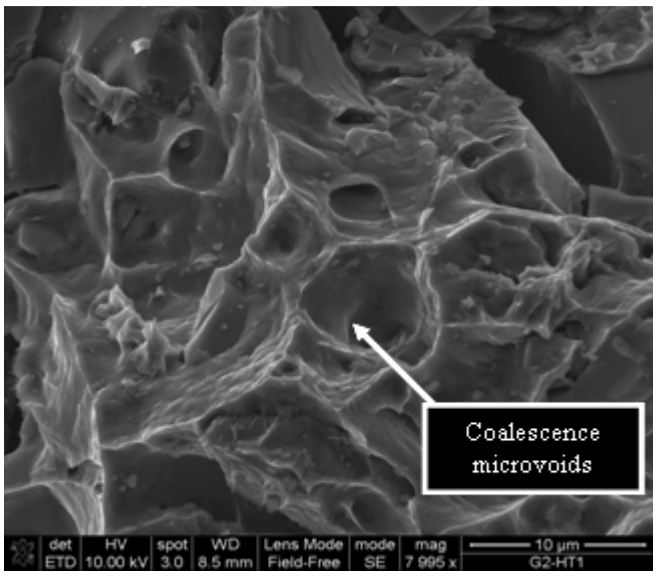

Figure IV.27c. T1 condition: Presence of coalescence microvoids indicating ductile behaviour.

From the examination of the microstructure in these materials it became evident that the heat treatment clearly improved the fracture properties of the composite. This was related to a precipitation hardening mechanism caused by the accumulation of precipitates at the interfacial region.

IV.5.5 Conclusions

The determination of valid plane strain fracture toughness (K_{IC}) for particulate-reinforced aluminium matrix composites subjected to different heat treatment conditions was achieved by satisfying all the validity criteria as per ASTM E399 standard. In addition, infrared thermography was used to monitor in real-time the various stages of crack growth up to the specimen's final fracture. The linear elastic fracture behaviour of the MMCs was thermographically assessed in relation to the validity of the fracture toughness calculations.

As was expected K_{IC} values for the MMCs were lower than the unreinforced aluminium alloys. However, higher toughness values were measured than reported in the literature for the same matrix/ reinforcement system, even for lower weight percentage of silicon carbide particles [110].

Heat treatment processing was the key to this improvement, with the T6 heat treated composite exhibiting the highest fracture toughness. This was attributed to a dominant mechanism associated to microstructural changes in the composite. This mechanism relates to the precipitates appearing in the microstructure of the composite at the vicinity of the interfacial region, which result to the enhanced toughness of the composite.

The thermographic examination of the materials showed that heat treated composite samples exhibit regular crack propagation behaviour. Stress concentration, due to the presence of particle reinforcements, produced controlled crack growth and higher stresses, which were related to regular energy release by the material during fracture, indicative of brittle fracture behaviour. On the other hand, the large plastic deformation of the aluminium alloy was associated with the absence of stress-peaks in conjunction with the monotonic temperature rise for a large part of the temperature / time curve prior to the specimen failure.

Chapter V – Predicting the interfacial fracture strength in Al/SiCp Composites

This Chapter focuses on the development of a thermodynamics – based damage model aiming in predicting the interfacial fracture strength in Al/SiCp composites. The experimental measurements obtained from the microstructural and macroscopic behaviour of the composite (see Chapter III and IV) are used as inputs into the model. This model serves in the design of a desirable SiC particulate reinforced aluminium alloy composite system as it correlates the micro with macro properties of the composite according to the needs for use.

V.1 Aims and Objectives

A micro-mechanics model, based on thermodynamics principles, is proposed to determine the fracture strength of the interface at a segregated state in MMCs. This model uses energy considerations to express the fracture toughness of the interface in terms of interfacial critical strain energy release rate and elastic modulus. The interfacial fracture toughness is further expressed as a function of the macroscopic fracture toughness and mechanical properties of the composite, using a toughening mechanism model based on crack deflection and interface cracking.

The model successfully predicts possible trends in relation to segregation and interfacial fracture strength behaviour in metallic alloys. Small changes in surface energy caused by segregation will result in very large changes in interfacial fracture stress.

The structure of the interfacial zone is important in determining the amount of predicted segregation and hence the change of the interfacial energy caused by the segregation. Relations have been developed to forecast the energy change in terms of the coincidence site stress describing the interface, and the formation energies of impurities on the interface.

Mechanical testing has been performed to obtain macroscopic data, such as the fracture strength, elastic modulus and fracture toughness of the composite, which are used as input to the model. Based on the experimental data and the analysis, the interfacial strength is determined for SiC particle-reinforced aluminum matrix composites subjected to different heat treatment processing conditions.

V.2 Introduction

In case of interfacial fracture a polycrystal exhibits brittle fracture behaviour [117-118], which is considered as major weakness of many advanced, high performance structural materials such as metal matrix composites used in high-temperature applications. In contrast, crack deflection at the interface has been associated with improved mechanical properties of the material at interface. Crack deflection is associated either with crack attraction or repulsion by second phase particles due to residual strains. An important factor regulating crack growth behaviour in metal matrix composites is the matrix-reinforcement interface property, which relates to precipitation hardening mechanisms [61].

The thermodynamics of vacancy and impurity absorption at interfaces and grain boundaries in solids has been studied in the recent years with theoretical models proposed in order to predict the behaviour of vacancies at interfaces in a stress gradient, as well the interface strength at fracture. It has been reported in literature that the

tendency for intergranular fracture is closely related to the type and structure of grain boundaries. Low-energy boundaries are resistant to fracture while high energy or the so-called random boundaries are favoured locations for crack nucleation and propagation. Lim and Watanaby [119] and Faulkner and Shvindlerman [120] have recognised the important role interface structure plays in determining the amount of predicted segregation and hence the change of interfacial energy caused by segregation.

Certain amounts of plastic deformation are involved with crack propagation along an interface. The parameters to be considered are the stain rate sensitivity to stress and the dislocation pile up behaviour at the advancing crack tip. Using this approach, the effective work parameter can be shown to be thousand times larger than the surface energy [120]. This implies that minute changes in surface energy caused by segregation would result in large changes in interfacial fracture stress.

In ductile materials such as metals, plastic deformation occurs at the crack tip. Much work is required in producing a new plastic zone at the tip of the advancing crack. Since the plastic zone has to be produced upon crack growth, the energy for its formation can be considered as energy required for crack propagation. This means that for metals R (crack propagation resistance) dW/dA is mainly plastic energy; the surface energy is so small that can be neglected [121].

V.3 Model

A model proposed by McMahon and Vitek [122] predicts the fracture resistance of a ductile material that fails by an intergranular mechanism. Based on this model, an effective work parameter can be developed to predict fracture strength of an interface at a segregated state using Griffith crack-type arguments.

Griffith [123] was the first who tried to relate the micro-defect fracture strength with the interatomic bond strengths. His model states that crack propagation will occur only if the total energy of the system is decreased. This implies that only if the energy released upon crack growth is sufficient to provide all the energy that is required for crack growth then this crack will propagate. The energy consumed in crack propagation is denoted by E_R = dW/da which is called the crack resistance. If E_R is a constant (da=constant), this means that for the crack to propagate the elastic energy release rate G must exceed a certain critical value G_{IC}. For metals, E_R is mainly the plastic energy; surface energy is so small that it can be neglected. Therefore, the energy criterion for plain stress conditions stipulates that (Equation V.1):

$$G_K = \frac{K^2}{E} \quad \text{and} \quad G_{IC} = \frac{K_{IC}^2\left(1-\nu^2\right)}{E} \quad \text{for plain strain conditions.} \qquad \text{V.1}$$

where, K_{IC} is the fracture toughness and E the Young's modulus of the material.

Davidson [124] has taken this energy approach and divided the energy G_{IC} into three terms; the work done in the plastic zone of the crack, the mechanical work expended in creating the voided surface, and the surface energy itself.

Based on Griffith's approach, the fracture toughness of the interface, K_{int}, can be expressed in terms of critical strain energy release rate, G_{int}, of the interface and the Young's modulus of the interface, E_{int} as shown in Equation V.2 [121].

$$K_{\text{int}} \cong \sqrt{G_{\text{int}} E_{\text{int}}} \qquad \text{V.2}$$

The Griffith's equation, which was derived for elastic body, is applied here because it is assumed that the yielding zone size ahead of the crack is small enough and the fracture is governed by the elastic stress field. The model further assumes that small

changes in interfacial energy caused by segregation of impurities at the interface will result in a much larger change in the work of fracture. This is due to the fact that the work of fracture must be provided by a dislocation pile-up mechanism around the advancing crack-tip on the interface. This implies that additional work must be provided to deform the material at the crack-tip in addition to the work needed to overcome the interface energy and to replace it with two surfaces. The definition of interfacial fracture strength, σ_{int}, is then given by Equation V.3:

$$\sigma_{\text{int}} = \sqrt{\frac{100\varepsilon_P E_{\text{int}}}{\pi d}} \qquad \text{V.3}$$

where,

E is Young's modulus,

d is the particle thickness, since it is assumed that cracks of the order of the particle size are present when considering crack propagation through the interface and the particulate,

$\boldsymbol{\varepsilon_p}$ is the energy required to create two fracture surfaces = $2\varepsilon_s - \varepsilon_{gb}$ (= ε_o), with ε_s, the surface energy, and ε_{gb}, the grain boundary energy.

The 100 ε_p component allows for dislocation interaction and movement ahead of the crack-tip in ductile materials. This refers to the work required for a total separation of the lattice planes, which is equal to the area under the force-extension curve. The energy ε_p required to create two fracture surfaces is basically related to the work of intergranular fracture, G_k, which is given, according to Faulkner et al. [125], by equation V.4:

$$G_k = A\ \varepsilon_p\ e^{n \ln\left(\frac{\varepsilon_a}{\varepsilon_o}\right)} \qquad \text{V.4}$$

where:

A, is the dislocation pile-up term describing the effectiveness of dislocations in providing stress concentration at the advancing interfacial crack tip (=100) in ductile materials,

n, is the work hardening exponent (= 10 for FCC aluminium).

Equation V.4 originally developed for intergranular fracture through grain boundaries, also applies to particulate/matrix interfaces. Interphase regions separate into two different phases whereas the grain boundaries separate into new portions of the same phase. Hence, the grain boundary system has one more degree of freedom than the interface system. Therefore, $G_k = G_{int}$, which is the work of interfacial fracture.

The quantity ε_a, in Equation V.4, is then the new interfacial energy caused by segregation, given by Equation V.5 [62]:

$$\varepsilon_a = \varepsilon_o - ZRT\ln\left(1-c+Bc\right) \qquad \text{V.5}$$

By replacing G_{int} from Equation V.4 into Equation V.2, the following relationship can be obtained (Equation V.5):

$$\frac{K_{int}^2}{E_{int}} = 100\varepsilon_p e^{n\ln\left(\frac{\varepsilon_a}{\varepsilon_p}\right)}$$

Also, considering Equation V.5 we get Equation V.6,

$$\frac{K_{int}^2}{E_{int}} = 100\varepsilon_p e^{n\ln\left(1-\frac{ZRT\ln\left(1-c+Bc\right)}{\varepsilon_p}\right)} \qquad \text{V.6}$$

or Equation V.7,

$$\frac{K_{int}^{2}}{100 E_{int}} = \varepsilon_p \left(1 - \frac{Z R T \ln\left(1 - c + B c\right)}{\varepsilon_p} \right)^{n} \qquad \text{V.7}$$

Where,

Z, describes the density of interface sites which are disordered enough to act as segregation sites (= D ρ_S),

D, is for the thickness of the interface region, and

ρ_S , stands for the density of the interface region (D=300 nm) (ρ= 2.6889 g/cm^3 for Aluminium and 3.22 g/cm³ for SiC),

R, is the gas constant (= 8.314472(15) J•K-1•mol-1),

T, is the absolute temperature (= 803.15 K for T6, = 723.15 K for HT1),

c, is the segregate concentration needed to cause embrittlement (= 0.1 for pure aluminium),

B, describes the modification of the boundary energy by impurities using the Zuchovitsky equations (Explained in detail in section V.7),

n, is the work hardening exponent (= 10 for FCC aluminium).

From Equation V.7 ε_p can be estimated if K_{int} (Interface fracture toughness) and E_{int} (Interface Young's Modulus) are known. Hence, from Equation V.3 the fracture of σ_{int} can be determined.

V.4 Interface fracture toughness K_{int}

In hard particle reinforced metal matrix composites the stress transfer from the matrix to the particles is mainly controlled by the misfit of the elastic constants between the two phases [126]. To measure the stress transfer to the particle, in an homogeneous material subjected to tensile loading, the stress carrying capability of the particle is defined as the ratio of the normal stress σ_N to the particle in the loading direction to the macroscopic tensile stress, σ_T, i.e. the ratio $L = \sigma_N / \sigma_T$. By using Eshelby's theory, the stress carrying capability of a spherical inhomogeneity can be written as (Equation V.8) [127]:

$$L = \frac{9x(2+3x)}{(1+2x)(8+7x)} \qquad \text{V.8}$$

where, $x = E_i / E_m$, and E_i and E_m are Young's moduli for inhomogeneity and matrix, respectively.

Furthermore, the shear lag model, originally developed by Cox [128] modified by Llorca [129], can be used to estimate the stress carrying capability of a particulate, assuming that the volume fraction of reinforcement is small and the average stress in the matrix is approximately equal to the applied stress (Equation V.9):

$$L = 1 + \frac{a}{\sqrt{3}} \qquad \text{V.9}$$

where $a = \overline{h} \big/ 2\overline{r}$ is the aspect ratio of the reinforcement, with $\overline{h}$ and $\overline{r}$ the average length and the average diameter of the particle.

A model has been proposed to estimate the effects of particle volume fraction on fracture toughness in SiC particle-reinforced aluminium alloy matrix composites. This model assumes that SiC particles are uniformly distributed in the matrix and that the pattern of particle distribution is similar to FCC structure in metals. The fracture toughness of the composite can then be written as (Equation V.10) [130]:

$$K_{IC} = \frac{K_p}{L_p} V'_m + \frac{2K_{\text{int}}}{L_p + L_m}\left(V_m - V'_m\right) + \frac{K_m}{L_m} 2V_m + K_m(1 - 3V_m) \qquad \text{V.10}$$

where K_{IC}, K_p = 3 MPa m-1/2, K_m = 35 MPa m-1/2, and K_{int} is the fracture toughness of the composite, SiC particulates, A359 aluminium alloy matrix, and interface, respectively. L_p and L_m are the stress carrying capabilities of a particulate and the matrix, respectively. On average, for SiC particles and aluminium alloy matrix, $L_p \sim L_m \sim 2$. The value of $L_m = 1$ is applicable for clean surfaces. However, due to processing conditions and the physical interaction at the matrix/reinforcement interface the interface contains partially contaminated surfaces, therefore $L_m = 2$ since it cannot be considered as a "clean surface". V_m and $(V_m\text{-}V'_m)$ are the area fractions for particle cracking and interface failure, respectively. These area fractions though are not accurately known. However Wang and Zhang [131] found that the ratio of particle cracking over interface failure $V_m/ (V_m\text{-}V'_m)$ was about 0.13 (= 1.4%/10.7 %) in a SiC particle-reinforced aluminium alloy composite.

V.5 Estimating Young's modulus of the interface region

The spherical particle in the unit cell is converted to a cubic particle. The diameter of the particle d, thickness of interphase region d_i, volume fraction of the particles including the interphase V'_f, the equivalent dimension of the particle is d_e and the overall dimension of the cubic unit cell s, are given by Equation V.11 [132] (see also Figure V.1):

$$\frac{\pi(d + d_i)^3}{6} = v'_f s^3 = \left(d_e + d_i\right)^3 \qquad \text{V.11}$$

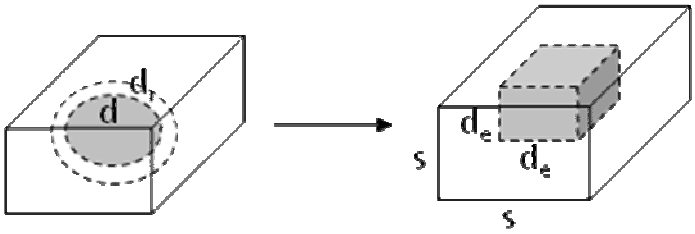

Figure V.1. Conversion of a spherical particle to a cubic particle

The volume fraction of the particles including the interphase region is therefore (Equation V.12),

$$v_f' = \left(\frac{d_e + d_i}{s} \right)^3 \qquad \text{V.12}$$

And the volume fraction of the particles is (Equation V.13)

$$v_f = \left(\frac{d_e}{s} \right)^3 \qquad \text{V.13}$$

Consider the unit cell is subjected to a uniaxial load in the longitudinal direction. The total load on the unit cell is defined from force equilibrium (Equation V.14):

$$P_C = P_p + P_m + P_i \qquad \text{V.14}$$

In an average sense (Equation V.15),

$$\sigma_C A_{unit\ cell} = \sigma_p A_p + \sigma_m A_m + \sigma_i A_i \qquad \text{V.15}$$

Dividing Equation V.15 by $A_{unit\ cell} = s^3$ and substituting the actual areas, one obtains (Equation V.16):

$$\sigma_C = \sigma_p \frac{d_e^2 s}{s^3} + \sigma_m \frac{\left(s^2 - \left(d_e + d_i\right)^2\right)s}{s^3} + \sigma_i \frac{\left(\left(d_e + d_i\right)^2 - d_e^2\right)s}{s^3} \qquad \text{V.16}$$

or (Equation V.17),

$$\sigma_C = \sigma_p v_f^{2/3} + \sigma_m \left(1 - V_f'^{2/3}\right) + \sigma_i \left(V_f'^{2/3} - V_f^{2/3}\right) \qquad \text{V.17}$$

Compatibility of longitudinal displacement requires that strain in the composite and each constituent be the same (i.e. $e_C = e_p = e_m = e_i$), so the Equation V.17 reduces to:

$$E_C = E_p v_f^{2/3} + E_m \left(1 - V_f'^{2/3}\right) + E_i \left(V_f'^{2/3} - V_f^{2/3}\right) \qquad \text{V.18}$$

So, the Young's modulus of a particulate composite E_C is given as a function of the moduli of the particles E_p, matrix E_m, and interphase E_i.

Due to the fact that the difference $\left(V_f' - V_f\right)$ is very small, a good approximation is to consider that the Young's modulus of the interface is close to that of the matrix; $E_i \cong E_m$ [133].

V.6 Constants calculations

The parameter B describes the modification of the boundary energy by impurities using the Zuchovitsky equations [134], given by (Equation V.19):

$$B = e^{\left(\frac{\varepsilon_1 - \varepsilon_2}{RT}\right)} \cong e^{\left(\frac{0.75\,\varepsilon_F}{RT}\right)} \qquad \text{V.19}$$

where ε_2-ε_1 is the difference between the formation energy in the impurity in the bulk and the interface region. It is assumed that the values of the surface energy and the impurity formation energy in the bulk are close, and therefore the numerator in the exponential term depends on the impurity formation energy in the interface region, which is assumed to be 0.75 ε_f, where ε_f is the formation energy of the impurity in the bulk.

Using Faulkner's approach [125], to the derivation of impurity formation energy,

$$\varepsilon_f = \varepsilon_s + \varepsilon_e \qquad \text{V.20}$$

where, ε_s is the surface energy required forming the impurity atom and ε_e is the elastic energy involved with inserting an impurity atom into a matrix lattice site. This is given by Equation V.21:

$$\varepsilon_f = \frac{0.5\varepsilon_S}{1.94} + \frac{8\pi G}{3e} a_m \left(a_i - a_m\right)^2 eV \qquad \text{V.21}$$

where,

ε_S is the surface energy (1.02 J m-2)

e is the electronic charge (1.60217646 *10^19 Coulomb)

a_i is the impurity atomic radius (0.118 nm for Si)

a_m is the matrix atomic radius (0.143 nm for aluminium)

G is the shear modulus (26 GPa for aluminium)

By performing the calculations the impurity formation energy, ε_f, for A359 aluminium alloy (Al-Si-Mg) can be determined and then substituted in equation 5 to calculate B (Zuchovitsky).

V.7 Al/SiCp Mechanical Properties

The mechanical properties of the 31% SiC aluminium matrix composite have been obtained from previews work (see chapter IV). The fracture toughness K_{1c} value has been measured for three different heat treatment conditions. Also, the young's modulus has been calculated. Table V.1 shows the values to be inputted in to the model.

Material	Heat Treatment	E (GPa)	$Rp_{0.2}$ (MPa)	K_{IC} (MPa √m)
A359 Al	-	71	75	35
A359/SIC/31p	AR	108	158	19,28
A359/SIC/31p	T6	116	290	22,05
A359/SIC/31p	HT1	110	155	20.75

Table V.1. Mechanical Properties of Al/SiCp Composite.

V.8 Results - Discussions

The micro-mechanics model, based on thermodynamics principles, is used to determine the fracture strength of the interface at a segregated state in MMCs. This model uses energy considerations to express the fracture toughness of the interface in terms of interfacial critical strain energy release rate and elastic modulus. The interfacial fracture toughness is further expressed as a function of the macroscopic fracture toughness and mechanical properties of the composite, using a toughening mechanism model based on stress transfer mechanism. Mechanical testing is also performed to obtain macroscopic data, such as the fracture strength, elastic modulus and fracture toughness of the composite, which are used as input to the model. Based on the

experimental data and the analysis, the interfacial strength is determined for SiC particle-reinforced aluminum matrix composites subjected to different heat treatment processing conditions and the results are shown in Table V.2. It is observed that K_{int} values are close to the K_{1c} values of the composites. Furthermore, σ_{int} values found to be dependent on the heat treatment processing with T6 heat treatment composite obtain the highest interfacial fracture strength.

Condition	K_{int} ***(MPa√m)***	$E_i \cong E_m$ ***(Nm^{-2})***	***T (K)***	***c***	***D (μm)***	***B***	ε_f	***N***	ε_p ***(Jm^{-2})***	σ_{int} ***(MPa)***
T1	22.4	7.1 x 10^{10}	300	0.1	17	1.5	0.303	10	1.42	94
T6	29.5	7.1 x 10^{10}	803.15	0.1	17	1.5	0.303	10	3.91	260
HT1	26.3	7.1 x 10^{10}	723.15	0.1	17	1.5	0.303	10	3.55	236

Table V.2. Interfacial Fracture strength of Al/SiC_p Composite.

V.9 Conclusions

A method of calculation has been applied to predict the interfacial fracture strength of aluminium, in the presence of silicon segregation. This model considers the interfacial energy caused by segregation of impurities at the interface and uses Griffith crack-type arguments to forecast the energy change in terms of the coincidence site stress describing the interface and the formation energies of impurities at the interface. Based on Griffith's approach, the fracture toughness of the interface was expressed in terms of interfacial critical strain energy release rate and elastic modulus. The interface fracture toughness was determined as a function of the macroscopic fracture toughness and mechanical properties of the composite using two different approaches, a toughening mechanism model based on crack deflection and interface cracking and a

stress transfer model. The model shows success in making prediction possible of trends in relation to segregation and interfacial fracture strength behaviour in SiC particle-reinforced aluminium matrix composites. The model developed here can be used to predict possible trends in relation to segregation and the interfacial fracture strength behaviour in metal matrix composites. The results obtained from this work conclude that the role of precipitation and segregation on the mechanical properties of Al/SiC_p composites is crucial, affecting overall mechanical behaviour.

Chapter VI – Conclusions

The role of segregation and precipitation on the interfacial strengthening mechanisms in SiC particulate reinforced aluminium alloy composite system, when subjected to thermo-mechanical processing has been studied in detail. The main objectives have been accomplished. Heat treatment processing was the key to this improvement of the microstructure of the materials studied. The microstructural modification and the tailoring of the interface properties enhanced the mechanical properties of the composites, mainly due to the precipitation hardening phenomena.

T6 heat treated composites clearly exhibited the highest mechanical properties according to the tensile, fatigue and fracture toughness tests. This was attributed to a dominant mechanism associated to microstructural changes in the composite. This mechanism relates to the precipitates of Mg_2Si appearing in the microstructure of the composite at the vicinity of the interfacial region, which result to the enhanced toughness of the composite.

Microhardness and tensile testing results showed that the composite micro-mechanical behaviour is influenced by certain factors such as: precipitates, the reinforcement percentage and interparticle distance.

It can be stated that the composite with higher volume fraction of SiC particles has lower strength in the T6 heat treatment and that is due to less precipitation formed around the reinforcement phase when SiC particles attract Si phases close to the interface regions and Mg_2Si precipitates formation decreases. Furthermore, Si phase tend to be absorbed by the SiC particles and this causes the matrix embrittelment due to the lack of Si phase remaining in the matrix, thus, eutectic regions are not any more formed and failure to strain decreases dramatically in comparison with the 20% SiC

composite where precipitation is more and well distributed homogenously around the reinforcement. In the HT-1 heat treated samples the Si phase showed an increase and has been expanded homogenously around the matrix. This explains the higher strain to failure value than the other two states, T1 and T6.

The fatigue behaviour of the composites showed that the exhibited endurance limits ranging are from 70% to 85% of their UTS. The T6 composites performed significantly better in absolute values but their fatigue limit fell to the 70% of their ultimate tensile strength. This behaviour is linked to the microstructure and the good matrix-particulate interfacial properties. In the case of the HT1 condition, the weak interfacial strength led to particle/matrix debonding. In the T1 condition the fatigue behaviour is similar to the HT1 condition although the quasi static tensile tests revealed a less ductile nature. Thermographic images delineated the plasticity areas in the case of the T6 condition well before the failure of the specimen.

The crack growth behaviour of particulate-reinforced metal matrix composites was investigated. Aluminium A359 reinforced with 31% of SiC particles has been examined. Heat treated composites, and especially those samples subjected to T6 aged condition, exhibited different behaviour of crack propagation rate and stress intensity factor range than the as-received composite specimens.

The determination of valid plane strain fracture toughness (K_{IC}) for particulate-reinforced aluminium matrix composites subjected to different heat treatment conditions was achieved. As was expected K_{IC} values for the MMCs were lower than the unreinforced aluminium alloys. However, higher toughness values were measured than reported in the literature for the same matrix/ reinforcement system, even for lower weight percentage of silicon carbide particles.

A method of calculation has been applied in order to predict the interfacial fracture strength of aluminium, in the presence of silicon segregation. The interface fracture toughness was determined as a function of the macroscopic experimental measurements (mechanical properties of the composite) and the microscopic modification parameters (tailoring of interface properties). The model shows success in making prediction possible of trends in relation to segregation and interfacial fracture strength behaviour in SiC particle-reinforced aluminium matrix composites. The model developed here can be used to predict possible trends in relation to segregation and the interfacial fracture strength behaviour in metal matrix composites.

The results obtained from this work conclude that the role of precipitation and segregation on the mechanical properties of Al/SiC_p composites is crucial, affecting overall mechanical behaviour.

Innovations in MMCs are beginning to pay off with new military and commercial developments underway. Engineered solutions, capitalising on the advantages of light weight and effective thermal performance, are proving the superiority of MMCs over traditional approaches and materials. As a technology-driven 21st century dawns, demand for better performance, productivity and/or efficiency in transportation, aerospace and industrial processes/products will increasingly require the use of these remarkable composite materials. More work can be done in optimising MMCs properties. The understanding of the interfacial strengthening mechanisms therefore is the key factor for optimising the properties.

Bibliography- References

[1] Matthews, F.L., Rawlings, R.D., 'Composite materials: engineering and science', (1999), p.8.

[2] Clyne, T.W., Withers, P.J., 'An Introduction to Metal Matrix Composites', Cambridge University Press, Cambridge, (1993).

[3] Clyne, T.W., 'An Introductory Overview of MMC Systems, Types and Developments, in Comprehensive Composite Materials', Elsevier, (2000), p.1-26.

[4] Taya, M., Arsenault R.J., 'Metal matrix composites: thermomechanical behaviour', (1989), Pergamon.

[5] Myriounis, D. P., Hasan, S. T., Matikas, T. E., 'Microdeformation behaviour of Al/SiC Metal Matrix Composites', Composite Interfaces, Volume 15, Number 5, (2008), p. 495-514(20).

[6] Clyne, T.W., 'Metallic Composite Materials, in Physical Metallurgy', Elsevier, (1996), p.2568-625.

[7] Gergely, V., Degischer, H.P. and Clyne, T.W., 'Recycling of MMCs and Production of Metallic Foams, in Comprehensive Composite Materials', (2000) p.797-820.

[8] Chawla, K.K., 'Composite materials: science and engineering' (1998) p.6.

[9] Hasselman, D.P.H., Donaldson, K.Y., Geiger A.L., 'Effect of Reinforcement Particle Size on the Thermal Conductivity of a Particulate-Silicon Carbide-Reinforced Aluminum Matrix Composite', Journal of the American Ceramic Society, Volume 75 Issue 11, (2005), p. 3137 – 3140.

[10] Gofrey, T.M.T., Goodwin P.S., Ward-Close, C.M., 'Titanium Particulate Metal Matrix Composites - Reinforcement, Production Methods, and Mechanical Properties Advanced Engineering Materials', Volume 2 Issue 3, (2000), p.85 – 91.

[11] Ibrahim, I.A., Mohamed, F.A., Lavernia, E.J., 'Particulate reinforced metal matrix composites—a review' - Journal of Materials Science, (1991), Springer.

[12] Barbero, E.J., 'Introduction to Composite Materials Design' Taylor & Francis, Philadelphia, Pa, (1999).

[13] Hexemer, R | Pierce, R Advances in MMCs and CMCs Ceramic Industry. Vol. 150, no. 6, (2000) p. 31-38.

[14] Jones, R.M., 'Mechanics of composite materials', (1999), p.31-37.

[15] Kreider, K.G., 'Composite Materials, Metallic Matrix Composites', Volume 4,

(1974), Academic Press, New York and London.

[16] Lloyd, D.J., 'Particle Reinforced Aluminium and Magnesium Matrix Composites', International Materials Reviews 39, (1994), p.1-23.

[17] Shang, J.K., Yu, W., Ritchie, R.O., 'Role of silicon carbide particles in fatigue crack growth in SiC particulate reinforced aluminum alloy composite', Mater Sci Eng.,A102 (1988), p.181–92.

[18] Crowe, C.R., Gray, R.A., Hasson, D.F., in Proc. Int. Conf on 'Composite materials', ICCM-V, (ed. W. C. Harrigan et al.), (1985), p.843-866, New York, AIME.

[19] Manoharan, M., Lewandowski, J.J., 'Effects of Aging Condition on the Fracture Toughness of 2XXX and 7XXX Aluminum Composites', Scripta Met., 23, (1989), p.301-305.

[20] Davidson, D.L., 'Fracture surface toughness as a gauge of fracture toughness: Aluminium particulate SiC composites', Mat. Sci., 24, (1989), p.681—687.

[21] Manoharan, M., Lewandowski, J.J., 'Effect of microstructure and notch root radius on fracture toughness of an aluminium metal matrix composite', Int. J. Fract., 40 (1989), R31-R34.

[22] Manoharan, M., Lewandowski, J.J. 'Fracture Initiation and Growth Toughness of an Aluminum Metal-Matrix Composite', Acta Met., 38 (1990), p.489-9.

[23] Mott, N.F., Nabarro, F.R.N., 'An attempt to estimate the degree of precipitation hardening, with a simple model', Proc Phys Soc 52, 85 (1940).

[24] Aaron, H.B., Aaronson, H.I., 'Growth of grain boundary precipitates in Al-4% Cuby interfacial diffusion, Acta Met 16, 789 (1968).

[25] Aaron, H.B., Fainstein, D., Kotler, G.R., 'Diffusion-Limited Phase Transformations: A Comparison and Critical Evaluation of the Mathematical Approximations', Journal of Applied Physics 41(11), (1970), p. 4404-4410.

[26] Shercliff, H.R., Ashby, M.F., 'A process model for age hardening of aluminium alloys—I. The model', Acta Met 38, (1990), p.1789-1802.

[27] Carolan, R.A., Faulkner, R.G., 'Grain boundary precipitation of M23C6 in an austenitic steel', Acta Met 36, (1988), p.257-266.

[28] Hasan, S.T., Beynon, J.H. Faulkner, R.G., 'Role of segregation and precipitates on interfacial strengthening mechanisms in SiC reinforced aluminium alloy when subjected to thermomechanical processing', Journal of Materials Processing Technology 153-154, (2004), p.757-763.

[29] Manoharan, M., Lewandowski, J.J., 'In-situ Deformation Studies of an Aluminum Metal-Matrix Composite in a Scanning Electron Microscope', Scripta Met. 23,

(1989), p.1801- 1804.

[30] Manoharan, M., Lewandowski, J.J., 'Effect of Reinforcement Size and Matrix Microstructure on the Fracture Properties of an Aluminum Metal-Matrix Composite', Materials Sci. and Eng. A150, (1992), p.79-186.

[31] Hasan, S.T., 'Effect of heat treatment on interfacial strengthening mechanisms of second phase particulate reinforced aluminium alloy', 14th International Metallurgical and Materials Conference (Metal 2005), Hradec nad Moravici, Czech Republic, (2005).

[32] Lewandowski, J.J., Liu, C., Hunt, Jr. W.H., 'Effects of Microstructure and Particle Clustering on Fracture of an Aluminum Metal Matrix Composite', Materials Sci. & Eng. A107, (1989), p.241-255.

[33] Rozak, G., Lewandowski, J.J., Wallace, J.F., Altmisoglu, A., 'Effects of Casting Conditions and Deformation Processing on A356 Aluminum and A356-20% SiC Composites', Journal of Composite Materials 26(14), (1992), p.2076-2106.

[34] Everett, R.K., 'Deposition Technologies for MMC Fabrication, in Metal Matrix Composites: Processing and Interfaces', Academic Press, (1991), p.103-19.

[35] Mortensen, A., Marchi, San C., Degischer, H.P., 'Glossary of terms specific to Metal Matrix Composites', Volume 1, MMC-Assess – Thematic Network, 2/13.

[36] Aghajanian, M.K., Rocazella, M.A., Burke, J.T. and Keck, S.D., 'The Fabrication of Metal Matrix Composites by a Pressureless Infiltration Technique', J.Mat.Sci., vol.26, (1991) p.447-54.

[37] Mortensen, A., Masur, L.J., Cornie, J.A. and Flemings, M.C., 'Infiltration of a Fibrous Preform bya Pure Metal', Metall. Trans., vol.20A (1989) p.2535-63.

[38] Mortensen, A., 'Melt infiltration of metal matrix composites', Comprehensive composite materials, volume 3: metal matrix composites, Pergamon Press, Oxford, UK, (2000), p. 521–554.

[39] Zhou, W., Xu, Z.M., 'Casting of SiC Reinforced Metal Matrix Composites', Journal of Materials Processing Technology, 63 (1997), p.358-363.

[40] Skibo, M.D., Schuster, D.M., US Patent 4,786,467 (1988).

[41] Ray, S., 'Synthesis of cast metal matrix particulate composites', Journal of materials science, (1993).

[42] Mortensen, A. and Jin, I., 'Solidification Processing of Metal Matrix Composites', Int. Mat. Rev.vol.37 (1992) p.101-28.

[43] Lloyd, D.J. and Jin, I., 'Melt Processed Aluminium Matrix Particle Reinforced Composites', in Comprehensive Composite Materials, Vol. 3: Metal Matrix

Composites, Elsevier, (2000) p.555-77.

[44] Lin, Ching-Bin, 'Process for making metal-matrix composites reinforced by ultrafine reinforcing materials products', thereof. US. Patent Document-Number 5,401,338, (1993).

[45] Willis, T.C., 'Spray deposition process for metal matrix composites manufacture', Metals and materials (London).

[46] Li, B. and Lavernia, E.J., 'Spray Forming of MMCs, in Comprehensive Composite Materials', Vol. 3: Metal Matrix Composites, T.W.Clyne (ed.), Elsevier, (2000), p.617-53.

[47] Matthews, F.L, 'Composite materials: engineering and science RD Rawlings – (1999) – p.125.

[48] McGraw-Hill 'Solidification processing', (1974), New York, p. 621–633.

[49] Georghe, I. and Rack, H.J., 'Powder Processing of Metal Matrix Composites, in Comprehensive Composite Materials, Elsevier, (2000) p.679-700.

[50] Hunt, Jr. W.H., ' Metal matrix composites - Handbook of Materials Selection for Engineering Applications', (1997), p.71-72.

[51] Englanda, J. and Halla, I.W., 'On the effect of the strength of the matrix in metal matrix composites', Scripta Metallurgica Volume 20, Issue 5, (1986), p. 697-700

[52] Mortensen, A. 'A Review of The Fracture Toughness of Particle Reinforced Aluminum Alloys', Proc. Int. Conf. Fabrication of Particulates Reinforced Metal Composites, Québec, Canada, (1990), p. 217-233.

[53] Anderson, T. L., 'Fracture mechanics: fundamentals and applications', (1995) p. 365-377 Technology & Engineering.

[54] Deo, R.B., Starnes, J.H., Holzwarth, R.C., 'Low-cost composite materials and structures for aircraft applications", (2001).

[55] Zweben, C. 'Metal-Matrix Composites for Electronic Packaging, JOM, v. 44, n. 7, (1992). p.15-23.

[56] Cantor, B., Dunne, F., Stone, Ian., 'Metal and Ceramic Matrix Composites: - Science', (2004).

[57] Metal Matrix Composites: The Global Market BCC Research, February 1, 2009 Pub ID: WA2107876.

[58] Myriounis, D.P., Hasan, S.T., Matikas, T.E., 'Influence of Processing Conditions on the Micro-Mechanical Properties of Particulate-Reinforced Aluminium Matrix Composites', Advanced Composite Letters, 17 (2008).

[59] Merle P., 'MMC-Assess Thematic Network, Thermal Treatments of Age-Hardenable Metal Matrix Composites', Volume 2, (2000).

[60] Myriounis D.P, Hasan S.T, Matikas T.E., 'Microdeformation Behaviour of Al/SiC Metal Matrix Composites", 6th International Symposium on Advanced Composites, Proceedings of Comp07, (2007), Corfu, Greece.

[61] Myriounis, D.P., Hasan S.T., Matikas T.E., 'Heat Treatment and Interface Effects on the Mechanical Behaviour of SiC Particle Reinforced Aluminium Matrix Composites,' J. ASTM Int. 5 (7) (2008).

[62 Papazian, J.M., 'Effects of SiC whiskers and particles on precipitation in aluminum matrix composites', Metallurgical and Materials Transactions A, Volume 19, Number 12, (1988), p.2945-2953.

[63] MC-21, Inc, Carson City, NV, USA, Technical Report, www.mc21inc.com.

[64] Strangwood, M., Hippsley, C.A., and Lewandowski J.J., 'Segregation to SiC/Al Interfaces in Al Based Metal Matrix Composites', Scripta Met, 24, (1990), p.1483-88.

[65] Massalski,T.B., 'Binary Alloy Phase Diagrams. ASM International', Metals Park (1986).

[66] Vasudevan, A.K. and Doherty, R.D., 'Aluminum alloys-Contemporary research and applications, Academic Press, Inc, London Ltd. (1989).

[67] Majumdar, B.S., Matikas, T.E, and Miracle, D.B., 'Experiments and Analysis of Fibre Fragmentation in Single and Multiple-Fibre SiC/Ti-6Al-4V Metal Matrix Composites', Journal of Composites B: Engineering, (1998), Vol. 29B, p. 131-145.

[68] Manoharan, M., and Lewandowski, J.J., 'Effects of Aging Condition on the FractureToughness of 2XXX and 7XXX Aluminum Composites', Scripta Met., (1989), 23, p. 301-305.

[69] Shaw, L.L, Matikas, T.E, Karpur, P, Hu, S, and Miracle, D.B., 'Fracture Strength and Damage Progression of the Fibre/Matrix Interfaces in Titanium-Based MMCs with Different Interfacial Layers', Composites Part B: engineering, (1998), Vol. 29B, p. 331-339.

[70] Manoharan, M., and Lewandowski, J.J., 'Fracture Initiation and Growth Toughnesses ofan Aluminum Metal-Matrix Composite', Acta Met., (1990), 38, p. 489-96.

[71] Manoharan, M., and Lewandowski, J.J., 'In-situ Observation of Crack Growth in Al-MMC's', Scripta Met., (1990), 24, p. 12-18.

[72] Liu, D. S., and Lewandowski, J.J. 'The Effects of Superimposed Hydrostatic Pressure on Deformation and Fracture: Part II 6061 Particulate Composites', Met. Trans. A, 24A, (1993), p. 609-617.

[73] Cocen, U., Onel, K., Ozdemir, I., 'Microstructures and age Hardenability of Al-5%Si-0.2%Mg Based Composites Reinforced with Particulate SiC', Composite Science and Technology, 57 (1997), p.801-808.

[74] Ramani, G, Pillai, R.M.B, Pai, C., Satyanarayana, K.G., 'Effect of dispersoid loading on porosity and Mg distribution in 6061-3% Mg---SiC composites', Scripta Metallurgica et. Materialia, 73 (1993), p.405-410.

[75] Annual Book of ASTM Standards. Standard Test Method for Microindentation Hardness of Materials (2005), E384-99. 03.01.

[76] Li, Y. and Ramesh, K.T., 'Influence of Particle Volume Fraction, Shape and Aspect Ratio on the Behaviour of Particle-reinforced Metal-matrix Composites at High Rates of Strain', Acta Material 46(16), (1998), p.5633-5646.

[77] Annual Book of ASTM Standards. Standard Test Methods for Tension Testing of Metallic Materials, E8-04. 03.01, (2007).

[78] Taya, M., Arsenault, R.J., 'Metal matrix composites: thermomechanical behavior', vol. 4. Elmsford, New York: Pergamon Press; (1989).

[79] Srivatsan, T.S., Al-Hajri, M., 'The fatigue and final fracture behavior of SiC particle reinforced 7034 aluminum matrix composites', Composites: Part B (2002), 33 p.391-404.

[80] Christman, T., Suresh S., 'Effects of SiC reinforcement and aging treatment on fatigue crack growth in an Al---SiC composite', Mater Sci Eng (1988), 102, p.211–20.

[81] Srivatsan, T.S., 'The low-cycle fatigue behaviour of an aluminium-alloy-ceramic-particle composite', International Journal of Fatigue (1992), 14, p.173-182.

[82] Zhang, R.J., Wang, Z., Simpson, C., 'Fatigue fractography of particulate-SiC-reinforced Al (A356) cast alloy', Materials Science and Engineering: A (1991), 148(1), p.53-66.

[83] Bloyce, A., Summers, J.C., 'Static and dynamic properties of squeeze-cast A357-SiC particulate Duralcan metal matrix composite', Materials Science and Engineering: A (1991) 135, p.231-236.

[84] Hall, J.N., Jones, J.W., Sachdev, A.K., 'Particle size, volume fraction and matrix strength effects on fatigue behavior and particle fracture in 2124 aluminum-SiCp composites', Materials Science and Engineering: A (1994), 183, p.69-80.

[85] Myriounis, D.P., Hasan, S.T., Matikas, T.E., 'Role of Interface on the Mechanical Behaviour of SiC-Particle Reinforced Aluminium Matrix Composites', In: Proceedings of the International Conference on structural analysis of advanced materials (ICSAM-07), Patras, Greece, September 2-6; (2007).

[86] Maldague, X.V., 'Theory and practice of Infrared technology for nondestructive Testing', John Wiley&Sons, Inc, New York, (2001).

[87] ASM Handbook, Nondestructive Evaluation and Quality Control, Vol. 17, (1989).

[88] Toubal, L., Karama, M., Lorrain, B., 'Damage evolution and infrared thermography in woven composite laminates under fatigue loading. International Journal of Fatigue (2006), 28(12), p.1867-1872.

[89] Davidson, D.L., 'Fatigue and fracture toughness of aluminium alloys reinforced with SiC and alumina particles', Composites (1993), 24(3), p.248-255.

[90] Shang, J.K., Yu, W. and Ritchie, R.O., 'Role of silicon carbide particles in fatigue crack growth in SiC particulate reinforced aluminum alloy composite', Mater Sci Eng. A102, (1988), p.181–192.

[91] Bruzzi, M.S., McHugh, P.E., 'Micromechanical investigation of the fatigue crack growth behaviour of Al–SiC MMCs', International Journal of Fatigue, 26, 8, (2004), p.795-804.

[92] Paris, P., and Erdogan, F., 'A critical analysis of crack propagation laws', Journal of Basic Engineering, Transactions of the American Society of Mechanical Engineers, (1963), p. 528-534.

[93] Lindley, T.C., Richards, C.E., and Ritchie, R.O., 'Mechanics and mechanisms of fatigue crack growth in metals: a review', Metallurgia and Metal Forming, (1976), 976, p. 268-280.

[94] Schijve, J., 'Four lectures on fatigue crack growth', Engineering Fracture Mechanics, (1978), 11, 1, p. 169-206.

[95] Wei, R.P., 'Fracture mechanics approach to fatigue analysis in design', Journal of Engineering Materials and Technology, (1978), 100, p. 113-120.

[96] Ritchie, R.O., 'Application of fracture mechanics to fatigue, corrosion fatigue and hydrogen embrittlement', Analytical and Experimental Fracture Mechanics, Proceedings of the International Conference held in Rome, G C Shih (editor), Sijthoff and Nordhoff, (1980).

[97] Allen, R.J., Booth, G.S., and Jutla, T., 'A review of fatigue crack growth characterisation by linear elastic fracture mechanics (LEFM) Parts 1 and 2', Fatigue and Fracture of Engineering Materials and Structures, 11, 1, (1988), p.

45-69, and p. 71-108.

[98] Suresh, S., 'Fatigue of Materials 2nd edition', Cambridge University Press, Cambridge, England (1998).

[99] Bremond, P., Potet, P., 'Cedip Infrared Systems, Lock-in Thermography, A tool to analyze and locate thermo-mechanical mechanism in materials and structure', Thermosence XXIII, (2001).

[100] Choi, M.Y., Park, J.H., Kang, K.S., Kim, W.T., 'Application of Thermography to Analysis of Thermal Stress in the NDT for Compact Tensile Specimen' 12th A-PCNDT Asia-Pacific Conference on NDT, 5th – 10th Nov, Auckland, New Zealand (2006).

[101] Annual Book of ASTM Standards, ASTM E647 - 08 'Standard Test Method for Measurement of Fatigue Crack Growth Rates'.

[102] Zhang, R.J., Wang, Z., Simpson, C., 'Fatigue fractography of particulate-SiC-reinforced Al (A356) cast alloy', Materials Science and Engineering: A, 148(1), (1991), p. 53-66.

[103] Roebuck, B., Lord, J., 'Plane strain fracture toughness test procedures for particulate metal matrix composites', Materials Science & Technology Materials Science & Technology, 6 (1990), p.1199-1209.

[104] Gorp, van A.C., Mussert, K.M., Janssen, M., Bakker, A., Zwaag, van der S., ,A Critical Appraisal of Fracture Toughness Measurements on AA6061 and an Al203-Particle Reinforced AA6061 Alloy for Various Heat Treatments', J. Test & Eval, 29 (2001, p.146-154.

[105] Perez lpina, J.E., Yawny, A.A., Stuke, R., Gonzalez O.C., 'Fracture Toughness in Metal Matrix Composites', Materials Research, 3 (2000), p.74-78.

[106] Mortensen, A., 'A Review of the Fracture Toughness of Particle Reinforced Aluminium Alloys', Proc. Int. Conf. Fabrication of Particulate Reinforced Metal Composites, Quebec, Canada, (1990), p.217-23.

[107] Anderson, T.L., 'Fracture Mechanics-Fundamentals and applications', CRS press LLC, (1995).

[108] Allison, J.E., Cole, G.S., 'Metal-Matrix Composites in the Automotive Industry: Opportunities and Challenges', JOM, 45 (1993), p.19-25.

[109] Doychak, J., 'Metal and Intermetallic Matrix Composites for Aerospace Propulsion and Power Systems', JOM, 44 (1992), p.46-51.

[110] Lord, J., 'Fracture Toughness Test Methods for PRM', MMC Assess EU Network MMC-Assess – Thematic Network.

[111] Annual Book of ASTM Standards, “Standard Test Method for Plane-Strain Fracture Toughness of Metallic Materials”, ASTM E399-90, 1997.

[112] Goolsby, R.D., Austin, L.K., Proc. 7th lnt. Conf on 'Fracture', ICF7, Houston, TX, University of Houston, 4 (1989), p.2423-2435.

[113] Arsenault, R.J., Fishman, S., Taya, M., ‘Deformation and fracture behaviour of metal-matrix composite materials’, Progress in Materials Science, 38 (1994), p.1-157.

[114] Singh, P.M., Lewandowski, J.J., ‘Effects of Heat Treatment and Particle Size on Damage Accumulation during Tension Testing of Al/SiC Metal Matrix Composites’, Met. Trans. A., 24A (1993), p.2451-2464.

[115] Myriounis, D.P., Kordatos, E.Z., Hasan, S.T., Matikas, T.E., ‘Crack-tip stress field and fatigue crack growth monitoring using infrared lock-in thermography in A359/SiCp composites’, Strain, (2009).

[116] Wong, B.S., Tui, C.G., Bai, W., Tan, P.H., Low, B.S. and Tan, K.S. ‘Thermographic evaluation of defects in composite materials’, Insight: NDT-and Cond Monit, 41, (1999), p.504-509.

[117] Briant, C.L., Banerji, S.K.,’ Embrittlement of Engineering Alloys’, Treatises on Mater. Sci. Tech., 25 (1983).

[118] Kamdar, M.H., ‘Embrittlement by Liquid and Solid Metals’, Mater. Soc. A.I.M.E. (1984).

[119] Lim, L.C., Watanabe, T., ‘Fracture toughness and brittle–ductile transition controlled by grain boundary character distribution (GBCD) in polycrystals’, Acta Met, (1990), 38(12), p.2507–2516.

[120] Faulkner, R.G., Shvindlerman, L.S., ‘Thermodynamics of Vacancies and Impurities at Grain Boundaries’, Materials Science Forum (1996), 207-209 (Part 1), p.157-160.

[121] Broek, D., ‘Elementary engineering fracture mechanics’, Kluwer Academic Publishers Group, 5-17 (1986).

[122] McMahon, Jr. C.J.., Vitek, V., ‘Effects of segregated impurities on intergranular Fracture Energy’, Acta Metall, 27(4), (1979), p.507-513.

[123] Griffith, A.A., ‘The phenomena of rupture and flow in solids’, Philosophical Transactions of the Royal Society of London, A 221: (1921), p.163–198.

[124] Davidson, D.L., ‘Fatigue and fracture toughness of aluminium alloys reinforced with SiC and alumina particles’, Composites (1993), 24(3).

[125] Faulkner, R.G, Shvindlerman, L.S., ‘Grain boundary thermodynamics, structure

and mechanical properties', Mater. Sci. Forum (1996), 207–209(1), p.157–160.

[126] Shoyxin, L., Lizhi, S., Huan, L., Jiabao, L., Zhongguang, W., 'Stress carrying capability and interface fracture toughness in SiC/6061 Al model materials', Journal of materials science letters 16, (1997), p.863–869.

[127] Xu, X.Q., Watt, D.F., 'Basic role of a hard particle in a metal matrix subjected to tensile loading', Acta Metal., Mater., 42(11), (1994),3 p.717-3729.

[128] Cox, H.L., 'The elasticity and strength of paper and other fibrous materials', Br. J. Appl. Phys., 3, (1952), p.72-79.

[129] Llorca, J., 'An analysis of the influence of reinforcement fracture on the strength of discontinuously- reinforced metal matrix composites, Acta Metall. Mater., 43(1), (1995), p.181-192.

[130] Myriounis, D.P., Hasan, S.T., Matikas, T.E., 'Thermodynamics based damage mechanics model for the estimation of interface strength in particulate composites', Advanced Composite Letters, in press (2009).

[131] Wang, Z., Zhang, R.J., 'Microscopic characteristics of fatigue crack propagation in aluminium alloy based particulate reinforced metal matrix composites, Acta metal. mater., 42(4), (1994), p.1433-1445.

[132] Mital, S.K., Murthy, P.L.N., Goldberg, R.K., 'Micromechanics for particulate reinforced composites', Mechanics of Advanced Materials and Structures, (1997), 4(3), p.251-266.

[133] Myriounis, D.P., Hasan, S.T., Matikas, T.E., 'Predicting interfacial strengthening behaviour of particulate reinforced MMC - A micro-mechanistic approach' Composite Interfaces (2009).

[134] Faulkner, R.G., 'Impurity diffusion constants and vacancy binding energies in Solids', Mater. Sci. Technol., 1(6), (1985), 442–447.